THE INFLUENCE OF TURBULENCE ON DUST EXPLOSION AND THE EFFECT OF METHANE ON COAL DUST EXPLOSION

Final Report

by

J.H.S. Lee, R. Kryslantas, F. Bond, N. Craft and P.Y. Kang

Shock Wave Physics Research Laboratory

Department of Mechanical Engineering, McGill University

Work on this project was conducted under the auspices of the Canada Centre for Mineral and Energy Technology, Energy, Mines and Resources, Canada.

DSS FILE NUMBER	:	12 ST 23440 - 4 - 9024
DSS CONTRACT SERIAL NUMBER	:	OST 84 - 00016
CANMET PROJECT NUMBER	:	23440 - 4 - 9024
CANMET SCIENTIFIC AUTHORITY	:	Dr. K.K. Feng

DATE: March 1984

This report should be cited as Contract Report No.: OST 84 - 00016

128 pp

MICROMEDIA JUL 03 1985

Final Report on an Investigation of Dust Explosion

by

Prof. J.H.S. Lee
Prof. R. Knystautas
Mr. François Bond
Mr. Neil Craft
Mrs. P.Y. Kang

Shock Wave Physics Research Laboratory
Department of Mechanical Engineering
McGill University
Montreal, Canada

March 26, 1985

TABLE OF CONTENTS

	PAGE
General Remarks	1
APPENDIX A: The Influence of Turbulence on Dust Explosions in Closed Vessels	
APPENDIX B: An Experimental Study of Hybrid Explosive Dust-Gas-Air Mixtures	

General Remarks

Dust explosions cause extensive human and material damage in coal mines, grain silos and industrial process equipment where dust is handled. The study of dust explosion is an increasingly active area of combustion research and will remain so at least until the structure and propagation mechanisms of dust flames are sufficiently well understood to permit the establishment of meaningful criteria for the design of safety measures to prevent or mitigate the effects of such explosions.

This report focusses on two topics which are of central interest in the study of dust explosions: the role of turbulence and the explosion of hybrid gas-dust-air mixtures.

The first part describes a series of experiments designed to elucidate the influence of turbulence on the extent and on the rate of burning of a dust-air mixture. Knowledge of the burning rate is especially important to the design of relief vents. The results of the experiments indicate that the burning rate is highly sensitive to the initial turbulence of the dust-air premixture and that the mechanisms of burning rate increase due to turbulence are probably similar to those which are known to affect the propagation of a premixed gas-air flame.

The second part is an experimental study of flame propagation in a mixture which contains combustible dust as well as combustible gas. It is well known that at the onset of a typical coal-mine explosion, the ignition of a combustible methane-air gas pocket creates a turbulent flow that raises into suspension coal dust lying on the floor and walls of the mineshaft, and that subsequent flame propagation takes place in a mixture that contains both dust and methane. Hence an understanding of the combustion of such hybrid mixtures

is very important. It is shown that small additions of coal dust to a mixture containing mostly methane and air, or small additions of methane to a mixture containing mostly dust and air, increases the burning rate substantially by affecting the stoichiometry of the combustible mixture.

APPENDIX A

The Influence of Turbulence on Dust Explosions in Closed Vessels

INTRODUCTION

The problem of dust explosion has received considerable attention since the series of grain elevator explosions in the United States, in December 1977[1]. The primary objectives in the study of dust explosion are to establish some meaningful parameters for the classification of the various types of explosive dust, to determine safety requirements in areas where dust accumulation can occur and to seek proper venting requirements for the design of grain elevators and industrial process equipment where dust is handled. To achieve these goals, one needs to have at least a qualitative understanding of the structure and propagation mechanisms of a dust flame.

In attacking the problem of dust explosion, it is wise to try to draw upon our knowledge of gas and vapor phase explosion. For homogeneous gases and vapors, the fundamental parameters that characterize the explosibility of a mixture (e.g., minimum ignition energy, laminar burning velocity, flammability limits, etc.) are well known and accessible to direct experimental measurements. The role played by turbulence in the propagation of premixed fuel-air flames is also fairly well understood[2], and there exists enough reliable experimental data on turbulent burning velocities to permit at least engineering estimates of the burning rate under different conditions. By contrast, no reliable fundamental parameters are as yet known for explosive dust-air mixtures. Turbulence is an intrinsic parameter in a dust-air mixture and the study of the role played by turbulence becomes an integral part of research on the fundamental mechanisms of propagation of a dust-air flame.

Since it is difficult to achieve stationary, adiabatic dust flames for detailed observation, dust explosions are usually studied in constant volume bombs of various sizes and shapes. The parameters measured in such experiments are the maximum overpressure and the maximum rate of overpressure

rise. The maximum overpressure, in principle, depends mainly on the energetics of the mixture but can be indirectly influenced by heat losses to the walls of the vessel. The magnitude of these losses depends in turn on the vessel geometry and on the rate of combustion. However, experimental data from a variety of apparatuses of different sizes and shapes appear to give reasonable agreement of maximum overpressure for practical purposes. The maximum rate of overpressure rise $((\frac{dp}{dt})_{max})$ on the other hand, has been found to vary considerably from one apparatus to another in a way that appears to be strongly related to the details of the flow field encountered by the propagating dust flame. Simple theoretical considerations of constant volume explosions[3] lead to the conclusion that if all explosion parameters except vessel size are the same, the maximum rate of overpressure rise should scale according to the so-called "cubic law":

$$(\frac{dP}{dt})_{max} V^{1/3} = Kst$$

where Kst is a constant of the dust-air mixture. It has been recognized by a number of authors that the fact that the Kst factor varies from one apparatus to the next is linked with the transient, decaying nature of the turbulent flow field generated by the process of dust dispersion in the different experiments performed. Yet there appears to have been no systematic study to date to elucidate the effect of the mean dust dispersion flow field on the Kst factor. The present investigation attempts to address this problem and recent results are presented in this paper.

EXPERIMENTAL APPARATUS AND PROCEDURE

A spherical vessel of 333 liter volume (Figure 1) and a cylindrical vessel of 180 liter volume (Figure 2), with 1 meter height and 0.5 m diameter, were used in the present study to assess the influence of turbulence on dust

and gas explosions in different geometries.

The spherical vessel was equipped with a 45 cm diameter copper tubing ring, on which ten holes of 1.1 mm diameter were drilled. The ring was fed by a high pressure air supply and the level of turbulence introduced by the round jets could be controlled by varying the mass flow rate of air to the ring. The dust was placed in a bowl at the bottom of the vessel and dispersion was achieved by an air blast from a 1.5 liter compressed air bottle (1380 kPa) discharging through a nozzle directed at the center of the dust bowl. The dispersion was triggered by opening a solenoid valve in the dispersion circuit. Ignition was achieved by either an exploding fuse wire or a bare flashbulb magnesium filament. The delay between dispersion and ignition could be controlled by means of an electric timer.

The sequence of operations for dust explosion experiments in the spherical vessel was as follows. The dust was first weighed into the cup at the bottom of the vessel. The vessel was then put under a vacuum (400 mm Hg). The air jets were then turned on, and air addition from the jets caused the vessel pressure to increase again. When atmospheric pressure was restored, the dispersion air blast was activated and ignition followed after a short delay.

For the methane-air experiments, the vessel was evacuated and then filled by partial pressure with an amount of methane resulting in the desired composition. The air jets were then turned on, and ignition was triggered when the vessel reached atmospheric pressure.

Similar accessories and experimental procedures were used in the cylindrical vessel. Turbulence was produced by six air jets spaced along two vertical arms 40 cm apart. As was the case in the spherical vessel, the holes were oriented in opposite directions on the two arms, thus producing a swirl around the axis of the vessel.

The dust used in the present study was cornstarch (ie., "Benson" brand). Cornstarch consists of a single chemical compound, with formula $(C_6H_{10}O_5)_n$.[4] It is a natural polymer formed by the linkage of many α-D-glucose ($C_6H_{12}O_6$) monomers. Upon polymerization, each glucose molecule yields one water molecule. For this reason, cornstarch is termed a condensation polymer of glucose. A schematic of the glucose molecule and of the polymerization process are shown below:

α-D-glucose (dextrose) monomer

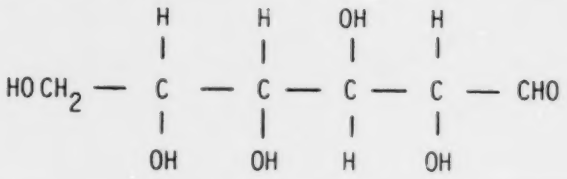

Polymerization process of cornstarch

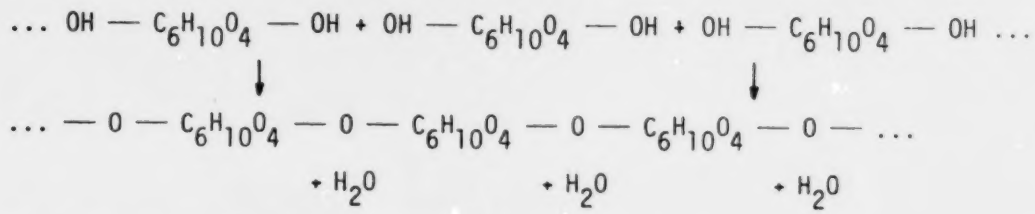

A single starch molecule may contain as few as 200 and as many as 600,000 monomers, with an average of about 500.[5]

The literature seems to contain no information on the devolatilization properties (ie., devolatilization products, devolatilization rates and enthalpy of devolatilization) of cornstarch. However, the devolatilization properties of cornstarch should be very similar to those of cellulose, since the structures of the two molecules are identical. Cornstarch and cellulose differ only by the number of monomers making up a single polymer molecule: cellulose contains an average of 3500 dextrose monomers joined in a linear chain which gives it its fibrous properties.[6]

Commercially available cornstarch usually contains about 10% moisture by weight.[7] Dried cornstarch should produce higher P_{max}, $(dP/dT)_{max}$ than moist starch.

The known chemical and physical properties of the starch material are summarized in the table below:

CORNSTARCH

Chemical formula:	$(C_6H_{10}O_5)_n$
Molecular weight of monomer:	162
Material density[8]:	1, 5
Stoichiometric concentration in air at S.T.P.	253.7 gm starch/m^3 air
Heat of combustion:	640 kcal/g mole

Scanning electron micrographs showed the particles to be remarkably spheroidal in shape, as indicated by the microphotograph of a single starch particle, Figure 3.

A particle size analysis shows the average size of the particles (mixed with the fluidizing agent CAB-O-SIL) to be 14.7 μm.[9] A simple Stokes' law force balance yields a free fall velocity of about 1 cm/sec. Hence a characteristic settling time for such single particles - defined as the ratio of apparatus radius to free fall velocity - is around 50 seconds. Yet experiments show that significant settling does occur in as short a time as one second, to the point that an explosion will not propagate if the mixture is ignited more than two seconds after the dust is dispersed.

From this we conclude that the dispersion consists of agglomerated starch particles, whose effective size is many times that of a single particle. The particles are initially present as one big agglomerate in the dust bowl.

The dispersion blast and subsequent flow field permit the separation of this single agglomerate into many small ones, but the process does not reach the stage where single starch grains are suspended in air.

A PCB quartz pressure transducer was used to record the pressure-time history inside the vessel. An ion gauge was mounted on the surface of the spherical vessel, to monitor the time of flame arrival on the vessel wall. Typical oscilloscope records of a dust explosion and of a methane explosion are shown in Figures 4 and 5.

RESULTS AND DISCUSSION

Figures 6 and 7 show the results of an experiment in which the only turbulence induced was that associated with the dispersion process itself. The delay between dispersion and ignition was varied to try to elucidate the role played by the transient turbulence of the dispersion process. The experiments were done with a 300 gm/m^3 cornstarch-air mixture in both the spherical and the cylindrical bomb. We have also plotted for comparison purposes, the data obtained by Nagy[10] in a similar experiment done with 9.5% methane-air in a 28.3 liter cubical vessel, in which 9.5% methane-air was also used as "dispersion" fluid. Figure 6 shows the maximum overpressure developed, while Figure 7 shows the ratio of Kst factor and Kg factor (the analogue of Kst for gas-air mixtures) to the maximum K factor observed. This provides a convenient way of normalizing the data to compare the influence of the flow field on gas-air flame and dust-air flame. For both the cylindrical and the spherical vessels, the maximum overpressure and the maximum Kst factor are obtained with an ignition delay of about 0.5 seconds. With shorter delays, it appears that the dust and air have had insufficient time to mix homogeneously, while for longer delays, the turbulence of the dispersion has begun to die down and can no longer act to enhance flame propagation. This finding led us to use an

ignition delay of 0.5 seconds in all subsequent dust-air explosions whose results are presented in this paper. With methane-air the oxidizer and fuel are already mixed so that the maximum Kg is obtained with zero ignition delay.

The phenomenon of the decay of turbulence in a closed vessel has been studied experimentally by Tsuge[11] who found that the characteristic decay time of the turbulence intensity was directly proportional to the smallest vessel dimension (D) raised to the power of 1.2. Hence for any particular vessel, the ratio

$$\frac{\tau_D - \tau_D\,(Kst_{max})}{D^{1.2}}$$

where τ_D is the delay between dispersion and ignition of the dust, is a normalized measure of the amount by which the vessel turbulence has decreased since the time at which it was a maximum - this time corresponding to the occurence of the maximum Kst factor. In Figure 8, we have plotted the ratio Kst/Kst_{max} versus the normalized turbulence decay time defined above, for a variety of vessel sizes and shapes: the Hartmann bomb used by Eckhoff[12], the 20-liter sphere of Cocks and Meyer[13], Bartknecht's[14] 1-m^3 cylinder, Swift's[15] 26-L sphere, Moore's[15] 1.75-L cylinder and 43-L sphere, as well as our own 180-L cylinder and 333-L sphere. It is quite remarkable that all the data follow fairly well a single pattern, despite the widely different characteristics of the apparatuses used.

Figure 9 shows the ratio of Kst to Kst_{max} as a function of the difference between ignition delay and ignition delay corresponding to Kst_{max}. This shows clearly how the rapidity of turbulence decay decreases with an increase in vessel size: the slowest decay is observed in Bartknecht's 1-m^3 vessel and the fastest occurs in Eckhoff's Hartmann bomb.

Figure 10 and 11 show maximum overpressure and Kst factor, respectively

as a function of cornstarch concentration for the 333 liter sphere and the 180 liter cylinder. For comparison purposes, results from Nagy[10], Hartmann[17] and Cocks[13] are also shown. The peak overpressures are found to be in fair agreement with one another, in spite of the widely different properties of the cornstarch used and of the characteristics of the experimental apparatuses. The Kst factor, on the other hand, is found to vary over a wider range. All the data for Δp_{max} show a similar trend, with Δp_{max} rising sharply from a "lean limit" concentration of about 100 gm/m^3 and asymptote to about 700 kPa when the concentration reaches 500 gm/m^3. No rich limit was observed up to a concentration of 1000 gm/m^3. The peak overpressure in the 333 liter sphere was consistently higher than that obtained in the 180 liter cylindrical vessel. This may be due to more severe heat losses to the walls in the cylindrical vessel since the flame is already in contact with the cylinder wall prior to complete consumption of the mixture at the ends of the vessel. The Kst from the cylinder bomb shows a maximum value of about 6000 kPa-m/s at a dust concentration of 200 gm/m^3 and then decreases with a further increase in concentration. The Kst from the spherical vessel does not show the same trend: it simply increases asymptotically to a peak value of about 3500 kPa-m/s. Thus the burning rate in the cylindrical vessel, as indicated by the Kst factor, is generally higher than that from the spherical vessel. This indicates the importance of vessel geometry not only on the quantitative but also on the qualitative behavior of the explosion processes.

Figure 12 shows the maximum overpressure developed in the 333 liter spherical vessel as a function of mass flow rate through the jets (ie., turbulence level) for a 300 gm/m^3 cornstarch-air mixture and for a 7.5% CH_4-air mixture. The methane data show a very slight increasing trend of Δp_{max} with increasing turbulence level, which indicates that turbulence enhances flame propagation and thus reduces the heat losses. On the average, the measured Δp_{max} was 6.7% less than the theoretical equilibrium pressure[18]. The maximum

overpressure in the dust explosions is remarkably constant, indicating that the amount of heat loss is independent of the turbulence level, except for the special case when the air jets are not used, ie., when the only turbulence present is that associated with the flow field generated by the dispersion process. The Kst factor measured in the latter case was 1400 kPa-m/s and the Kg measured for laminar methane-air was 2676 kPa-m/s. In Figure 13, we have plotted as a function of jet mass flow rate the ratio of K factor to the reference K factor described above. Since models of constant volume combustion in a closed vessel[10] show that the burning velocity of a fuel-air mixture is directly proportional to $(\frac{dP}{dt})$, the ratio K/K_{ref} can be interpreted to be equivalent to the ratio of turbulent to laminar burning velocity (u_t/u_ℓ), although the reference dust-air explosion, as already pointed out, is not truly laminar. The Kg factor shows a remarkably linear increase with jet flow rate, up to a ratio Kg/K_{ref} of about 8 at the maximum flow rate. Comparison of these data with the data published by Abdel-Gayed and Bradley[19] leads to the plausible conclusion that the turbulent r.m.s. velocity increases linearly with jet flow rate and that the level of turbulence induced by the jets is low compared to the level required to bring about the onset of quenching mechanisms. The Kst factor ratio is about the same as for the methane up until a jet flow rate of 8 gm/sec. Further increase in the flow rate causes the Kst factor ratio to drop below the Kg factor ratio. Over the range of flow rates studied, the ratio of Kg to Kst varies between two and four. The faster burning of the methane-air mixture clearly brings to light the extra steps involved in the propagation of a dust flame compared to a gas flame, namely, devolatilization of the raw fuel particles and mixing of the volatiles with the surrounding air.

Figure 14 and 15 show the results of a series of experiments very similar to that described above, but performed in the 180 liter cylindrical vessel. The results obtained for the methane-air mixture agree qualitatively

with those in the spherical vessel. The maximum overpressure developed in the cylindrical vessel is roughly 10% lower than in the spherical vessel, probably because the higher surface-to-volume ratio in the cylinder causes a greater heat loss to the wall. Although the maximum flow rate used in the cylindrical vessel was only about one fourth that used in the spherical vessel, a K factor ratio of 10.5 was achieved for methane-air. By contrast with the curve of K/K_{ref} for the methane-air in the spherical vessel, the analogous curve for the cylindrical vessel shows significant flattening at the higher flow rates and it is possible that the turbulence intensity there is sufficiently high to begin quenching the flame.

The results for the dust-air mixture are qualitatively quite different from those obtained in the spherical vessel. Here it appears that turbulence has the effect of retarding flame propagation and by the same token, increasing the time available for heat loss to the wall to decrease the maximum overpressure. The maximum overpressure and maximum rate of overpressure rise are highest with zero jet flow rate and both decrease monotonously as jet flow rate is increased. The only satisfactory explanation to this is that in this smaller vessel the dispersion and the jets induce a level of turbulence already sufficient to cause quenching of the flame. It is worth pointing out that the turbulent flow field encountered by a dust-air and a gas-air flame in apparatuses with the same geometry and jet flow rates are not necessarily equivalent since it is possible that the air flow interacts with the dust particles in a manner that alters the relevant turbulent parameters.

CONCLUSION

This study shows that for dust flames as well as gas flames, turbulence can play the dual role of enhancing as well as retarding the flame

propagation. It appears that the study of gas explosion in conjunction with dust explosion can help speed up the learning process for the elucidation of the structure and propagation mechanisms of dust-air flames, as the effects observed in dust and gas explosions often appear to be correlated.

Although more experimental data are required to ascertain this finding, it would seem that the onset of quenching mechanisms appears at lower turbulent intensities in cornstarch-air flames than in methane-air flames with approximately equivalent energetics.

More data on fundamental parameters for dust flames (ie., laminar flame thickness, laminar burning velocity, minimum ignition energy, etc.) are required before the role of turbulence displayed in this study can be properly interpreted. Recently, Bradley and Lee[20] have speculated that there may exist a great deal of similarity between the structure of turbulent dust-air and gas-air flames. Their argument rests on the idea that since most of the burning occurs after a dust particle has devolatilized, the main effect of turbulence is to increase the rate of mixing between volatiles and air around a particle, and to enhance the transport of heat from the flame front to the unburned mixture ahead. In Tables 1 and 2, we have attempted to summarize the characteristic length and time scales on which a model of turbulent dust explosion in a closed vessel must be based.

REFERENCES

1. Kaufmann, C.W.: "Agricultural Dust Explosions in Grain-Handling Facilities", Proc. International Meeting on Fuel-Air Explosions, SM Study 16, Eds. C.M. Guirao and J.H. Lee, University of Waterloo Press, Waterloo, 1982.

2. Andrews, G.E., Bradley, D. and Lwakabamba, S.B., Combustion and Flame 24, 285-304 (1975).

3. Bartknecht, W.: "Brenngas-Und Staubexplosionen. Forschung-Bericht F45, Bundesinst. f. Arbeitschutz, Koblenz (1971).

4. Holdness and Lambert: A New Certificate Chemistry, 4th ed., London 1969, p. 187.

5. Brescia, F., Arents, A., Meislich, H. and Turk, A.: Fundamentals of Chemistry: A Modern Introduction. Academic Press, New York, 1966, p. 755.

6. Ibid.

7. Letter from F. Tamanini to J.H. Lee, 21/11/83, and our own measurements.

8. Banks, W. and Greenwood, C.T.: Starch and Its Components. Halsted Press, 1975, p. 242.

9. Letter from P. Nelson to J.H. Lee, 17/10/84.

10. Nagy, J., Seiler, E.C., Conn, J.W. and Verakis, H.C.: "Explosion Development in Closed Vessels", U.S. Bureau of Mines Report of Investigations 7507, 1971.

11. Tsuge, M., Kido, H. and Yanagihara, H.: Bull. J.S.M.E., V. 16, No. 92 (1973), pp. 244-251.

12. Eckhoff, R.K.: 1st International Colloqiuium on Explosibility of Industrial Dusts, Baranow, Poland, 1984.

13. Cocks, R.E. and Meyer, R.C.: "Fabrication and Use of a 20 liter Spherical Dust Testing Apparatus", Process Specialities Section, Engineering Division, Procter & Gamble, Cincinnati, Ohio.

14. Bartknecht, W., 18th Annual Loss Prevention Symp. AIChE, Philadelphia, Aug. 19-22.

15. Swift, I.: Fuel-Air Explosions, SM Study No. 16, Eds. C.M. Guirao and J.H. Lee, University of Waterloo Press, Waterloo 1982.

16. Moore, P.: Chemistry and Industry, July 7, 1979, pp. 430-434.

17. Hartmann, I., Cooper, A.R. and Jacobson, M: "Recent Studies on the Explosibility of Cornstarch", U.S. Bureau of Mines Report of Investigation 4725, 1951.

18. Gordon, S. and McBride, B.J.: "Computer Program for Calculation of Complex Chemical Equilibrium Compositions, Rocket Performance, Incident and Reflected Shocks, and Chapman-Jouguet Detonations", National Aeronautics and Space Administration, Washington, 1971.

19. Abdel-Gayed, R.G. and Bradley, D., Proc. Trans. Royal Soc. London, 301, A1457 (1981).

20. Bradley, D. and Lee, J.H.S.: "On the Mechanisms of Propagation of Dust Flames", First International Colloquium on Explosibility of Industrial Dusts, Baranow, Poland, 1984.

ACKNOWLEDGEMENTS

The authors would like to gratefully acknowledge the contributions of Mr. Moris Fresko in performing some of the experimental work and of Dr. Lloyd Nelson of Sandia National Laboratories for procuring particle size analyses and s.e.m. photographs of cornstarch dust.

TEST APPARATUS
(V = 0,333 m³)

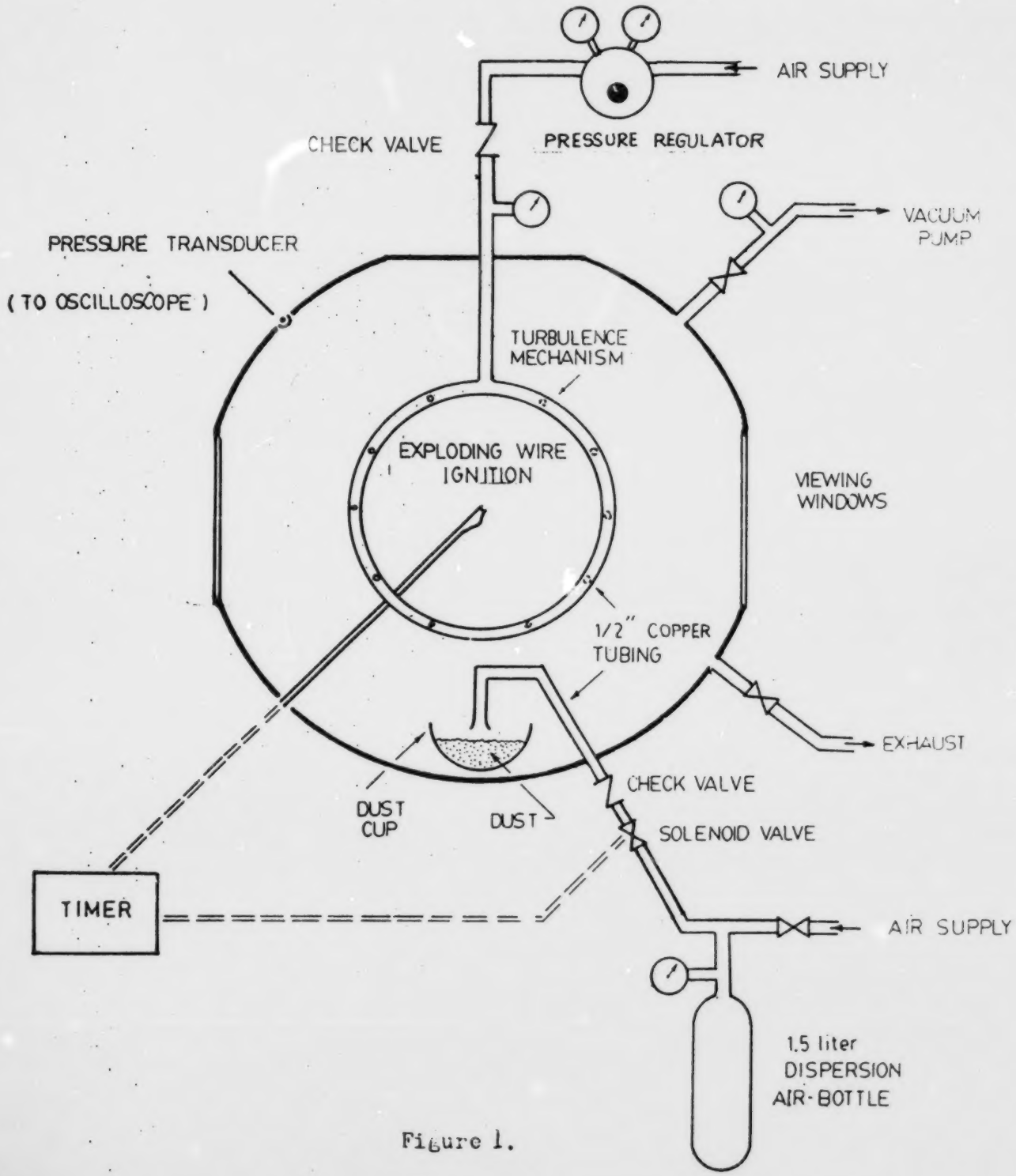

Figure 1.

TEST APPARATUS
(V = 0.180 m^3)

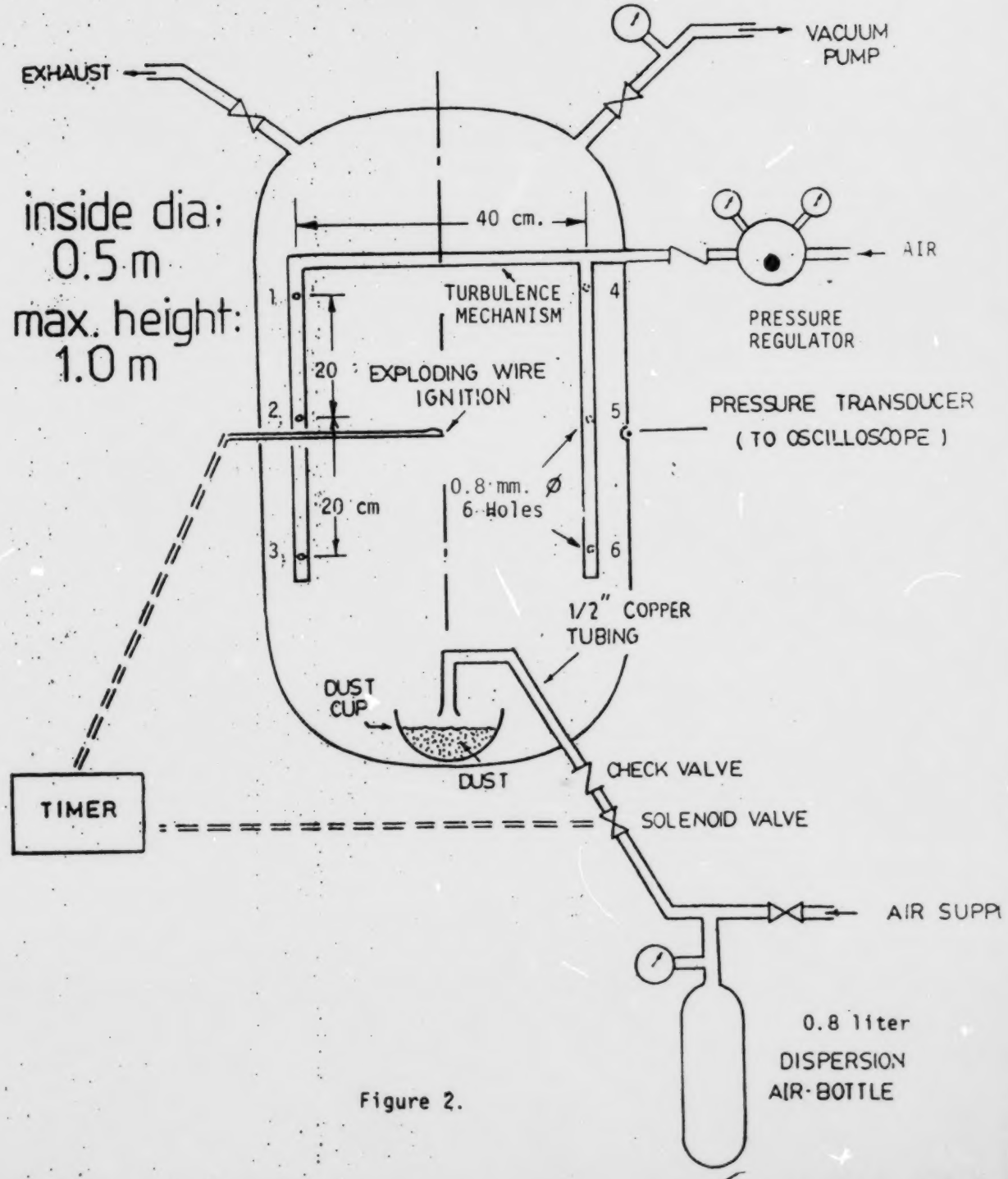

Figure 2.

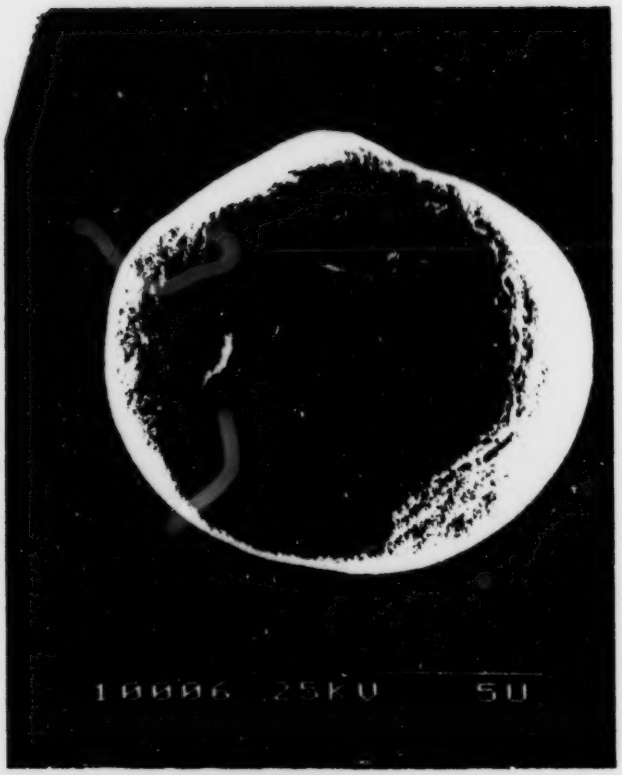

Figure 3 - Typical microphotograph of a single cornstarch dust particle, magnified 5000 times. Particle diameter: 13.8 microns.

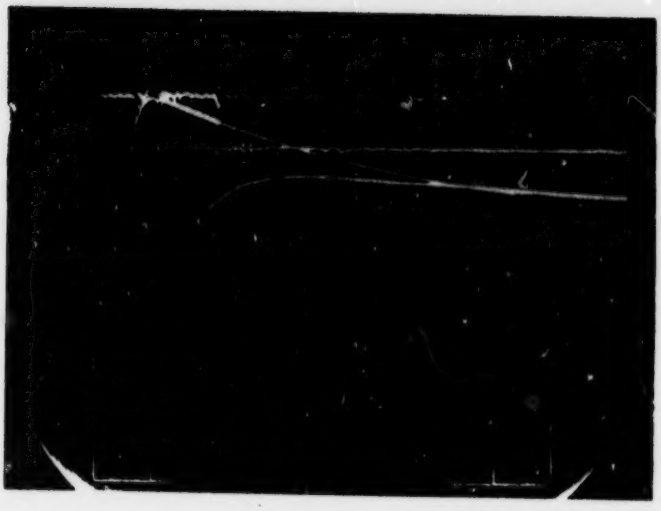

Figure 4 - Typical oscilloscope record of a dust-air explosion. Top two traces show slow sweep and fast sweep ion gauge currents. Bottom two traces show slow sweep and fast sweep pressure at 20 psi per vertical division. Fast sweep rate: 0.02 s/div. Slow sweep rate: 0.1 s/div.

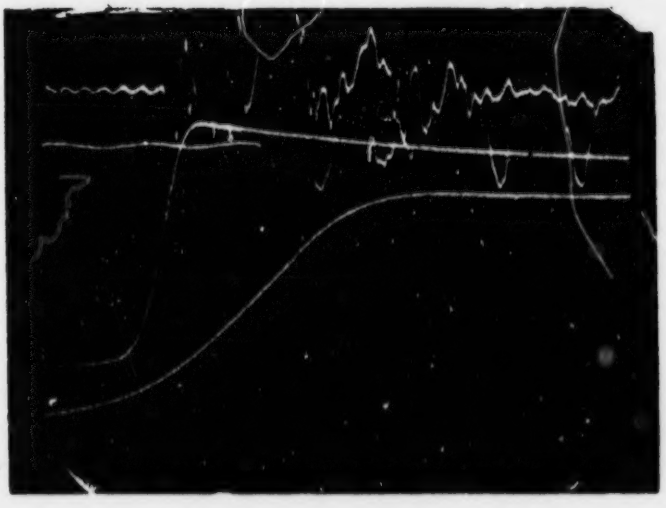

Figure 5 - Typical oscilloscope record of a methane-air explosion. Diagnostics are identical to that of the dust explosion trace. Fast sweep rate: 0.01 s/div. Slow sweep rate: 0.05 s/div.

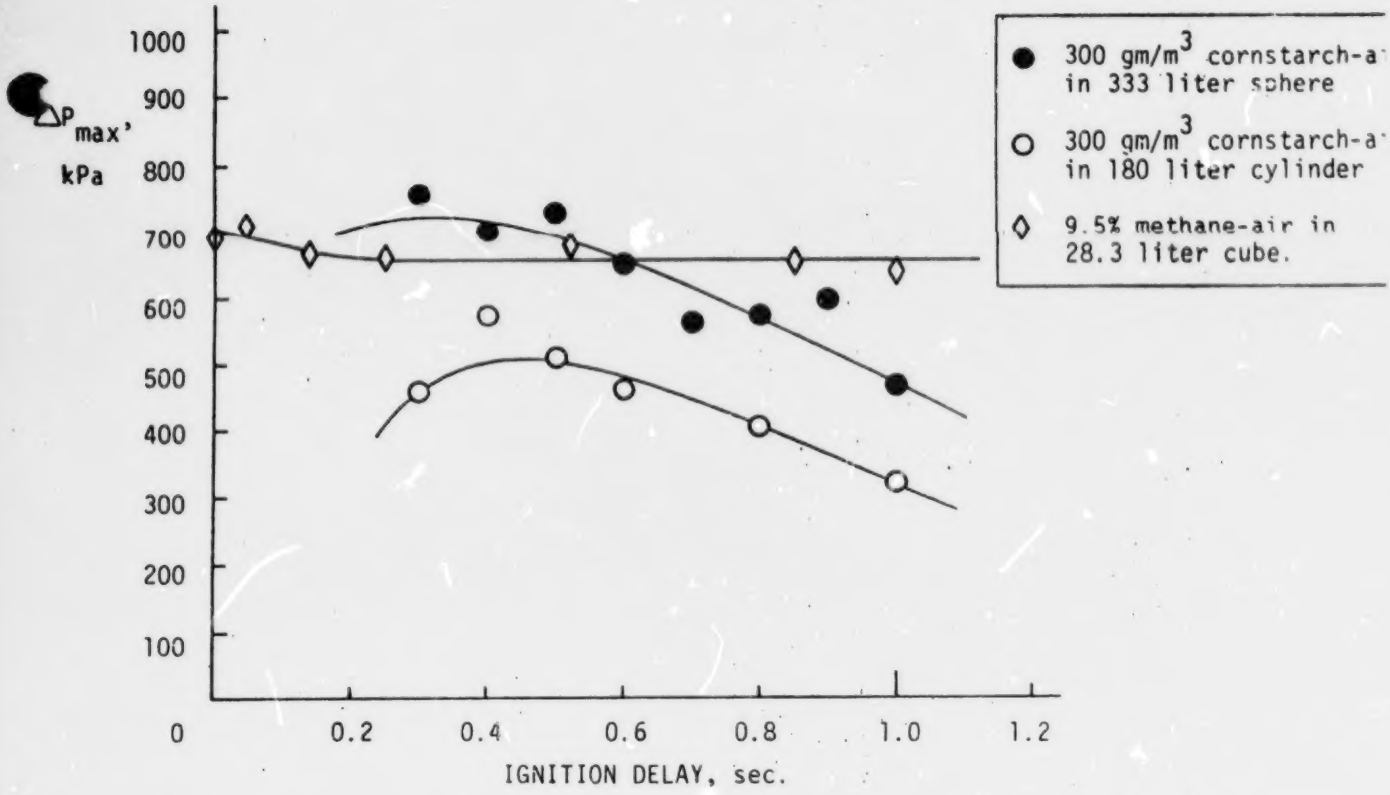

Figure 6 - Variation of maximum pressure with ignition delay

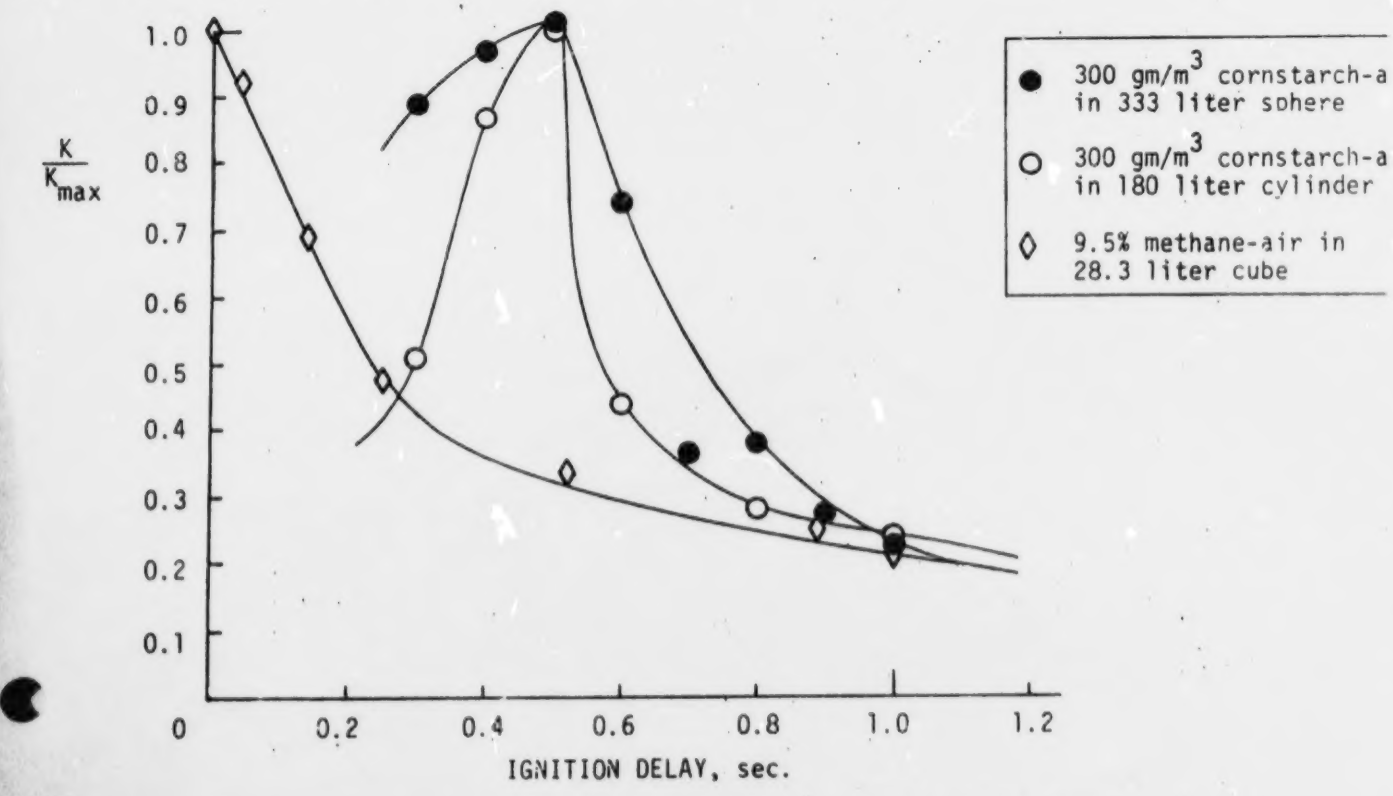

Figure 7 - Variation of normalized K factor with ignition delay

EFFECT OF NORMALIZED TURBULENCE DECAY TIME ON Kst RATIO

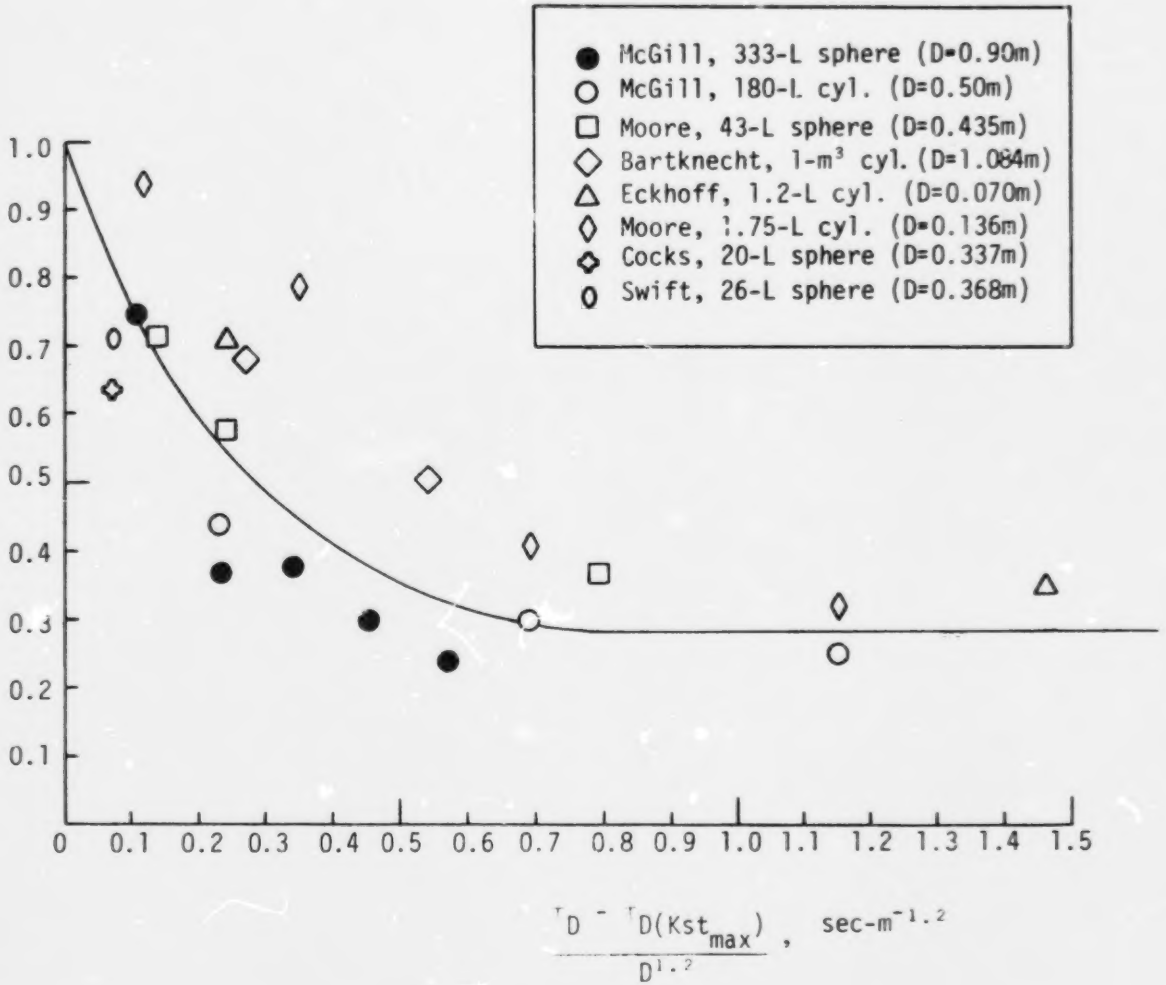

FIGURE 3

EFFECT OF TURBULENCE DECAY TIME ON K_{st} RATIO

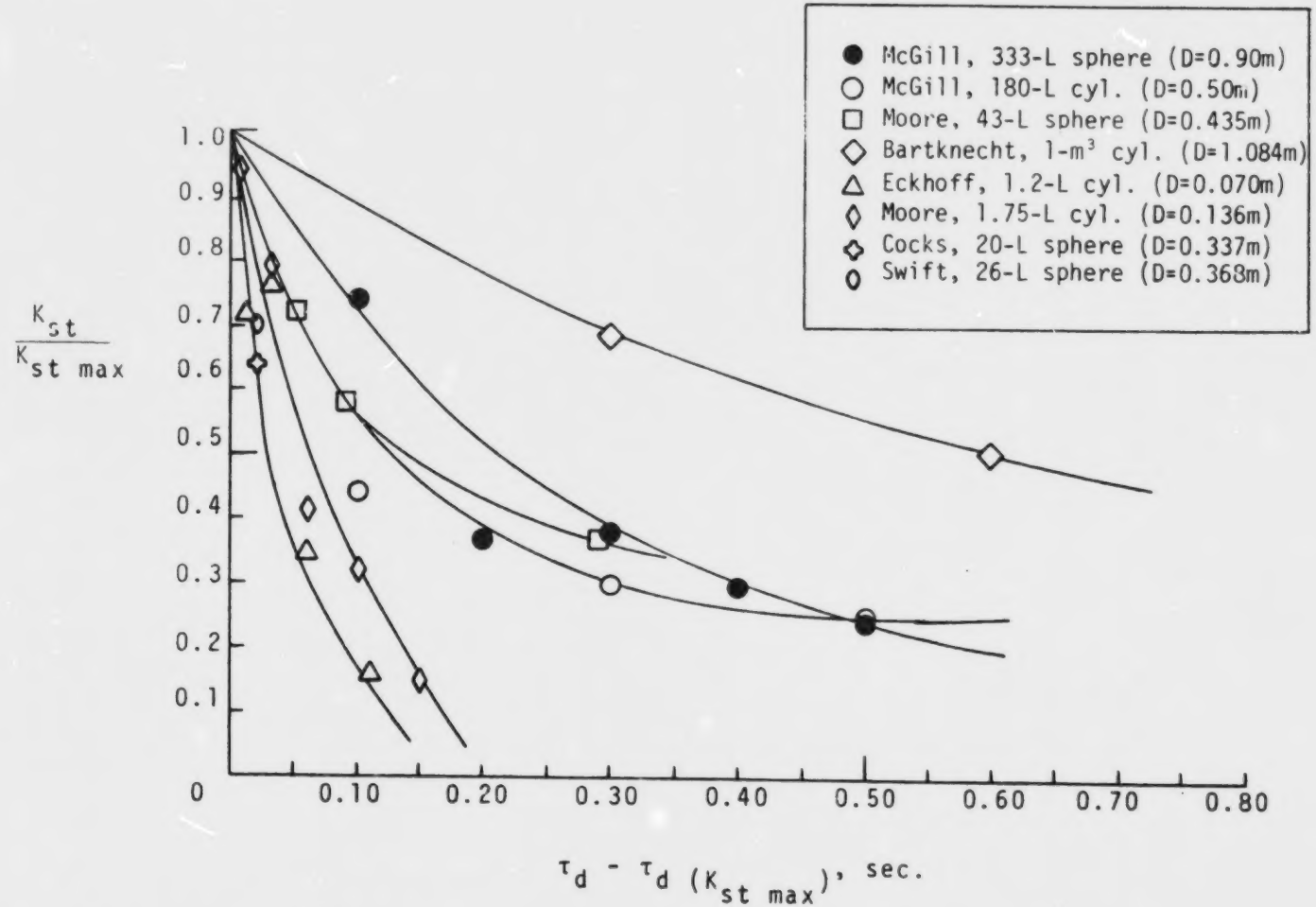

FIGURE 9

Figure 10 - MAXIMUM OVERPRESSURE vs. AVERAGE CONCENTRATION

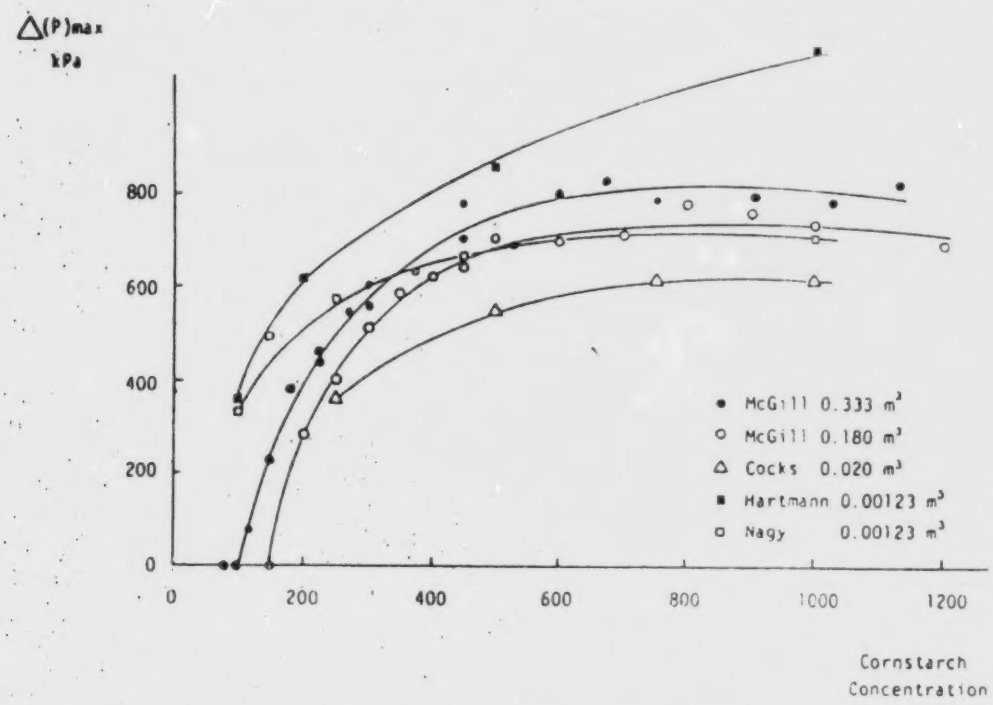

Figure 11 - (K)st vs. AVERAGE CONCENTRATION

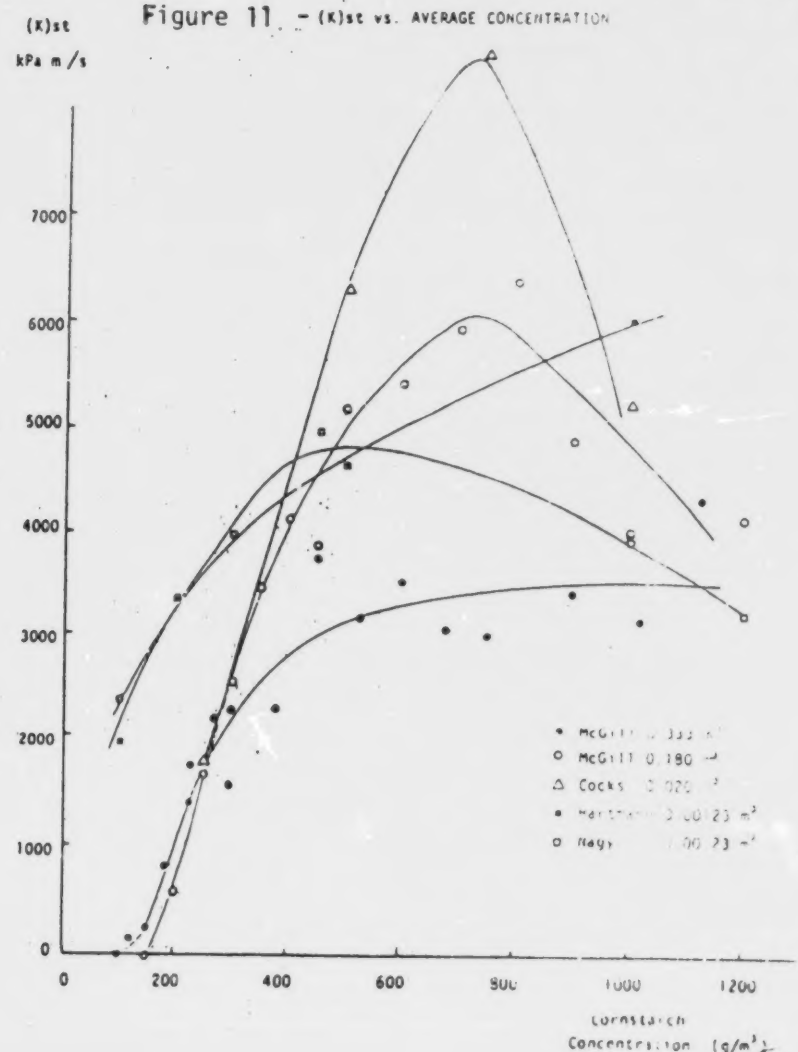

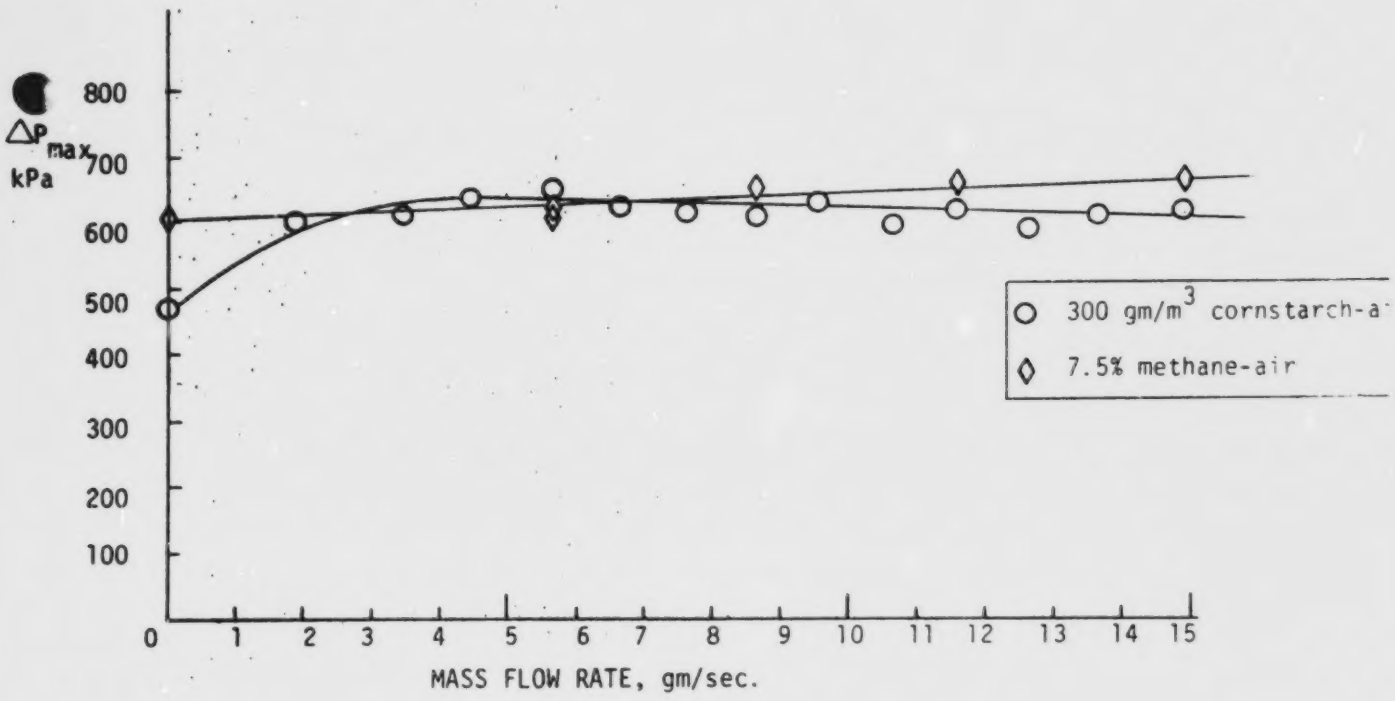

Figure 12- Variation of maximum pressure with jet flow rate in 333 liter sphere

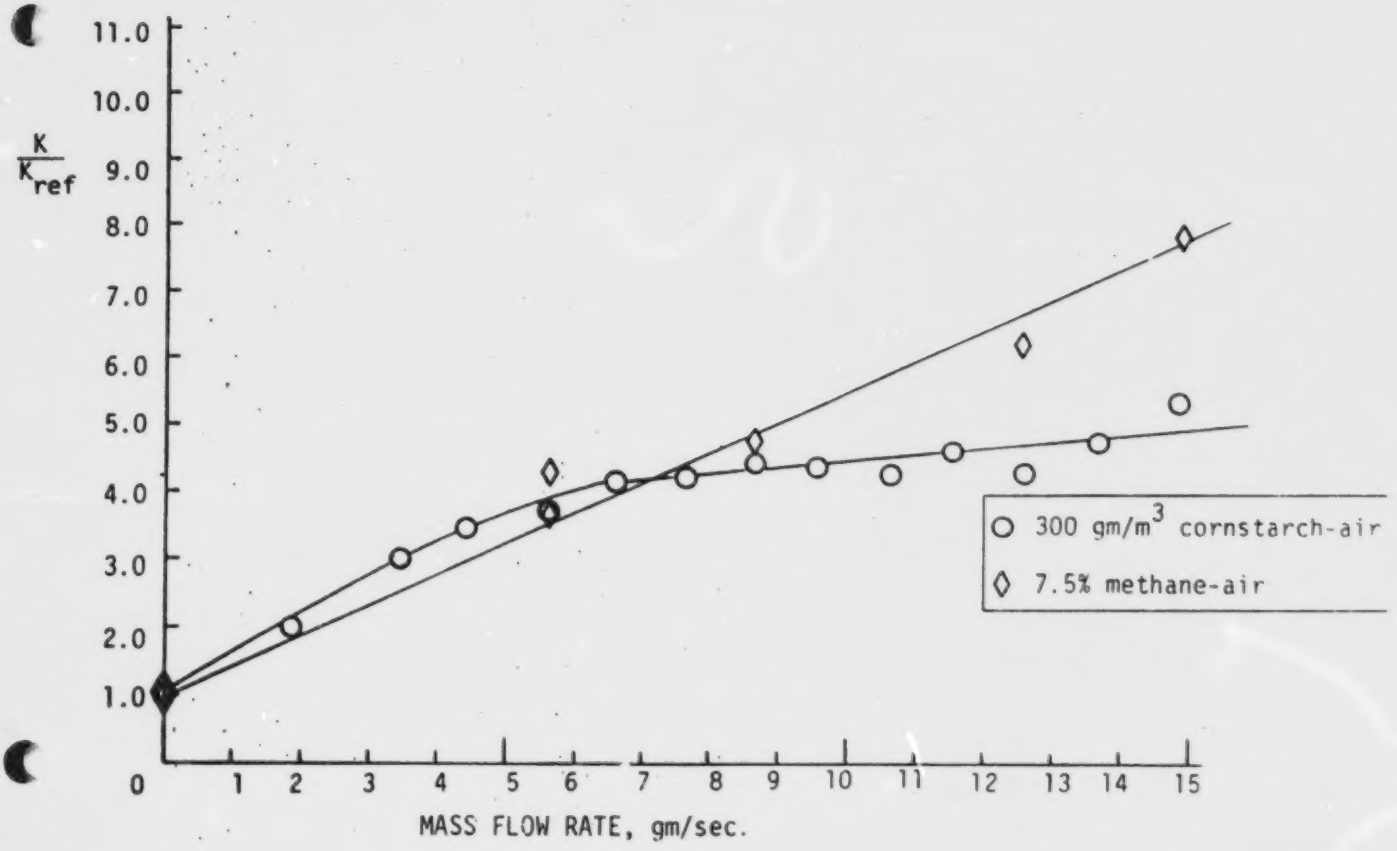

Figure 13 - Variation of K factor with jet flow rate in 333 liter sphere

Figure 14 - Variation of maximum pressure with jet flow rate in 180 liter cylinder

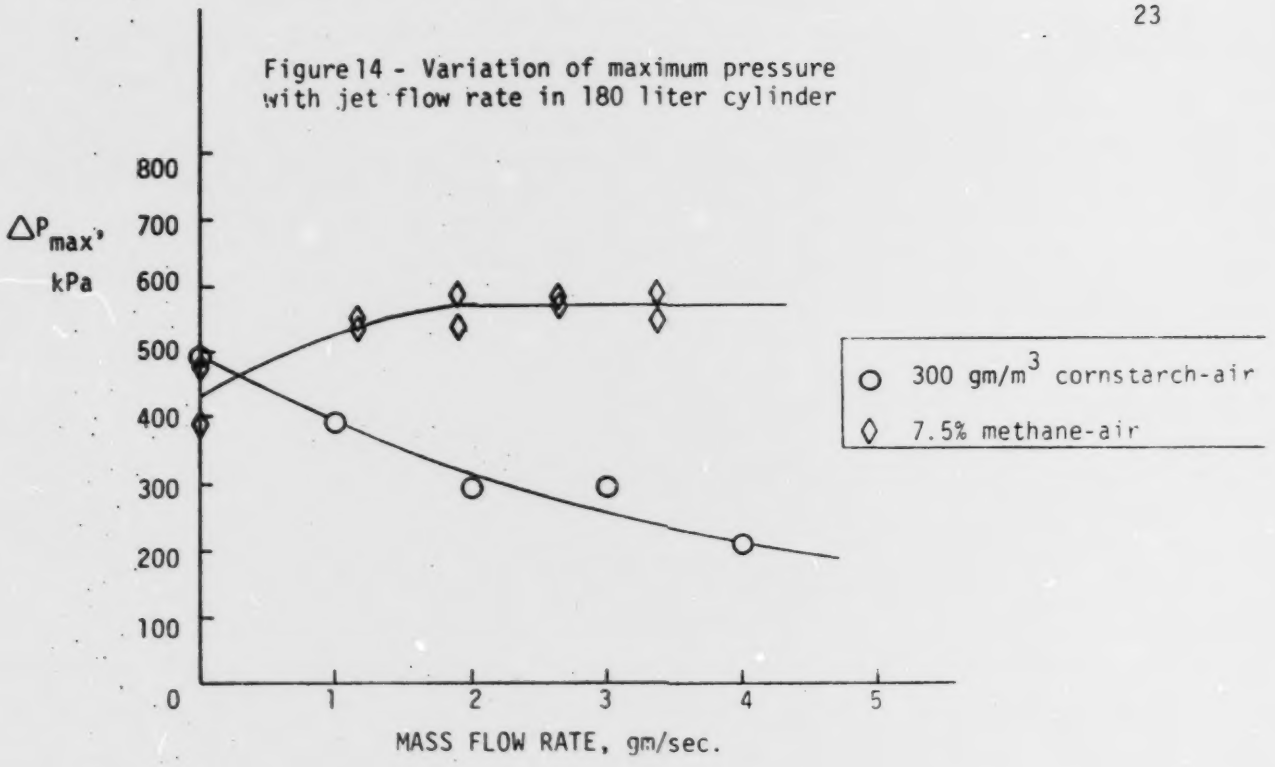

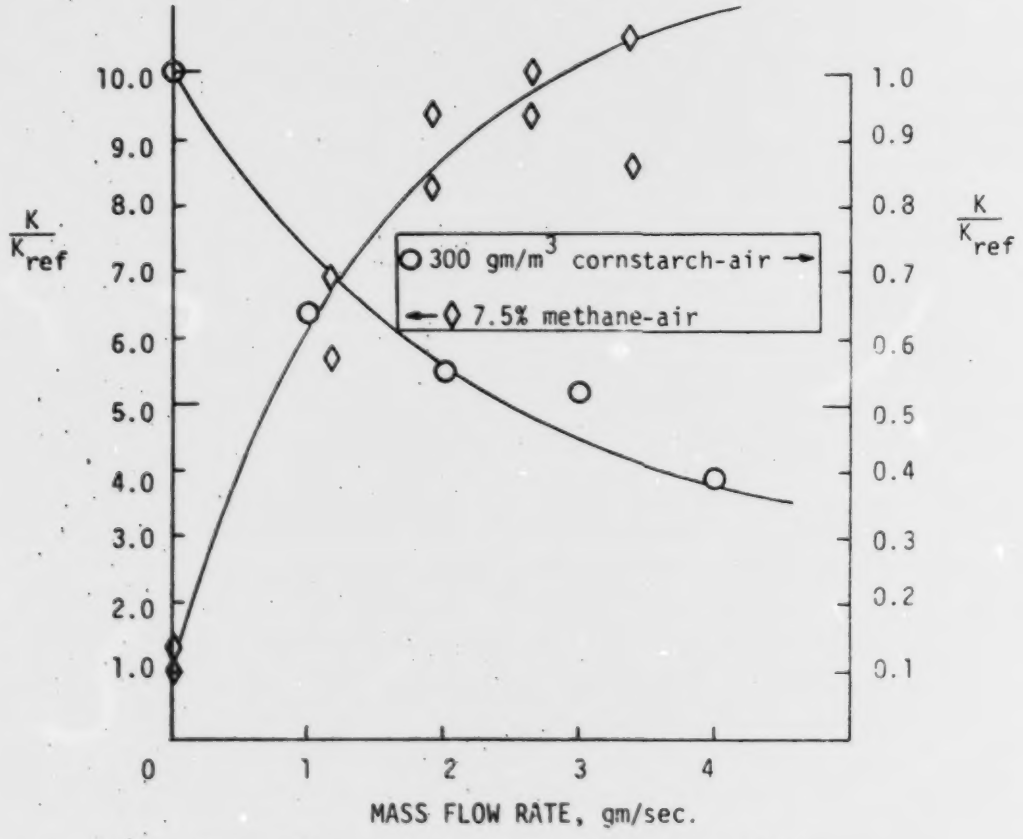

Figure 15- Variation of normalized K factor with jet flow rate in 180 liter cylinder

TABLE I. LENGTH SCALES INVOLVED IN TURBULENT DUST FLAME PROPAGATION

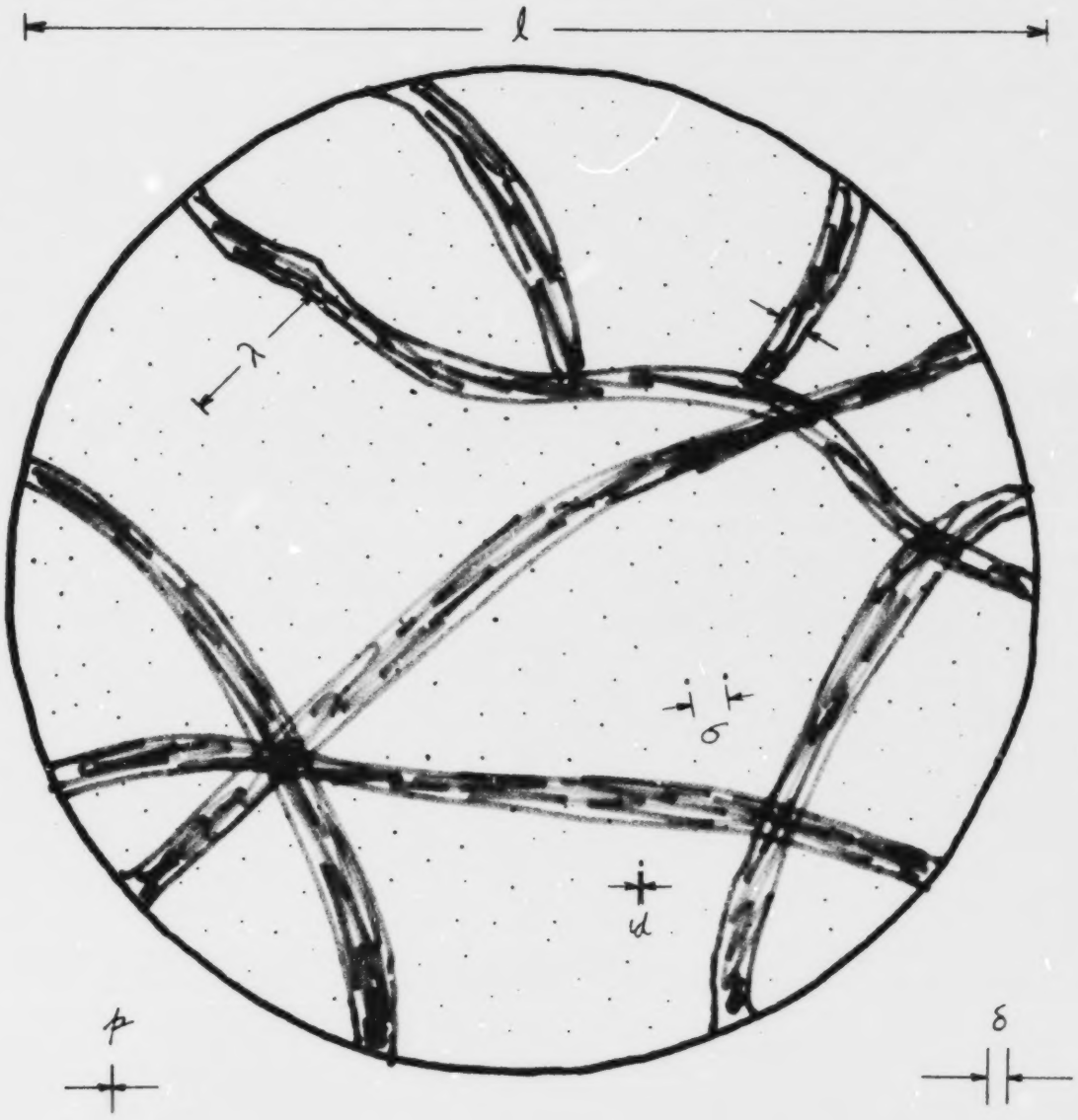

LENGTH SCALE	SYMBOL	ORDER OF MAGNITUDE	COLOR
INTEGRAL LENGTH SCALE	ℓ	10^{-2} m	BLACK
TAYLOR MICROSCALE	λ	10^{-3} m	BLACK
KOLMOGOROFF SCALE	η	10^{-4} m	YELLOW
PARTICLE SIZE	d	1.5×10^{-5} m	RED
INTER-PARTICLE SPACING	σ	1.5×10^{-4} m	BLACK
GASEOUS LAMINAR FLAME THICKNESS	δ	10^{-4} m	BLACK
MOLECULAR MEAN FREE PATH	p	10^{-8} m	BLACK

TABLE II. TIME SCALES INVOLVED IN TURBULENT DUST FLAME PROPAGATION

TIME SCALE	SYMBOL	DEFINITION	FORMULA	ORDER OF MAGNITUDE
IGNITION TIME	τ_{ign}	Period between ignition of exploding wire and onset of pressure rise.	--------	10^{-1}
PRESSURE RISE TIME	τ_{pr}	Time between zero pressure and maximum pressure.	--------	2 x 10
EXPLOSION DURATION	τ_{exp}	Period between ignition of exploding wire and attainment of P_{max}.	$\tau_{ign} + \tau_{pr}$	3 x 10
EXPERIMENTAL HEAT LOSS TIME	τ_{hl}	Period of the exponential decay of the temperature of combustion products.	$\left[\frac{-1}{\Delta P}\left(\frac{dP}{dt}\right)\right]^{-1}_{P_{max}}$	1.5
IGNITION DELAY	τ_d	Delay between dispersion and ignition.	---------	0.5
SETTLING TIME	τ_{set}	Time required for a single dust particle to travel one sphere radius at its free fall velocity.	$\frac{9\mu R}{2R_i^3 \rho_i g}$	5 x 10
VELOCITY RISE TIME	τ_{vr}	Period of the exponential decay of initial slip velocity of a single dust particle.	$\frac{2\rho_i R_i^2}{9\mu}$	10^{-3}
LIFETIME OF MACROSCALE EDDIES	τ_l	Characteristic decay time of integral length scale eddies.	l/μ'	10^{-2}
VISCOUS DISSIPATION TIME OF MACROSCALE EDDIES	τ_{lv}	Characteristic time of viscous dissipation of the integral length scale eddies.	l^2/ν	5 s
LIFETIME OF MICROSCALE EDDIES	τ_η	Characteristic decay time of Kolmogoroff length scale eddies.	$\left(\frac{\nu l}{\mu'^3}\right)^{1/2}$	4 x 10
DISPERSION BOTTLE EMPTYING TIME	τ_b	Time to discharge the dispersion bottle from 150 psig to 15 psig.	$\frac{2.92\,V}{(\gamma-1)\sqrt{RT_i}\,A^2}\left(\left[\frac{p_i}{p_f}\right]^{\frac{\gamma+1}{2\gamma}}-1\right)$	3 x 10
MOLECULAR COLLISION TIME	τ_m	Average time between molecular collisions.	p/ν_{RMS}	10^{-1}
EDDY BURNING TIME	τ_e	Time required for the combustion of a single eddy at the laminar burning velocity.	λ/S_1	10^{-2}
DUST PARTICLE TEMPERATURE RISE TIME	τ_{tr}	Period of the exponential decay of the temperature difference between a single dust particle and the surrounding air.	$\frac{\rho_i R_i^2 c_p}{3k_a}$	3 x 10
FLAME RESIDENCE TIME	τ_f	Time spent in the reaction zone of a dust-air flame.	δ/S_1	10^{-2}

APPENDIX B

An Experimental Study of Hybrid Explosive Dust-Gas-Air Mixtures

An Experimental Study of Hybrid Explosive Dust-Gas-Air Mixtures

by

Neil H. Craft

Department of Mechanical Engineering
McGill University
Montreal, Canada

March 26, 1985

ABSTRACT

This report describes an experimental investigation into hybrid dust-gas-air explosions. It is well known that admixture of flammable gas will enhance the burning rate and maximum explosion pressure of a dust-air mixture. The objective of the present work is to elucidate the major influence of the flammable gas when present at various concentrations.

A brief review is given of existing experimental evidence which indicates that a dust-air flame progagates in the volatiles generated in the preheat zone and reaction zone of a thin flame which resembles a premixed gas flame. Thus, the behaviour of a dust-air flame should resemble that of a premixed gas flame.

A long horizontal tube constant volume bomb was developed with a novel dust dispersal system. Experiments were conducted with fine cornstarch dust, methane and hydrogen gases. The burning rates and maximum explosion pressures for various hybrid compositions are compared to those obtained from single component mixtures. The results indicate that the flammable gas added to the dust-air mixture acts to increase the flame temperature and hence the burning rate in a manner similar to increasing the equivalence ratio of a lean gas mixture. Excess dust present in a rich hybrid mixture is shown to act as a thermal sink, similar to an inert dust, reducing the flame temperature, and hence retarding the burning rate.

LIST OF SYMBOLS AND ABBREVIATIONS

C	-	Frequency factor in equation (8), [s^{-1}].
$\bar{C}_v$	-	Specific heat capacity at constant volume, [kj/kg-^{0}k)
d	-	Diameter [m, μm]
E	-	Activation energy [kcal/mole]
E_{min}	-	Minimum ignition energy
G	-	Gas concentration [%(vol)]
LEC	-	Lower explosible concentration, [g/m^3, %(vol)]
LHT	-	Long horizontal tube
M_p/M_r	-	Number of moles pf products to mactants
P	-	Pressure, [bar]
P_o	-	Initial atmospheric pressure [bar]
P_e	-	Maximum explosion pressure in absolute units [bar]
ΔP_e	-	$P_e - P_o$
$\Delta \bar{P}_e$	-	$\Delta P_e/P_o$
(dP/dt)	-	Rate of pressure rise, [bar/s]
Q	-	Heating value of fuel, [kJ/kg]
R	-	Universal gas constant, [kcal/kmole-^{0}K]
R_f	-	Flame speed with respect to laboratory reference frame, [m/s]
S_L	-	Laminar burning velocity, [m/s]
T	-	Temperature, [^{0}K]
T_o	-	Initial gas temperature [^{0}K]
T_e	-	Equilibrium temperature of combustion products of constant volume explosion [^{0}K]
T_f	-	Flame temperature at constant pressure [^{0}K]
ΔT_f	-	$T_f - T_o$ [^{0}K]
ΔT_e	-	$T_e - T_o$ [^{0}K]

W	-	Dust concentration, [g/m^3]
W_s	-	Apparent stoichiometric dust concentration [g/m^3]
x	-	Distance downstream from ignition [m]
α	-	Thermal diffusivity, [m^2/s]
γ_b	-	Ratio of specific heat capacities in burnt products
δ	-	Flame thickness [mm]
ρ	-	gas density [kg/m^3]
ϕ	-	Equivalence ratio
τ_b	-	Burnout time of explosion, [s]
τ_{ch}	-	Chemical time scale of gaseous flame, [s]
τ_{th}	-	Thermal time scale for particle heat up, [s]

TABLE OF CONTENTS

DESCRIPTION		PAGE
I.	INTRODUCTION	1
II.	GENERAL COMMENTS	6
	1. Review of Research into Hybrid Combustion	6
	2. Physical Model for Dust Flame Propagation	9
III.	EXPERIMENTAL CONSIDERATIONS	16
	1. Apparatus	16
	2. Dust Properties	18
	3. Ignition System	19
	4. Measurement of Burning Rate	20
IV.	EXPERIMENTAL RESULTS AND DISCUSSION	22
	1. Flammability of Methane-Air Mixtures	22
	2. Flammability of Cornstarch-Air Mixtures	23
	3. Flammability of Hybrid Starch-Methane-Air Mixtures	28
	4. The Effect of Flame Temperature Upon the Burning Rate	32
	5. Effect of Inert Dust Upon Methane-Air Flames	40
	6. Effect of Hydrogen Upon a Lean Starch-Air Flame	42
	7. On the Lean Flammability Limits of Hybrid Mixtures	44
V.	CONCLUSIONS AND RECOMMENDATIONS	47
	REFERENCES	50
	LIST OF FIGURES	53
	FIGURES	56

I. INTRODUCTION

When an explosion occurs in an environment containing combustible dusts and flammable gases, it is called a Hybrid Explosion. It is now generally recognized that the potential hazard of a hybrid explosion can be greater than that of either component considered individually. The coal mining industry was the first to recognize the significance of hybrid explosions when it was realized that small amounts of methane gas, known as "firedamp", greatly enhanced the violence of an ensuing coal dust explosion. As the demands for energy continue to increase and as there is a growing tendency to reduce our dependence on petroleum, coal mining has shifted from shallow mines to deeper ones, with the result that they are increasingly "gassy". Although laws generally prohibit the buildup of flammable gas concentrations beyond fifty percent of the lower flammability limit, the gases are still present in small amounts and contribute to the explosion hazard.

Also with the idea of conserving energy many large municipalities have established facilities for converting light industrial and commercial refuse into energy by combustion. The primary process in this operation is to shred the finely divided materials containing: plastics, wood and paper products, metals and food products. This process can produce massive amounts of dusts from all these materials. Also, flammable vapours may be present as a result of disposed containers. Coupled with the explosible dusts the vapours can contribute to large scale explosions in these shredder machines.

Hybrid explosions occur in the plastics industry as well, where powdered plastics are often present along with solvent vapours in the manufacturing operations and stored near solvent vapours during transportation. In some operations in the grain industry, extraction plants producing large quantities of flammable vapours are located near grain storage silos. Explosions in these facilities can involve large quantities of both solid and gas phase fuels. Typical examples of flammable mixtures include: hexane with soya bean meal, pentane with styrene and polysterene, vinyl chloride with polyvinyl chloride and cyclopentane with wood.

Most industrial facilities are not designed to withstand the pressures developed by even weak dust explosions. Thus these places are equipped with various types of explosion mitigation schemes of which the three most common are: relief venting whereby large vents open to exhaust expanding gases before significant overpressures develop; explosion barriers whereby powdered chemical flame suppressants are dispersed into the path of a propagating flame and high speed valves used to isolate an explosion inside the chamber in which it originates when that chamber is a very sturdy structure. To effectively design an explosion protection scheme based on any of these techniques it is essential to be able to anticipate the potential overpressure that may develop and the burning rate as well.

In order to be able to supply industry with accurate guidelines for protection from dust and hybrid explosions, a knowledge of the fundamental mechanisms which govern the phenomenon is needed. Currently, the exact mechanism by which combustion of the solid and gas fuels occurs is not well understood. This is because as yet the fundamental nature of dust combustion only is not well understood. Only in the past two decades has there been a significant amount of research

into the nature of dust combustion. Hitherto, researchers have not been able to propose a satisfactory comprehensive model which can predict the flame speed and rate of pressure use in a closed vessel using primarily the composition of the dust as the initial condition. Added to this the complication of reactions occurring uniformly in the gas phase as well as heterogeneously near the particle surface and the problem becomes much more complicated.

The present work describes an investigation of the influence of admixed flammable gas to fully confined dust explosions. A long horizontal tube is filled with a dust-gas-air suspension and ignited at one end. The maximum explosion pressure and the burning rate of different dust-gas compositions are examined to determine the relative explosion hazard of the hybrid mixtures as compared to the single component mixtures. The data are analyzed to determine the predominant factors which are altered by the admixed flammable gas.

In the subsequent chapter details of pertinent hybrid results are presented. These results are concerned mostly with the influence of admixed gas on the burning parameters of dust-air mixtures. There is also a review of some important results concerning dust combustion which lead to the development of a physical model for the propagation of a dust flame through the volatiles generated in the preheat and reaction zones. This model is later used to interpret and give physical meaning to the present results.

Chapter III provides details of the experiment and procedure used, including a description of the dust dispersal system. The appealing properties of cornstarch for use as an experimental dust are discussed. The ignition system used and the method of measurement of the burning rate are also presented.

Chapter IV presents the experimental results and the proceeding discussion. The flammability characteristics of the vessel are first discussed in relation to homogeneous methane-air explosions in order to determine the effects of non-adiabacity and the turbulence generated by the dust dispersal system. The flammability data for dust only mixtures are presented in comparison to other investigators to establish confidence in the dust dispersal system and the experimental procedure. Furthermore, this data serves as a basis for comparison with the subsequently done hybrid tests. Various combinations of cornstarch and methane concentrations were tested to determine the maximum explosion pressures and burning rates. Following this, the effect of the flame temperature upon the burning rate is established. It is first discussed with respect to methane explosions for which the burning rate is known to depend upon the flame temperature. This analysis is extrapolated to dust mixtures and then to hybrid dust-gas mixtures. It is shown that this analysis is fairly simple and indicates that dust and hybrid dust-gas mixtures exhibit a temperature dependence similar to the methane-air explosions. These results give further credence to the idea that dust flames propagate mainly through the volatiles generated ahead.

Cornstarch-hydrogen-air tests are presented as well to determine the influence of the chemistry of the admixed gas. It has previously been concluded that the influence of gases with a high normal burning velocity are less severe

than the influence of methane [1]. According to the present model, if the admixed gas is by itself and non-flammable, then the burning rate of the hybrid mixture will be determined by the burning rate of the mixture of volatiles and admixed gas. If the gas is itself flammable then it is more relevant to discuss the influence of the dust upon the gas flame.

Finally, the flammability limits for hybrid mixtures is discussed briefly and the usefulness of the present apparatus for determining these limits is also discussed.

Chapter V outlines the significant conclusions arrived at in the present study. Also a few recommendations are made for future work in the field of hybrid combustion.

II. GENERAL COMMENTS

1. Review of Research into Hybrid Combustion

Historically, much of the research into the dust explosion phenomena has been concerned with flammability or explosibility limits since most explosion prevention schemes involve minimizing airborne dust concentrations. In the past forty years, thousands of materials have been tested for their lower explosible concentration in laboratories the world over. Coal dusts have probably undergone the most scrutiny with investigators examining the effects of particle size, composition, and initial temperature as well as ignition energy requirements [2,3]. Similarly, of all possible hybrid combinations coal-dust-methane mixtures have attracted the most attention.

It is now well known that an explosible hybrid mixture can be formed despite that the concentrations of the individual components, dust and gas, are themselves below the explosibility limit. Furthermore, the lower explosibility limit for hybrid mixtures can be estimated by a modified form of Le Chatelier's principle which is normally applied to premixed gases. Simply:

$$\frac{W}{(\overline{LEC})\text{dust}} + \frac{G}{(\overline{LEC})\text{gas}} = 1 \qquad (1)$$

where W and G are the dust and gas concentrations for the hybrid limit mixture, (LEC)dust and (LEC)gas are the lower explosible concentrations of the dust alone and gas alone respectively. The values reported in the literature for the lower explosible concentration of coal dust contain a tremendous amount of scatter with values ranging from $5 g/m^3$ to $300 g/m^3$ [2]. This is due to the strong apparatus dependency of this parameter and the widely different apparatus used. However,

this linear, or in some cases nearly linear, decrease in the explosible dust concentration with gas concentration has been observed in closed volume bombs [4,5], as well as horizontal and vertical open channels [6,7]. These results demonstrate conclusively that the burning mechanisms of the two fuels are intimately coupled.

There are comparatively few investigators concerned with the problem of turbulent flame propagation in hybrid mixtures. It is, however, generally agreed upon that the presence of small acounts of flammable vapours in the atmosphere, even below the lean flammability limit, can significantly enhance the burning rate of a combustible dust-air mixture. Furthermore, the vapours affect all dust concentrations from very lean to rich. Nagy [5] found that there is an optimum methane concentration for each particular coal dust-air mixture, to generate each the maximum explosion pressure and the maximum burning rate and these need not be the same. For example: with $500g/m^3$ coal dust the maximum rate of pressure rise occurs with 4% methane however the optimum explosion pressure occurs with no methane at all.

Similarly Bartkneckt [1] reports results from tests in a $1m^3$ vessel with propane gas and different dusts. In general it was found that the optimum propane concentration in terms of the explosion pressure is close to the lower flammability limit of propane (2%), whereas the maximum burning rate occurs with stoichiometric propane air. These results appear to be different from those of premixed gas explosions in which the maximum burning rate and explosion pressure usually occur at the same concentration which is near stoichiometric.

In a premixed gas, altering the fuel air composition will affect the flame temperature which will in turn affect the rate of energy production. In

hybrid explosions the change in flame temperature is more difficult to assess and so there are no correlations available between the measured flame temperatures and burning rates. If the burning rate for the hybrid mixture is solely dependent upon the flame temperature, as is a gaseous flame, then why are rich dust air flames also affected by admixture of methane? Presumably, admixture of methane to a rich fuel-air mixture should not increase the flame temperature. Both closed bomb [1,5,8] tests and laminar burner experiments [9] indicate that rich dust air flames are affected by admixture of methane.

Physical processes also may be important in determining the influence of the admixed gas. Ballal [10] reports that the laminar burning velocity of fine particles is more affected than the burning velocity of the coarse particles. From this, the author concludes that admixture of flammable gas has a greater effect upon the kinetically controlled burning processes which dominate combustion of fine particles as opposed to the diffusional processes which dominate combustion of large particles.

There lacks data, however, from which it may be shown conclusively that the role of admixed gas acts one way or another. There is not sufficient information to determine to what extent admixture of flammable gas may affect the diffusional and kinetic dominated process for dust combustion which must be known to be able to predict the maximum effect of the gas upon the overall burning process. This is partly a result of the fact that the nature of dust combustion is only recently (twenty years) being investigated in a fundamental manner.

2. Physical Model for Dust Flame Propagation

To be able to properly analyse and interpret experimental results of hybrid explosions one must first have a physical model of the burning process of a turbulent dust explosion. To date, however, there are no unified theories which can accurately explain qualitatively nor quantitatively all the processes involved, from the preheating zone through the reaction zone. It is possible though to establish some understanding of the basic phenomena from a composite of the many researchers' works on the macroscopic features of the flame structure and on the microscopic features of individual particle burning. It has been well documented that a dust flame-propagates as a wave, with a preheat zone followed by a reaction zone of some thickness δ in which heat released causes the temperatures within the zone to rise as shown below. The heat released within

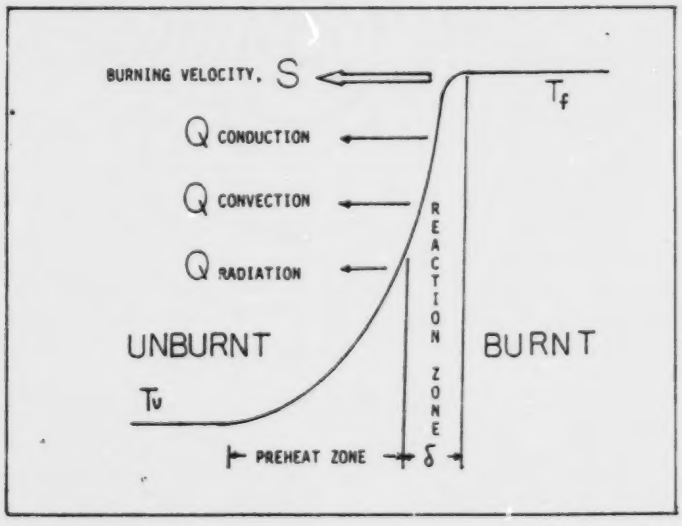

the reaction zone is transported forward by conduction, convection and radiation, the relative importance of each mode will depend upon the nature of the dust, particle size, cloud density and turbulence levels of the mixture. The disagreement amongst current researchers on the importance of each transport mechanism makes it impossible to rule in favour of any one in particular.

In order to further elucidate the structure of a dust flame some of the available experimental evidence will be examined. This evidence concerns some of the fundamental parameters associated with laminar flame propagation: the laminar burning velocity, lean flammability limits, minimum ignition energy anf flame thickness. The dust flames being considered here involve those particles which emit significant amounts of volatile vapours upon being heated. This group includes bitumous coals, lignites, vegetable grains, powdered foodstuffs and plastics.

It is well known that for premixed hydrocarbon gases the flame speed versus gas concentration curve has the shape of an inverted "u", as shown below, with the peak value occurring very close to the stoichiometric concentration. The burner results of Smoot et. al. [9] for fine coal dust particles shows similar behaviour. With very fine particle sizes (diameter $d_p \cong 9\mu m$) the inverted "u" shape is clearly evident, with the maximum laminar burning velocity near 33cm/s.

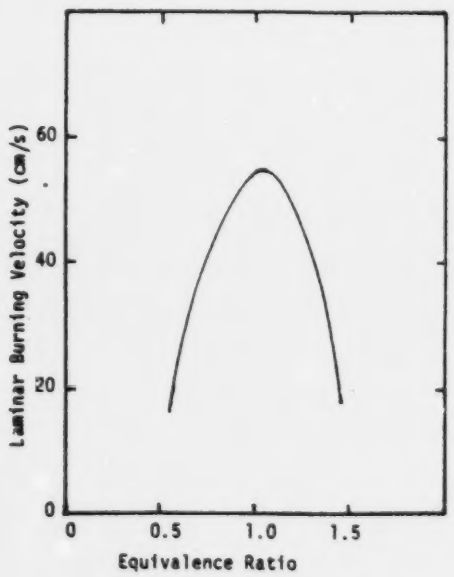

With larger particlesizes the curve has the same trend as with the fine particles except the maximum value decreases and the curve broadens. Three different types of coal were tested and all three produced maximum burning velocities near 30cm/s and 35cm/s for identical particle size distributions. Other investigators also report laminar burning velocities for coal dusts between 20cm/s and 70cm/s in a variety of different apparatus [10,11,12]. These values are well within the range of many hydrocarbon gases.

Hertzberg [13] has correlated the lean flammability limits for various dusts with the volatile content from rapid pyrolysis tests. Experiments with low and high volatile coals, polyethelyne, anthracite, gilsonite and methane indicate that the heating values of volatiles generated by a lean limit mixture are almost uniform at 11.8 kcal/mole. This value is also similar to that measured independently for other gaseous hydrocarbons [14]. Because of the similar heating values of the volatiles in the limit mixtures the flame temperatures for these mixtures are also close to that observed for hydrocarbon gases, namely 1500^{0}k. These lean flammability limits, measured in an 8 liter bomb agree well with those reported in reference [9]. Thus, from these experiments it appears that the contribution of carbon or char residue oxidation to the heat released in a lean mixture is not significant.

Other evidence of combustion of coal particles occurring mainly in the volatiles comes from the direct observations of Seeker et. al. [15] and McLean et. al. [16]. In these experiments pulverized coal was injected into a lean methane air burner flame. Both investigators noticed, on open shutter photographs, that the particles ignited behind the gas flame after a brief period of about 2-5 msec. This was followed by a period of intense yet diffuse

luminescence lasting 2-3 msec followed by a longer period of less intense but sharply defined radiating streaks. Rapid exposure shadowgraphs and schlieren photographs revealed that initially there is a rapid evolution of volatiles which burn vigorously followed by a longer period during which char particles glow due to heterogeneous oxidation.

Essenhigh and Howard [17] measured the volatile content of the char samples collected at various points upstream and downstream of a stabilized burner flame and found that it decreased slightly before the visible flame front and subsequently quite rapidly within the flame zone. In fact, the ratio of volatile matter to fixed carbon decreases to 18% of its original value in the char particles. Subsequent analysis revealed that most of the mass lost during combustion occurs by devolatilization not direct heterogeneous combustion. Methane and hydrogen gas concentrations have actually been measured in coal dust burner flames [18].

Currently there is a large amount of conflicting data concerning dust flame thickness for state of the art combustion experiments in the literature. Values from 5mm to several cm are reported for similar mixtures. This is a result of a wide variety of experimental apparatus, particle sizes, and dust dispersion techniques. Also it may result from a lack of a clear definition of the term flame thickness. Buksowitz and Wolanski report that an upward propagation, lean limit lignite-air flame consists of a thin flame front in which the temperature gradient is steep and a thick flame region where reactions continue to occur for a long period of time. These conclusions are based on observing a steep temperature rise of about 7×10^6 ^{0}k/s or 100^0 k/mm in front of the visible flame so that the maximum temperature occurs 1.5 cm

after the start of the temperature rise. This is followed by a longer period during which the gas temperature remains elevated for up to 175 msec before significant temperature drops are observed. This is the region in which the bright particles and particle streaks are observed. Based on the temperature increase, the lower density exhaust gases move at a velocity 5 times that of the leading front so that visible zone corresponds to a 5 x 0.7 m/s x 0.175s=0.6 m thickness.

Slezak [11] also reports a "bushy" flame structure that appears to be at least 15 cm thick. However, thermocouple (1 mil) traces from different points downstream of the ignition indicates that the temperature rise occurs within a much smaller region, perhaps a few millimeters. Other burner flames indicate that most reactions are completed just a few millimeters from the ignition point[9,18]. Thus it appears that the burning rate of the dust particles are capable of producing quite thin flames.

However, the thickness of a gas flame is of the order of 0.1 mm, about 100 times smaller than the 1 cm dust flame thickness. Additional evidence supports the notion that the dust flame may be thinner than the observed 1 cm thickness [19]. From thermal flame theory the minimum ignition energy, E_{min} can be shown to be proportional to the cube of the flame thickness, δ. If the constant of proportionality is approximately the same for the dust and gas, then:

$$\frac{(E_{min})dust}{(E_{min})gas} \simeq \left[\frac{\delta_{dust}}{\delta_{gas}}\right]^3 \qquad (2)$$

E_{min} for many dust-air mixtures have been shown to be of the order of 10^{-3} to 10^{-2} Joules as compared to 10^{-4}J for premixed gas [20]. In some cases for sulfur and fine aluminum flakes E_{min} is as low as 10^{-4}J as well. Based on these values $\delta_{dust}/\delta_{gas}$ should be of the order of $10^{1/3}$ or $100^{1/3}$ (2.1 or 4.6). Also from thermal flame theory the laminar burning velocity, S_L, can be approximated as $S_L = \alpha/\delta$ where α is the thermal diffusivity of the gas, if the reactions are assumed to take place mostly at the flame temperature. If S_L is of the same order as that for gas flames and the gas diffusivity is also similar, then one would expect that δ would also be of the same order as for gas flames. Thus the actual measure of the dust flame thickness might be over-estimating the effective thickness.

With the evidence presented indicating that combustion of organic dusts such as constarch and coal proceeds mainly in the volatiles, it is possible to speculate on the physical model of this phenomenon. Particles entering the preheat zone of the flame are heated by conduction, convection and radiation from the flame front. As they are being heated small amounts of volatiles are released, primarily from the finer particles(a). At some critical temperature the volatiles surrounding the particles will ignite(b). The rapid beat release will be conducted to the particle and cause the particle to generate a more vigorous release of volatiles in which the gaseous flame stablizies(c). Proceeding this the fixed carbon or char (if any remains) may continue to glow due to slower heterageneous reactions that occur within the remaining oxygen(d).

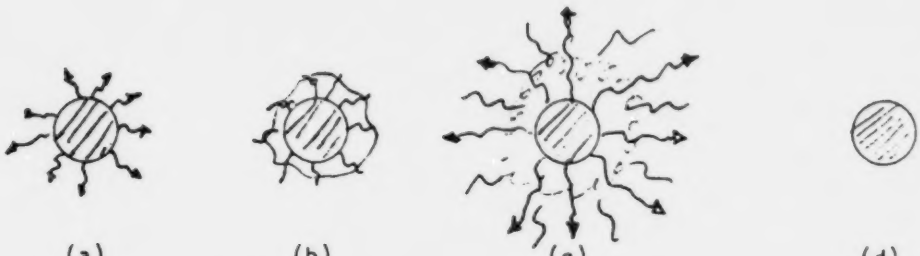

(a) (b) (c) (d)

It is the rapid combustion of volatiles pictures in (c) that occurs in the distinct reaction zone which contributes most of the energy released in the flame. It has also been shown that for very fine particles the surface oxidation of the particle may be considerably enhanced by the presence of high concentrations of O, OH and H radicals in the gaseous zones [21]. These processes can be rapid enough to occur largely within the thickness of a gaseous flame. Subsequent combustion of the larger particles behind this flame front may occur but will unlikely influence the burning rate of the front, which is controlled mainly by the steep gradients of temperature and species within.

As the dust flame propagates predominantly through the volatile vapours generated ahead of it, the burning rate is probably sensitive to the same parameters as is a gaseous flame. It is unlikely that admixture of a gaseous fuel to the unreacted mixture significantly alters the diffusivity of the unburned gas. However, the mixture energetics will change and hence the flame temperature too will change. It is known that the chemical kinetic processes which determine the rate of heat release have an exponential dependence upon the flame temperature. The temperature effect upon the burning rates of gas-air, dust-air and hybrid dust-gas-air mixtures is examined in more detail in Chapter IV.

III. EXPERIMENTAL CONSIDERATIONS

1. Apparatus

The experiments reported in this text were conducted in a long horizontal tube (LHT), closed at both ends, with an internal volume of 156 liters. The tube measures 2.18 m (7 ft.) long and has an internal diameter of 0.30 m (1 ft.) forming an aspect ratio of L/D = 7. The tube is constructed of ordinary steel of 12 mm thickness. There are six threaded ports located along a single longitudinal axis spaced 0.3 m apart in which diagnostics can be mounted, as well as gas flow inlets. An additional port is located 100 mm from one end (ignition end) in which the igniter may be mounted. At the opposite end a valve is mounted on the end flange to exhaust combustion products.

To create a uniform dust cloud within the vessel a novel dust dispersion system was designed. A nominal mass of dust is spread uniformly along a 5 cm x 5 cm V-channel 2.0 m long. The V-channel is mounted inside the tube, 4 cm above the tube floor. Prior to ignition the dust is dispersed by twenty impulsively started jets emerging from a perforated shock tube which runs the central axis of the LHT. The perforated shock tube is a 38 mm diameter copper tube with 4.0 mm holes drilled every 100 mm and is mounted to the flange near the ignition end. The holes are aligned so that they directly oppose the V-channel and the jets impinge directly upon the dust. The shock tube is driven by a $63 \times 63\ mm^2$ tube, 1 m long mounted on the external side of the end flange. The driver and driven sections are separated by a plastic diaphragm. The driver section is pressurized to 10 bars, containing the same gas mixture as the test volume.

The gas mixture in the test volume was prepared by flow-through method, displacing five to six times the volume of the vessel within 25 minutes to ensure a good mixture. The gas mixture was formed by flowing extra dry laboratory air and commercially pure methane through a pair of calibrated rotameters into a small mixing chamber then to the vessel. The mixture in the driver section was prepared by filling the methane and air to the appropriate partial pressures.

Instrumentation consists of a single PCB piezoelectric pressure transducer (5.0 mV/psi) with very high frequency response (MHz) located at $x = 1.22$ m where x is the distance measured from the ignition end flange. Two ionization probes protruding 63 mm from the tube wall are located at $x = 0.91$ m and $x = 1.83$ m respectively. These measure time of arrival of the flame at these locations. The measurements are recorded on an oscilloscope and permanent photographic records are made of these. A schematic of the apparatus is shown in Figure 1.

After the gas mixture has been prepared and the dust loaded into the vessel, the driver section is pressurized. The test begins when the diaphragm between the driver and driven sections is ruptured by a pneumatically driven plunger. The stress waves generated in the tube by the bursting diaphragm are registered by a piezoelectric crystal attached to the tube. The electronic pulse is delayed electronically, then the delayed pulse is used to turn on the ignition system. The delay time used was 85 msec for all experiments.

2. Dust Properties

In the present experiments cornstarch was selected for use as a combustible dust because it has many advantageous properties: a) it is readily available in pure form and in large quantities at a reasonable expenditure; b) the particles have a regular shape and a fairly narrow particle size distribution with an average particle diameter near 15 μm; c) its chemical composition is relatively simple and is representative of many agricultural and carbonaceous dusts; d) it is readily dispersable.

Figures 2 and 3 show some photomicrographs of cornstarch particles and the particle size distribution for a random sample. It can be seen that the particles are nearly spheroidal in shape and do not appear highly porous. The mean particle size based on a frequency average is 14.7 μm and the largest particle size is 30 μm. Normally, such small particles are cohesive and easily agglomerate making uniform dispersion quite difficult. To facilitate dispersion and reduce agglomeration the starch was dried overnight at 70^{0}C and mixed with 1% by mass of fumed silica, a fluidizing agent. This fluidizing agent significantly reduces the weak electrostatic forces which make the particles cohesive and thus reduces agglomeration. In Figure 2 cornstarch particles are shown from samples with and without the fluidizing agent and in Figure 3 the particle size distributions are shown for both samples.

Cornstarch has a simple chemical composition. It is basically a polymer of dextrose molecule shown below. Cornstarch consists of 80% linear

chain polymers (amylose) and 20% branched chain polymers (amylopectin). Typically 300 to 400 dextrose molecules form a chain. The basic chemical formula is $(C_6H_{10}O_5)_n$.

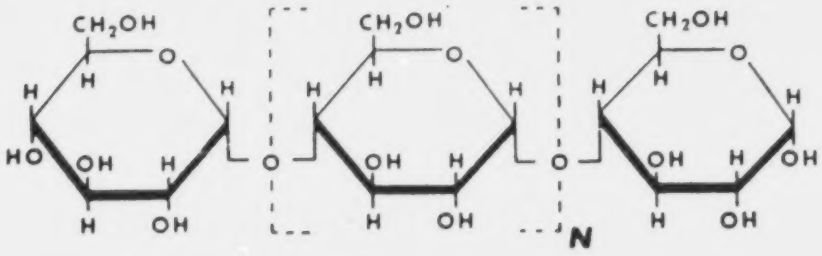

3. Ignition System

In all experiments exploding wire ignition sources were used. Initially, the igniter used consisted of a brass wire 0.076 mm in diameter 25 mm long connected to a 115 VAC source. For mixtures that were more difficult to ignite, the igniter strength was augmented by wrapping ultra-fine zirconium filaments around the brass wire to produce a flash bulb effect. The duration of this ignition source was several times longer than the brass wire alone. For all experiments except where noted otherwise, the mixtures were ignited 100 mm from the tube end, 30 mm from the central axis. This igniter is sufficient for igniting most dust mixtures except near the lean limit at which point the use of chemical pyrotechnic devices such as electric matches might have been preferable. However, as the ultimate lean limit was not the objective of these experiments, it was decided not to radically change the igniter. Although less energetic than high energy capacitive sparks, the present ignition system was found to be preferable. This may be a result of the pressure waves generated by short capacitive sparks which can convect the dust away from the

ignition zone. Furthermore, if the ignition induction period is longer, then the energy deposited by a short spark may be dissipated before the flame kernel is formed.

The ignition delay period was kept constant at 85 msec. This value leads to the most vigorous combustion of a 400 g/m^3 mixture, as shown in Figure 4. The ignition is delayed so that the dust cloud may be properly formed before the mixture is ignited. With excessively long delay times the turbulence generated by the dispersion process decays and the dust begins to settle out of suspension.

4. Measurement of Burning Rate

It is important to have an understanding of the rate at which an explosion will propagate to be able to adequately size relief venting or to employ other explosion mitigation schemes in hazardous environments. Some insight is also given into the complicated phenomena which govern dust explosions. Even though there are several ways by which we can measure the explosion rate, none of them are essentially fundamental for dust explosions. For premixed flammable gases, the laminar burning velocity is a fundamental property of the mixtures dependent upon the fuel type and the initial thermodynamic state of the mixture. However, in most explosible dust-air environments on earth the dust is dispersed by turbulent air motion and moves randomly through the air, rendering it impossible to generate a truly laminar flame as it exists with gaseous fuels. Thus when one measures the burning rate, flame speed or any other characteristic rate one is doing so for a turbulent flame. In most experiments the turbulence parameters are not known. Thus, what is measured is not really fundamental and must be considered in a relative context. That is the burning rates from one mixture may be compared to those of another.

The rate of pressure rise in a closed vessel is proportional to the mass rate of consumption of fuel and hence is an important parameter. It is also readily obtained from the pressure history. However, as the rate of pressure rise (dP/dt) is not constant throughout the explosion there is some arbitrariness in choosing a particular value. For spherical and nearly spherical geometries there is a clearly discernable maximum value of dP/dt. As the flame ball grows the pressure and temperature of the unburned gases increases and so then does the burning rate. Near the vessel wall increased heat losses cause the burning rate to decline. In vessels with large L/D ratios as in the present case when the mixture is ignited near one end, the flame kernel initially grows spherically. As it expands some areas of the flame contact the vessel wall and are extinguished. The flame surface area eventually diminishes and the flame assumes a more planar shape. The characteristic pressure history reflects these changes and is shown in Figure 5. It is important to note that in the present text, dP/dt is measured in the region where the flame is planar. It is felt that the flame in this region is also less influenced by the ignition characteristics.

To measure the actual flame speed with respect to laboratory co-ordinates, the distance between the two ionization probes is divided by the time interval between the signals from these probes. Thus it is a measure of the average flame speed, $\dot{R}_f$, at a location 1.37 m from ignition. If the flame shape is not exactly planar then the measured value may not be a true indication of the flame speed, however, when considered relative to other tests it is useful.

IV. EXPERIMENTAL RESULTS AND DISCUSSION

1. Flammability of Methane-Air Mixtures

Most dust bombs have an aspect ratio (length/diameter) of the order of unity, however, in the present experiments the L/D ratio is seven, hence it was necessary to assess the flammability characteristics. The first tests conducted in the long horizontal tube involved premixed methane-air. The object was to study the burning characteristics at different compositions, the effects of the turbulence generated by the impulsive jets of the dust dispersal system and the heat losses associated with the large surface area to volume ratio of this particular geometry. Figure 6 shows comparative pressure histories of 9% methane, (ϕ = 0.95), burning through a quiescent mixture and a turbulent mixture, where the jet strength and ignition delay time were identical to those used in the later dust experiments. The turbulent burning rate is 4.5 times that of the quiescent mixture as characterized by the burnout time. This results in reduced heat losses to the cold boundary as can be seen by the peak explosion pressure ratios, the turbulent flame obtains 98% of the adiabatic constant volume pressure while the slower flame only 73%. All the other experiments reported in this test were conducted in a turbulent environment.

Experiments were done with successively leaner methane-air mixtures and the resulting maximum overpressures are shown in Figure 7. For the more energetic mixtures the observed $\Delta\bar{P}_e$ is close to the adiabatic value but the discrepancy broadens as the mixture is made leaner. The burnout time (time from ignition to 95% of the peak pressure) for different mixtures and the relation

between the burnout time and heat loss can be seen in Figures 8a) and 8b). The burnout time increases in an exponential manner from 0.11 seconds to 0.41 seconds at 6% methane where the heat loss is 18%. Thus despite the large surface area to volume ratio of cylinders of high aspect ratio, the heat lost to the cold walls by the hot gases is small except for very lean near limit mixtures which burn very slowly.

The observed lean limit in the present apparatus is 6% which is slightly higher than the horizontal propagating limit (5.38%). This is probably due to strong turbulent motion from the dispersion jets quenching the very lean flame kernel.

These gas flame experiments will form a basis to which further experiments with dust-air and dust-gas-air flames can be compared. They also demonstrate the strong dependence of the burning rate upon the mixture composition. Furthermore, the influence of the turbulence generated by the dispersion jets upon the burning rate of a gas flame has been shown.

2. Flammability of Cornstarch-Air Mixtures

Extensive tests were next conducted with cornstarch at various concentrations. The object was to ascertain the flammability characteristics of the dust-air mixture alone first to form a basis for comparison with the hybrid (i.e. dust-gas-air) mixtures studied later. It is also important that the long horizontal tube and accompanying dust dispersal system yield results that are valid and reproducible. This is done by demonstrating that the present results are compatible with other researchers doing similar experiments.

The maximum explosion pressures, $\Delta\bar{P}_e$, obtained in the long horizontal tube, (LHT), with cornstarch-air mixtures are shown in Figure 9 along with results of several other investigators [22,23,24]. It can be seen that the agreement with other researchers is very good, well within the experimental accuracy. That the present results are not lower than those of the other investigators within the range of 200 g/m^3 to 500 g/m^3 is encouraging. Each of the investigators quoted used a different dust dispersal system and the concentrations quoted are based on the nominal loading, that is the mass of dust placed in apparatus divided by the vessel's volume. By far the most adiabatic of these is the large 333 liter sphere, having the smallest surface area to volume ratio, yet the $\Delta\bar{P}_e$ from the LHT are comparable except at very high concentrations. This indicates that the present dispersion system is adequate. Ideally, $\Delta\bar{P}_e$ for an adiabatic explosion of a monodisperse cloud is a function of the chemistry of the dust, the particle size and surface area, the dust concentration and the initial thermodynamic state of the mixture, but in actuality boundary conditions will be significant.

At 200 g/m^3, $\Delta\bar{P}_e$ is 4.5 and decreases rapidly at concentrations below. At 100 g/m^3 no pressure is measured and no burned residue is present after the test. Between 125 g/m^3 and 200 g/m^3 burning occurs but with a frequency less than one. 200 g/m^3 is the minimum concentration that will allow a flame to propagate the entire length of the tube. The optimum value of $\Delta\bar{P}_e$ is 7.0 and is obtained at 500 g/m^3. Subsequent addition of dust produces little change. Some investigators report no change in $\Delta\bar{P}_e$ up to 1 kg/m^3. This peak pressure is consistant with the value obtained for most hydrocarbons at stoichiometric concentration.

That $\Delta\bar{P}_e$ obtained in the present experiments is identical to that obtained in other vessels with different geometries and different dispersion systems indicates that the maximum explosion pressure is apparatus-independent. Hertzberg [2] has correlated measured values of the consumed oxygen concentration with the peak explosion pressure and found that it increases almost linearly. That is when the optimum value of $\Delta\bar{P}_e$ is achieved all the oxygen has been consumed and so the quantity of heat released will be limited by combustion with the finite amount of oxygen in the vessel.

In all tests in which there was a successful explosion, there still remained a considerable amount of slightly charred and even unburned residue. This is especially true for the high dust concentrations, even the "apparent stoichiometric concentration", W_s = 500 g/m^3. This is consistent with the fact that the theoretical stoichiometric concentration is 226 g/m^3. That the optimum concentration is usually much higher than the theoretical stoichiometric, even in the burner experiments where the dust concentrations are well known [9], indicates that the dust only partially burns. This is further evidence for the hypothesis that the dust flame burns as a thin gas flame in the volatiles generated within the preheat zone and thin reaction zone. Only those particles capable of burning within the time scale of the flame will contribute to the flame, those which burn more slowly (large particles and agglomerations), will pass through the flame zone unburned or only partially burned.

In the present experiments it was found that the effective heating value of the dust is $Q_{c.s.} \approx 8663 \frac{kj}{kg}$ based on the nominal dust concentration. The maximum overpressures could then be estimated using the following two equilibrium relations:

$$(W\,\bar{C}_{V_{c.s.}} + \rho_g \bar{C}_{V_g})\Delta T_e = W\,Q_{c.s.} \tag{3}$$

$$\frac{P_e}{P_o} = \frac{T_e}{T_o}\frac{M_p}{M_r} \tag{4}$$

In the above relations W is the lean cornstarch concentration (less than W_s=500 g/m^3), ρ_g is the density of the gaseous mixture, $\bar{C}_{V_{c.s.}}$ and $\bar{C}_{vg}$ are the mean specific heat capacities at constant volume for the cornstarch and gaseous products, P_e and P_o are the maximum explosion pressure and initial pressure in absolute units and T_e and T_o are the equilibrium explosion temperature and initial temperature in absolute units. The ratio M_p/M_r is the ratio of moles of gaseous products to reactants. For most hydrocarbon combustion this value is close to unity, for combustion of one mole of solid cornstarch this ratio is 1.175 based on the chemical formula for cornstarch $C_6H_{10}O_5$. The value for $\bar{C}_{V_{c.s.}}$ is approximated as 1.2 kj/kg and $\bar{C}_{vg} \approx 1.0$ kj/kg which is average for combustion products in the temperature range considered. A comparison of the approximated value and the experimentally obtained values for $\frac{P_e - P_o}{P_o}$ is shown in Table I below:

TABLE I

Concentration	$\Delta\bar{P}_e$ estimated	$\Delta\bar{P}_e$ observed
100 g/m^3	2.3	--
200 g/m^3	4.2	4.5
300 g/m^3	5.8	5.75
400 g/m^3	7.2	6.7
500 g/m^3	8.4	7.0

Within the accuracy of these crude estimations it can be seen that the approximate value of $Q_{c.s.} = \frac{kj}{kg}$ is valid. The heating value for most hydrocarbons is 45000 ± 5000 kj/kg and that of methane is 50167 kj/kg.

The low heating value for the starch is likely from the fact that the value obtained was based on the nominal dust concentration, however, the actual concentration of cornstarch that burned is probably much less.

It is worthwhile to compare the burning rate as characterized by the rate of pressure rise, dP/dt, obtained in the present experiments with those from other investigators to ensure that similar trends are observed. In order to compare the present data with those from other bombs, it is necessary to scale the rate of pressure rise with the apparatus size, the so-called "cubic law" [25] is employed and the K_{st} factor is plotted in Figure 10. The K_{st} factor is defined as $K_{st} = (dP/dt)_{max} \cdot V^{1/3}$. It appears the K_{st} values for the present results exhibit the same trend as the other results quoted. However, for a tube with a large aspect ratio, the scale factor $V^{1/3}$ is not meaningful. It was developed for spherical bombs and cylindrical bombs with aspect ratios of the order of unity, where $V^{1/3}$ is characteristic of the length of flame travel. Thus in a long tube, this should be given as the distance from ignition to the far end, in this case $L_{char} = 2.0$ m. The new K_{st} factor is replotted in Figure 11, again with the results of Bond [22] Cocks [23] and Nagy [24] in a 333 l sphere, 20 liter sphere and the 1.2 l Hartmann bomb respectively. K_{st} increases sharply from 200 g/m^3 to the optimum value at 500 g/m^3. This optimum concentration is slightly lower than that of Cocks and Bond as was also the case for $\Delta\bar{P}_e$. However, the trend is in good agreement.

That the K_{st} values in the LHT are significantly higher than those from the other apparatus is indicative of a high degree of self-generated turbulence in the tube. It has been demonstrated that the rate of pressure rise in a dust explosion is sensitive to the turbulence level inside the vessel prior to combustion [25, 26].

3. Flammability of Hybrid Starch-Methane-Air Mixtures

The flammability of cornstarch-air mixtures in atmospheres containing different amounts of methane has been studied. The explosion pressures for the various hybrid mixtures are plotted in Figures 12 and 13. Also shown for comparison is the best fit curve from the starch only data. With 2% methane admixed $\Delta\bar{P}_e$ increases for each particular dust concentration and the optimum concentration is slightly lower than that with no methane. Furthermore, mixtures that were not ignitable without methane (100 g/m^3) are readily explosible with 2%. With 4% methane the trend with various dust concentrations is similar to the 2% curve except it is shifted slightly more to the lean side, and the optimum $\Delta\bar{P}_e$ is also slightly higher. Similarly, with 6% admixed the $\Delta\bar{P}_e$ is shifted still further to the lean side, so that it is flammable with no dust. In an atmosphere with nearly stoichiometric methane, 9% (ϕ = 0.95), small amounts of dust have a net contribution to $\Delta\bar{P}_e$, but further increase in dust concentration causes $\Delta\bar{P}_e$ to decrease. This is due primarily to the fact that the energy released by combustion has to raise the temperature of an increasing by larger mass. The bulk density of a mixture containing 500 g/m^3 cornstarch is 45% greater than the gas only misture. As in any rich fuel-air mixture the energy released is limited by the amount of O_2 available for combustion, therefore, there will naturally be a competition for the oxidizer. The methane being homogeneously premixed will be consumed first and

the cornstarch will burn with the remaining oxygen. That fuel which does not burn acts to dilute the mixture.

The above data is cross plotted with the methane concentration as the abscissa in Figure 14. It can be seen that the initial 2% methane admixed has a more significant effect upon $\Delta\bar{P}_e$ than does subsequent admixture. This is likely due to the increased uniformity of the burning. Within the dust cloud, small variations in particle density might cause small regions to be void of dust, as well there will be regions near the corners where the dust has not dispersed. The gas being homogeneously premixed will burn uniformly throughout these regions. Smoot [9] also found that addition of 2% methane to a coal dust burner flame reduces irregularities in the flame shape.

With the lean dust mixtures the optimum value for $\Delta\bar{P}_e$ occurs with the 9% methane air mixtures, however, with 600 g/m^3 the optimum methane concentration reduces to 6%. The excessively rich mixtures reduce $\Delta\bar{P}_e$. In rich mixtures with high methane concentrations (e.g. 9% CH_4 + 300 g/m^3 starch) the residue contains large agglomerations of singed cornstarch, indicating the particles were airborne when the flame passed but did not burn.

The maximum overpressure is therefore a function of the mixture energetics only, however, increases in the uniformity of the burning with small amounts of methane will result in minor contributions to the total energy released.

Since it is a function of mixture energetics alone, it is possible to estimate the maximum overpressure by considering the combined heat released

from the dust and gas. It has been found that for lean hybrid mixtures the constant volume explosior temperature, T_e, and pressure P_e, can be estimated in a manner analogous to equations 3 and 4.

$$(W\,\bar{C}_{V_{c.s.}} + \rho_g \bar{C}_{V_g})(T_e - T_o) = W\,Q_{c.s.} + G\rho_{CH_4}\,Q_{CH_4} \tag{5}$$

$$\frac{T_e}{T_o} \simeq \frac{P_e}{P_o} \tag{6}$$

In the above relation ρ_{CH_4} is the density of methane gas that is present in the environment, ρ_g is the density of gas phase mixture before combustion and $\bar{C}_{V_g}$ is the mean specific heat capacity for the gaseous products. For mixtures that are not lean the correlations are somewhat different. It is assumed that the methane gas, being homogeneously premixed will react with the oxygen entirely and the fraction of cornstarch burned will be that necessary to completely deplete the oxygen content in the vessel.

If ϕ is the equivalence ratio of the admixed methane then the optimum dust concentration of the hybrid mixture will be $W_s' = (1 - \phi)W_s$. Thus for rich mixtures where $W \geq W_s'$ the explosion energy can be estimated by:

$$(W\,\bar{C}_{V_{c.s.}} + \rho_g \bar{C}_{V_g})(T_e - T_o) = W_s'\,Q_{c.s.} + \rho_{CH_4}\,Q_{CH_4} \tag{7}$$

The estimates are shown with respect to the experimentally observed values in Figures 13 and 15 for some sample mixtures. In performing the estimates the value of $\bar{C}_{vg}$ used is the mean value for the combustion products (H_2O, CO_2, N_2) at

the approximated mean temperature. The value for $\bar{C}_{V_{c.s.}}$ is constant at 1.2 kj/kg^{0}k. The estimated values appear to be in reasonable agreement with the experimental observations. The approximately linear decrease in the optimum dust concentration with increasing methane concentration has also been observed by Bartknecht [1] experimenting with PVC dust and methane. The good agreement with the experimental results also lends further support to the assumption that the dust suffers in a competition for oxygen with a premixed flammable gas.

The effect of admixing increasing amounts of methane on the burning rates of various dust air mixtures can be seen in Figure 16. For any particular dust concentration the rate of pressure rise increases when methane is admixed, even in small amounts. With admixture of 2%, 4%, and 6%, the dP/dt versus dust concentration curve exhibits the same trend as with no methane except the values are higher and the optimum concentration is shifted to the lean side, in a manner similar to ΔP_e. The maximum burning rate of the optimum dust-air mixture is exceeded even by leaner dust-methane-air mixtures. The measured values of the flame speed, $\dot{R}_f$, shown in Figure 17, correlate well with the dP/dt data in terms of the curve shape, the relative increase in value of $\dot{R}_f$ and the shift in the optimum dust concentration to leaner mixtures with increased methane content.

The data from Figures 11 and 12 are cross-plotted in Figures 18 and 19. Here it can be seen that the optimum burning rate for hybrid mixtures occurs with relatively high gas concentrations. For low dust concentrations (i.e. $W < 500$ g/m^3) the optimum mixture contains stoichiometric methane, however, for higher concentrations the optimum mixture contains somewhat less methane, in the present case the optimum mixture contains 6% methane.

When the gas concentration itself is nearly stoichiometric the inclusion of combustible dusts acts to lower the burning rate as can be seen in Figures 20 and 21. For those mixtures of 9% methane and small amounts of dust ($50\ g/m^3 < W < 200\ g/m^3$) in which $\Delta\bar{P}_e$ increased from 7.6 to 8.1, the burning rate continues to decrease. The trend of the dP/dt curve and $\dot{R}_f$ are almost identical, with the value at $800\ g/m^3$ being about 35% of the value with no dust.

4. The Effect of Flame Temperature Upon the Burning Rate

It will now be shown that the above data substantiates the model for the propagation of a dust flame in which the reactions occur mainly in the volatiles generated at the flame front. According to this model, as the particle temperature increases in the preheat zone of the flame the particles will begin to pyrolyze and emit volatiles which quickly mix with the surrounding gas. This process is probably largely completed before the end of the gaseous reaction zone, especially for the very fine particles. For larger particles or agglomerations, subsequent oxidation of the remaining char is slow by comparison and not as significant. The characteristic burning rate of a flame is determined by the steep gradients of species and temperature in the front.

Thus the admixture of methane gas to a lean dust air mixture, in making the mixture more energetic, should affect the burning rate in a manner similar to that of a premixed gas when made more energetic. According to the theory of Mallard and LeChatelier [27] the laminar burning velocity is related to the flame temperature in the following manner:

$$S_L = \frac{R\,T_f^2}{E(T_f - T_o)} \sqrt{2C\alpha \exp\left(\frac{-E}{R\,T_f}\right)} \qquad (8)$$

In the above equation T_f is the flame temperature, α is the thermal diffusivity of the gas, R is the gas constant, E is the activation energy and C is a frequency factor. It is well known that the turbulent burning velocity of a premixed gas is proportional to the laminar burning velocity of that mixture.

The validity of this statement can be seen in a comparison of the change in the laminar burning velocity with the changes in the $\frac{dP}{dt}$ and $\dot{R}_f$ when the composition of a methane air flame is altered. In Table II below the flame temperatures quoted are adiabatic constant pressure temperatures calculated using the NASA equilibrium code [28]. The burning rates are compared to that of a 9% methane air mixture denoted by the subscript "o". The ratios of the laminar burning velocity is given by:

$$\frac{S_L}{S_{L_o}} = \frac{T_f^2}{T_{f_o}^2} \left[\frac{T_{f_o} - T_o}{T_f - T_o}\right] \sqrt{\frac{E}{RT_{f_o}} - \frac{E}{RT_f}} \qquad (9)$$

in which the value of E = 20 kcal/mole is used. This was found to give a perfect fit by equation 8 to the accepted values for the laminar burning velocities of methane as reported by Bradley et. al. [29].

TABLE II

CH_4 MIXTURE (% vol)	T_{fad} · ^0k	S_L/S_{L_o}	$\left(\frac{dP}{dt}\right)\Big/\left(\frac{dP}{dt}\right)_o$	$\dot{R}_f/\dot{R}_{f_o}$
9%	2135	1.0	1.0	1
8%	1982	0.81	0.80	0.88
7%	1805	0.61	0.27	0.55
6%	1616	0.42	0.14	0.29

Similarly, Table III illustrates the same dependence except the values of T_f were estimated from the maximum overpressure as follows:

$$\frac{P_e}{P_o} = \frac{T_e}{T_o} \tag{6}$$

$$T_f \simeq \frac{T_e}{\gamma_b} \tag{10}$$

where $1.20 < \gamma_b < 1.25$ for the combustion products in this temperature range.

TABLE III

CH_4 MIXTURE (% vol)	$\frac{P_e}{P_o}$	T_f (^{0}k)	$\frac{S_L}{S_{L_o}}$	$\frac{(dP/dt)}{(dP/dt)_o}$	$\frac{\dot{R}_f}{\dot{R}_{f_o}}$
9	8.6	2163	1.0	1.0	1.0
8	7.75	1927	0.68	0.90±.2	0.8 ±.1
7	6.9	1710	0.45	0.27±.06	0.55±.07
6	5.6	1380	0.19	0.14±.05	0.29±.05

Note that the temperature of lean flames differs somewhat from the adiabatic value because the maximum overpressure, from which it is derived, suffers from the heat loss from the hot products. Most likely the flame is closer to the adiabatic temperature. However, for the more energetic mixtures the agreement is much better. In general, the agreement is quite good considering the sensitivity of the burning rate to the turbulence intensity and ignition source both of which can fluctuate, as well as the simplicity of the analysis. Thus the turbulent burning rate scales directly with the laminar burning rate. Note that between the most energetic and least energetic mixtures the Reynolds number of the flow in the tube is between 10^5 and 5×10^5. Considering also that there

are no obstructions in the path of the flow, it is unlikely that the flow-induced turbulence varies from one run to the next. Also, the turbulence generated by the dispersion process is also constant for each run. However, this latter turbulence decays exponentially with time after ignition, and so the slower burning flames will have a lower average turbulence intensity which may also account for the larger discrepancies in Table II between S_L/S_{L_o} and the observed burning rates of the leaner mixtures.

The burning rate data for cornstarch-air mixtures can be analyzed in a similar fashion, in which the constant pressure flame temperature is estimated from the maximum overpressure. In general, the flame temperatures calculated in this manner are lower than those for the methane only mixtures. This is probably a result of the higher bulk heat capacity of dust air mixtures. In Table IV below the ratio of the laminar burning velocities have been estimated using an activation energy of E = 10 kcal/mole. This value is within the range reported for the pyrolysis of various coals by Niksa[30]. The change in laminar burning velocity for different starch concentrations is shown below along with the experimentally observed changes in dP/dt. Also shown are the observed values of P_e/P_o. The burning rates are normalized with respect to the values at the optimum concentration, W_s = 500 g/m^3, and denoted by the subscript "o".

TABLE IV

STARCH g/m^3	$\frac{P_e}{P_o}$	T_f (^{0})	$\frac{S_L}{S_{L_o}}$	$\frac{\frac{dP}{dt}}{(dP/dt)_o}$	$\frac{\dot{R}_f}{\dot{R}_{f_o}}$
500	8.0	2016	1.0	1.0 ±.05	1.0 ± .1
400	7.25	1753	0.74	0.71±.07	0.80±0.08
300	6.75	1568	0.57	0.53±.06	0.60± .1
200	5.5	1277	0.34	0.38±.05	0.20± .1

The good agreement between the change in laminar burning velocities and rates of pressure rise can also be seen graphically in Figure 23 in which S_L/S_{L_o} is represented by the solid line and $(dP/dt)/(dP/dt)_o$ by the triangular points. In Figure 24 $\dot{R}_f$ is plotted similarly along with S_L/S_{L_o}. Thus the observed increase in the turbulent burning rate of a dust-air mixture when the concentration is increased is largely a temperature effect. Furthermore, that the temperature dependence of the burning rate agrees in parametric form with the thermal theory of Mallard and LeChatelier for premixed gas is strong evidence in favour of combustion in the volatiles phase. That the activation energy for the dust-air mixture is lower than that of methane-air mixtures may be due to the difference between the chemistry of the volatiles and methane, as well as the chemical reactions that occur during the pyrolysis of the cornstarch.

It is assumed for gaseous flames with high E, that most of the reactions occur at the flame temperature so that the ignition temperature and flame temperature are nearly identical. The lower activation energy of the dust implies that reactions occur over a broader temperature range and so there is a finite difference between the ignition temperature and the flame temperature. From thermal flame theory [26] it is known that

$$\delta = \frac{\alpha}{S_L} \cdot \frac{T_f - T_i}{T_i - T_u} \tag{11}$$

where T_i is the ignition temperature and α is the thermal diffusivity. It can be seen from here that if the activation energy is low, hence T_i is low and the flame thickness will increase. Hence this may explain the thicker laminar flames observed for laminar dust combustion from the burner experiments discussed in Chapter II.

Since the admixture of methane to a lean dust-air mixture has the effect of increasing the combustion temperature, the burning rate of the volatiles will also increase. The magnitude of these changes are compared to the observed values for the changes in dP/dt and $\dot{R}_f$ in Table V below. In this table the flame temperatures used were estimated from the maximum overpressure and were found to agree well with those estimated from equations 3 and 5. The burning rates of mixtures containing various amounts of methane are compared to the burning rates of dust-air mixtures denoted by the subscript "o".

TABLE V

MIXTURE STARCH + CH_4 (g/m^3) (% vol)	$\frac{P_e}{P_o}$	T_f (^0k)	$\frac{S_L}{S_{L_o}}$	$\frac{(dP/dt)}{(dP/dt)_o}$	$\frac{\dot{R}_f}{\dot{R}_{f_o}}$
200 + 0%	5.5	1277	1.0	1.0 ±.05	1.0 -
" + 2%	7.25	1753	2.17	2.1 ±.2	2.6 ±.05
" + 4%	7.6	1904	2.60	2.6 ±.3	4.2 ±.3
" + 6%	8.1	2040	3.0	3.8 ±.2	-
300 + 0%	6.75	1568	1.0	1.0 ±.05	1.0 ±.05
" + 2%	7.75	1927	1.59	1.7 ±.1	1.70±.1
" + 4%	8.15	2052	1.81	2.2 ±.05	2.60±.05
" + 6%	8.4	2114	1.93	2.9 ±.1	2.6 ±.3
600 + 0%	8.0	2016	1.0	1.0 ±.1	1.0 -
" + 2%	8.0	2016	1.0	1.05 -	1.25 -
" + 4%	8.5	2138	1.13	1.48±.2	1.35 -
" + 6%	8.0	2016	1.0	1.7 ±.1	1.50 -

These results are also shown graphically in Figures 25-27, in which S_L/S_{L_o} is shown as the solid line connecting the values at 0%, 2%, 4% and 6% methane. Throughout all the calculations the value of the activation energy was assumed to be 10 kcal/mole. Perhaps slightly better agreement between S_L/S_{L_o} and the measured parameters could be achieved by adjusting the activation energy to an intermediate value depending on the relative concentrations of dust and methane. This can be seen in Figure 26 where the experimental values of $(dP/dt)/(dP/dt)_o$ and $\dot{R}_f/\dot{R}_{f_o}$ lie between the two S_L/S_{L_o} curves using $E=10\frac{kcal}{mole}$ and E=20kcal/mole. However, it was decided not to involve another adjustable parameter to the calculations, since the trends are already evident. It can be seen that the increased burning rates caused by admixture of methane to a dust-air mixture is primarily a temperature effect. It was noted that 6% methane in air is flammable without any dust. That the burning rate increases when dust is added indicates that a significant amount of volatiles are generated within the preheat zone and reaction zone of this gaseous mixture, causing the flame temperature to increase. The characteristic time scale of the premixed gas flame is given by $\tau_{ch} \simeq \delta/S_L$, the flame thickness divided by the laminar burning velocity. For 6% methane $\tau_{ch} \simeq 0.2\times10^{-3}m/0.15m/s = 1.3$ msec. Also from an analysis of heat transfer to a particle by conduction, it can be shown that the characteristic heating time of a particle is proportional to $\tau_{th} = \rho_p C_p d_p^2/12K_f$ $\rho_p C_p$ and d_p are the particle density, specific heat capacity and diameter respecitvely, and K_f is the conductivity of the gas. For cornstarch particles with diameter about 15 μm this value is about 0.2 msec. Thus it is reasonable to assume that most particles can heat up and devolatilize within the preheat zone and reaction zone of the flame. The flame thickness of this hybrid mixture is then of the same order as the gas flame thickness, which is about 0.2 mm.

Although the increased burning rate of dust-air mixtures when flammable gas is admixed can be explained primarily in terms of the effect on the flame temperature it must be recognized that other factors are altered as well. By admixing a quantity of flammable gas to a dust-air mixture the quantity of volatiles that need be generated from the dust is reduced. This was seen in the lean shift in the optimum dust concentration, W_s, for hybrid mixtures. This will have the effect of reducing the characteristic time associated with the production of the volatiles, which in turn will reduce the flame thickness and increase the overall burning rate. This factor may explain the observed increase in the burning rate for rich dust-air mixtures when methane is admixed. It was observed that $\Delta\bar{P}_e$ did not change hence S_L/S_{L_o} did not change either; yet dP/dt and $\dot{R}_f$ increase with increased methane concentration, (see Figure 27). However, it is difficult to quantify this result as the devolatilization rates are unknown. It is though, intuitively obvious that as the methane concentration increases the devolatilization rate of the dust becomes a decreasingly significant factor. When the concentration of methane is flammable by itself then the progress of the flame is not limited by the dust's devolatilization rate.

It was observed that dust added to a nearly stoichiometric mixture of methane and air (ϕ = 0.95) acted to retard the burning rate of the flame, even when added in small amounts. Figure 13 shows that $\Delta\bar{P}_e$ increases when dust is added, up to 200 g/m^3, and the optimum dust concentration with 9.0% methane was found to be 25 g/m^3. However, $\dot{R}_f$ and dP/dt decrease monotonically with added cornstarch.

It appears then that the rate of energy released by oxidation of the starch in the gaseous reaction zone is slower than the rate of heat absorption by conduction to the particles. Subsequent oxidation behind the gas flame can result in a net increase in the final gas temperature for low dust concentrations. With higher dust concentrations the heat lost by conduction to the particles is greater than the heat released by the starch oxidation and so $\Delta\bar{P}_e$ decreases. The slower relative reaction rate of the dust is due in part to the lack of oxygen available for dust combustion. With 9% admixed methane only 5% of the initial oxygen content is available for combustion of the dust whereas with 6% admixed methane there is 37% of the initial oxygen content left to react with the dust.

5. Effect of Inert Dust Upon Methane-Air Flames

In order to further verify the thermal effect of cornstarch upon a 9% methane-air flame it can be compared to the thermal effect of an inert dust. Hence, experiments were conducted to investigate the influence of aluminum oxide (alumina) dust upon a 9% methane-air flame. The mean particle diameter of the alumina is d_p = 9 μm and the thermal time constant is τ_{th} = 0.34 msec, about 0.8 the value of cornstarch. The experimental results are shown graphically in Figures 28-31.

In Figure 28 the experimental values of $\Delta\bar{P}_e$ are shown for concentrations of 50 g/m^3, 100 g/m^3, 300 g/m^3, and 800 g/m^3. Also shown in the figure are the values for $\Delta\bar{P}_e$ calculated from equation 6 and equation 5 modified as:

$$(W_{a1}\bar{C}_{a1}^{\cdot} + \rho_g\bar{C}_{V_g})(T_e-T_o) \doteq G\rho_{CH_4}Q_{CH_4} \qquad (12)$$

where W_{al} and $\bar{C}_{al}$ are the alumina concentration and the specific heat capacity (calculated at $(T_e + T_o)/2$). For the temperature range encountered $\bar{C}_{al} \cong 1.25 kj/kg\text{-}^0k$ The agreement between the estimated and observed values for $\Delta\bar{P}_e$ is very good, the discrepancies are due mainly to errors in the actual dust concentrations. This is more pronounced at 800 g/m^3, which is difficult to disperse properly. It can be seen that $\Delta\bar{P}_e$ decreases linearly with increasing concentration, to 4.75 with 800 g/m^3 (observed value = 5.5).

The burning rate for the hybrid mixtures decreases monotonically with increasing alumina concentration (see Figures 29 and 30). This reduction in observed burning rate can be attributed solely to reduction in flame temperature. In Figure 31 the rate of pressure rise, flame speed and calculated laminar burning velocity are normalized with respect to the value with no dust and plotted against the dust concentration. In the calculation of S_L/S_{L_o}, the flame temperature T_f was estimated from the value of T_e calculated in equation 12 and E = 20 kcal/mole.

The good agreement between S_L/S_{L_o} and the observed values for dP/dt and $\dot{R}_f$ indicates that the flame temperatures were estimated correctly. Furthermore, this implies that the particles equilibriate with the hot gases within thin gas flame, that is, the temperature lag of the particles in the flame is neglibible.

That the shape of the curves in Figures 29-31 are congruent with those for cornstarch in 9% methane-air is further evidence that the cornstarch particles act as an inert dust in the thin gas flame of the nearly stoichiometric methane-air mixture. Thus for very reactive dust mixtures, the burning rate may be limited by the rate of pyrolysis of dust which governs the production of volatiles. Furthermore, this burning rate is just lower than that of a stoichiometric methane-air flame.

This may also explain why the laminar burning velocities of coal dust air flames generally reported have a maximum value near 0.35 m/s while that for methane is 0.45 m/s.

6. Effect of Hydrogen Upon a Lean Starch-Air Flame

In order to ascertain the role of the chemistry of the flammable gas admixed to a dust-air mxiture, some tests were run with constarch-hydrogen-air mixtures. The experiments were conducted with 100 g/m^3 cornstarch and various hydrogen concentrations from 0% to 12 % by volume. As noted earlier, 100 g/m^3 of starch alone is not ignitable in the present experiment, however, it readily ingites and propogates with 3% H_2. The maximum overpressures observed experimentally are shown graphically in Figure 32, along with those values calculated by use of equations 3 and 4, (broken line). In these calculations Q_{H_2} = 121,000 kj/kg. The similarity between the observed and calculated values for $\Delta\bar{P}_e$ indicate that $\Delta\bar{P}_e$ is a function only of the energetics of the individual components of the mixture. Note that at high concentrations of H_2 (near stoichiometric) the value of Mp/Mr=0.85 however, at lower concentrations the value is much closer to unity, so that the calculations are not significantly affected.

The rate of pressure rise data for these mixtures is shown in Figure 23. Between 3% and 9% H_2, dP/dt increased at a mild rate from 22 bar/s to 55 bar/s respectively. However, at 12% H_2, the burning rate increases dramatically to 250 bar/s, a 4.5 fold increase from the value at 9% H_2. This sudden change in the burning rate is indicative of a change in the burning mechanism of the mixture.

For H_2-air mixtures alone, the horizontal flammability limit is near 6.5% by volume. Thus, in the mixtures containing 7%, 9% and 12% H_2, the gas is capable of sustaining flame propagation without the contribution from the oxidation of the starch. The $\Delta\bar{P}_e$ data, however, indicate that starch oxidation does occur.

It has been shown by Scholte et. al. [31,32,33] that the burning velocity of many hydrocarbons increases with the square root of added H_2 gas $S_L \alpha [H_2]^{1/2}$. This is qualitatively observed in the present experiments in mixtures containing up to 9% H_2. The sudden increase at 12% H_2 can be explained from the reaction kinetics of hydrogen combustion. Lee et. al. [34] observed experimentally a sudden increase in the turbulent burning rate of H_2-air mixtures at 13% H_2. This is attributed to a changeover in the competing reation between $H_2 + O_2 + M \rightarrow HO_2 + M$ and $H + O_2 \rightarrow OH + O$ which occurs around 1300^{0}K in favour of the more rapid OH branching reaction. That the transition was observed, in the present case, to occur between 9% and 12% whereas Lee et. al. observed this change at 13% indicates that heat released by combustion of the starch is sufficiently rapid to occur within the reaction zone of gaseous mixture. This is further demonstrated by a comparison with the flammability of a 12% H_2-air mixture with no cornstarch shown below.

MIXTURE	$\Delta\bar{P}_e$	dP/dt
12% H_2	4.1	45 bar/s
12% H_2 + 100 g/m^3 starch	7.0	250 bar/s

Clearly the cornstarch acts to decrease the concentration of H_2 at which the sudden transition of burning rates occurs.

It thus appears that for lean amounts of hydrogen admixed to the dust, the increased burning velocity can be explained by the increased burning rate of the volatiles-gas mixture. This is due to the higher burning velocity of hydrogen gas and due to the increased flame temperature which results from the more energetic mixture. That the observed increase in burning rate within the range of 0% - 9% is because of the low heating value of hydrogen on a molar basis. $Q_{CH_4}/Q_{H_2} \doteq 3.3$ per mole of fuel burned. This is also seen from the fact that stoichiometric concentration of hydrogen in air is 29.5% as opposed to 9.5% for methane. Thus when comparing the equivalence ratio of admixed gas the relative effect of lean methane and lean hydrogen are similar.

7. <u>On the Lean Flammability Limits of Hybrid Mixtures</u>

To further elucidate the coupling between the two components of the hybrid cornstarch-methane-air mixtures the lean flammability limits will be examined. This is not so straight forward as the definition of lean limit propagation is vague, hence the definition used in the present context will be explained. The mixture is considered to be explosible if the overpressure generated is greater than 1.5 bar. It was generally observed in the present experiments that no explosions occurred which generated overpressures between zero and 1.5 bar, either $\Delta\bar{P}_e \geq 1.5$ or no pressure at all. Furthermore, the vessel was inspected after each test to examine the residue. Burned char present throughout the tube length is indicative of flame propagation along the entire tube length. Ion probe signals also indicate if the flame has propagated as far as the probe locations (x = .91 m, x = 1.83 m).

To determine the "lower explosible concentration",(LEC), of a hybrid mixture tests were done at a particular dust concentration at decreasing methane concentrations until the mixture was no longer explosible. The lowest dust concentration tested was 50 g/m^3, below this value it was felt that the dispersal system was not reliable. Table VI below presents the results from these tests, showing the lowest explosible hybrid concentrations:

TABLE VI

LEC (g/m^3)	CH_4 (% vol)	CH_4 (g/m^3)
125	0	0
100	2	13
50	4	26
0	6	39

The results are shown graphically in Figure 29 and it can be seen that a linear decrease in LEC with increase in CH_4 exists. Also shown on the figure are the highest concentrations that were non-explosible in the present experiments. The slope of the explosibility line is about -20.8 g cornstarch/g CH_4.

The linear variation of LEC with methane content might indicate that similar mechanisms are responsible for the extinguishment of the dust flame as in the gaseous flame. The lean flammability limit for horizontal propagation of methane in the present case is 6.0%. The energy stored in this mixture is about 1965 kj/m^3 of mixture and $\Delta\bar{P}_e = 4.6$. That for the lean limit mixture for cornstarch is 1083 kj/m^3. This latter value is based upon LEC = 125 g/m^3 and $Q_{starch} = 8663$ kj/kg. In fact, the total energy of the hybrid lean limit mixture

decreases with decreasing methane concentrations. This is incongruent with the proposed model since it implies that the dust combustion is capable of propagating at much leaner mixtures than that of a premixed gas. It is more likely that the dust flame propagates at lower concentrations because some spacial non-uniformities allow the flame to propagate through regions with more favourable concentrations. If a harder criteria of $\Delta\bar{P}_e = 3$ is imposed which more closely resembles the pressure developed by the lean limit gaseous mixtures then the LEC with no methane is 175 g/m^3. However, as can be seen in Figure 29 this causes the flammability curve to be slightly non-linear. The higher concentrations of dust required for mixtures containing less methane may be a result of dust settling. As shown earlier most limit mixtures propagate at flame speeds near 4 to 5 m/s and have burnout times of the order of 0.4 seconds. By this time a considerable amount of dust can fall out of suspension. In the ignition experiments the mixtures could not be ignited at all when the ignition time delay was 0.4 seconds. This factor will more influence mixtures containing little or no flammable gas. Thus the criteria of $\Delta\bar{P}_e = 3$ might be unduly hard, and the linear variation of LEC with methane is probably accurate. It may be concluded then, that long horizontal tubes are not ideal for measuring lean limits, nor studying near limit dust flames, because this particular geometry enhances the problem of dust settling during the explosion process.

V. CONCLUSIONS AND RECOMMENDATIONS

A long horizontal tube constant volume bomb was developed to study dust-air and hybrid dust-gas-air explosions. The bomb employs a novel dust dispersal system to generate quite uniform dust clouds within. Maximum explosion pressures obtained with the new apparatus are comparable to those values obtained by other investigators (despite that much of the dust does not burn).

It has been demonstrated that the maximum explosion pressure and the burning rate of a dust-air mixture are enhanced by the presence of flammable gas in the atmosphere. Admixed methane gas has a greater effect upon lean dust-air mixtures and a very small effect upon rich dust-air mixtures. The maximum explosion pressure was shown to be a function of the combined mixture energetics and is readily estimated from equilibrium thermodynamics. The maximum feasible explosion pressure that can be generated in the closed volume is limited by the amount of oxidizer available for combustion. The optimum dust concentration, at which the greatest explosion pressure is generated, decreases almost linearly with increasing methane content.

It was also demonstrated that the turbulent burning velocity of all cornstarch-air mixtures increases when methane is admixed. The enhanced burning rate is attributed to increased flame temperatures generated by the hybrid mixtures. Furthermore, changes in the turbulent burning rates with fuel concentration, for gas-air, dust-air and hybrid dust-gas-air mixtures were shown to be proportional to changes in the laminar burning velocities. The latter were calculated from the thermal flame propagation theory of Mallard and LeChatelier. That the gas-air and dust-air mixtures behave similarly supports the proposed qualitative model for dust flame propagation, in which a thin gaseous flame propagates through the volatiles generates within the preheat and reaction zones.

Excess dust that is present in rich hybrid mixtures was shown to act as a thermal sink, absorbing heat from the flame front. In doing so, the flame temperature is reduced, thereby retarding the burning rate. The influence of a combustible dust upon the burning rate of a nearly stoichiometric premixed gas flame is similar to the influence of an inert dust.

The influence of admixed hydrogen is similar to that of admixed methane. The less significant effect of lean hydrogen is because combustion of one mole of hydrogen yields 30% of the heat released by combustion of one mole of methane. However, starch added to a 12% hydrogen air mixture results in a dramatic increase in the burning rate. It was concluded that the heat contributed by the dust oxidation acts to increase the flame temperature beyond some critical value at which the faster chain branching reactions are favoured. That the starch burns within the thin gas flame attests to rapid rate at which the small particles may devolatilize and react.

Finally it may be concluded that the lower explosible concentration for cornstarch decreases nearly linearly with increasing methane content. This result is consistent with other investigators and further supports the model of flame propagation in the volatiles. However, it must be mentioned that the relatively weak ignition and long flame travel in the present experiment provide too many variables for distinguishing a true limit flame, hence it is not ideally suited for this measurement. The author recommends that lean limit measurements are best made in manner outlined in references [2,12].

In the proposed physical model for dust flame propagation the reaction zone is similar to that of a premixed gas. The laminar flame is thin since the burning occurs in the volatiles generated in the preheat zone. Some evidence in support of this claim is given as well, however, no really conclusive evidence exists to show that the dust flame is as thin as a premixed gas flame. In correlating the present starch-air data with the theory of Mallard and LeChatilier, an activation energy E = 10 kcal/mole was proposed as compared to E = 20 kcal/mole used to correlate the methane-air flammability data. This would indicate that reactions in dust-air flame occur over a broad temperature and this in turn implies a thicker flame. Hybrid mixtures correlate with an in between value for the activation energy. This evidence would imply that the devolatilization rate may not be infinitely fast and so cause the dust-air flame to be slightly thicker. It would thus be beneficial to have a more detailed description of the properties of a laminar dust-air flame including the role of the devolatilization rate and the temperature and species profiles. This might be best achieved and the results more easily applied with a dust whose physical and chemical properties are well known and relatively simple to model.

REFERENCES

1. Bartknecht, W., "Explosions - Course, Prevention, Protection", Sprinker Verlag, New York, (1980), p 31.

2. Hertzberg, M., Cashdollar, K., and Operman, J.J., "The Flammability of Coal Dust-Air Mixtures: Lean Limits Flame Temperatures, Ignition Energies and Particle Szie Effects", *United States Bureau of Mines Report of Investigations RI 8360*, (1979).

3. Conti, R.S., Cashdollar, K.L., Hertzberg, M., and Liebman, I., "Thermal and Electrical Ignitability of Dust Clouds", *United States Bureau of Mines Report of Investigations RI 8798*, (1983).

4. Hertzberg, M., Richmond, J.K., Cashdollar, K.L., "Flammability Limits and the Extinguishment of Explosions in Gases, Dusts, and their Mixtures: Theory Experiment and Problem of Scale", *First Specialists Meeting (Int.) of the Combustion Institute, Bordeaux, France*, (1981), p 202.

5. Nagy, J., Portman, W.M., "Explosibility of Coal Dust in an Atmosphere Containing a Low Percentage of Methane", *United States Bureau of Mines Report of Investigations RI 5815*, (1961).

6. Singer, J.M., Bruszak, A.E., and Grummen J., "Limits of Flame Propagation of Coal Dust-Methane-Air Mixtures", *United States Bureau of Mines Report of Investigations RI 7103*, (1968).

7. Klemens, R., and Wolanski, P., "Flame Structure in Dust and Hybrid Mixtures Near the Lean Flammability Limit", *20th Symposium (International) on Combustion, The Combustion Institute*, (1984), in press.

8. Feng, K.K., "Hazardous Characteristics of Canadian Coal Dusts", *Energy Research Program, Division Report ERP/MRL 82-132*, (OP)(J).

9. Horton, M.D., Goodson, F.P., and Smoot, L.D., "Characteristics of Flat, Laminar Coal-Dust Flames", *Combustion and Flame, Vol. 28*, (1977), pp 187-195.

10. Ballal, D.R., "Flame propagation through dust clouds of carbon, coal, aluminum, and magnesium in an environment of zero gravity", *Proc. R. Soc. Lond. A 385*, 21-51 (1983).

11. Slezak, S.E., Fitch, D.J., Krier, H., and Buckius, R.O., "Coal Dust Flame Propagation in a Laboratory Flammability Tube", *Combustion and Flame, Vol. 54*, (1983), pp 103-119.

12. Buksowicz, W., Klemens, R., and Wolanski, P., "An Investigation of the Structure of Dust-Air Flames", *Oxidation Communications 5, Nos. 1-2*, (1983), pp 175-188.

13. Hertzberg, M., Cashdollar, K.L., and Lazzara, C.P., "The Limits of Flammability of Pulverized Coals and Other Dusts", *18th Symposium (Int.) on Combustion, The Combustion Institute* (1981), pp 717-729.

14. Zabetakis, M.G., "Flammability Characteristics of Combustible Gases and Vapours", *U.S. Bureau of Mines Bulletin 627*, (1965).

15. Seeker, W.R., Samuelsen, G.S., Heap, M.P., and Trolinger, J.D., "The Thermal Decomposition of Pulverized Coal Particles", *18th Symposium (Int.) on Combustion, The Combustion Institute*, (1981), pp 1213-1226.

16. McLean, W.J., Hardesty, D.R., and Pohl, J.H., "Direct Observations of Devolztilizing Pulverized Coal Particles in a Combustion Environment", *18th Symposium (Int.) on Combustion, The Combustion Institute*, (1981), pp 1239-1248.

17. Howard, J.B., and Essenhigh, R.H., "Mechanism of Solid-Particle Combustion with Simultaneous Gas-Phase Volatiles Combustion", *18th Sumposium (Int.) on Combustion, The Combustion Institute*, (1981), pp 399-408.

18. Milne, T.A. and Beachey, Z.E., "Laboratory Studies of the Combustion, Inhibition and Quenching of Coal Dust-Air Mixtures", *Paper presented at the Western States Section of the Combustion Institute*, (1976) Spring Meeting.

19. Bradley, D., Lee, J.H.S, "On the Mechanisms of Propagation of Dust Flames", *First International Colloquium on the Explosibility of Industrial Dusts Book of Papers Vol. 2*, (1984), Polish Academy of Sciences. In Press.

20. Eckhoff, Rolf K., "Towards Absolute Minimum Ignition Energy For Dust Clouds?", *Combustion and Flame, Vol. 24, No. 1*, (1975).

21. Bradley, D., Dixon-Lewis, G., El-Din Habik, S., and Mush, E.M.J., "The Oxidation of Graphite Powder in Flame Reaction Zones", *20th Symposium (Int.) on Combustion, The Combustion Institute*, (1984). In Press

22. Bond, F., Fresko, M., Knystautas, R., and Lee, J.H.S., "Influence of Turbulence on Dust Explosion", *First International Colloquium on the Explosibility of Industrial Papers; Vol. 1*, (1984), Polish Academy of Sciences.

23. Cocks, R.E., and Meyer, R.C., "Fabrication and Use of a 20 Liter Spherical Dust Testing Apparatus", *Process Specialties Section, Engineering Division, Procter and Gamble, Cincinnati, Ohio.*

24. Nagy, J., Seiler, E.C., Conn, J.W. and Verakis, H.C., "Explosion Development in Closed Vessels", *U.S. Bureau of Mines Report for Investigations RI 7507*, (1971).

25. Eckhoff, R.K., "Use of (dP/dt) max From Closed-Bomb Tests for Predicting Violence of Accidental Dust Explosions in Industrial Plants", *First International Colloquium on the Explosibility of Industrial Dusts, Book of Papers Vol. 1*, (1984), Polish Academy of Sciences.

26. Cassel, Hans, M., "Some Fundamental Aspects of Dust Flames", *U.S. Bureau of Mines Report of Investigation RI 6551*, (1964).

27. Lee, J.H.S., "Physics of Explosions", *Course Notes Presented at SANDIA National Laboratories*, N.M., (1984).

28. Bittker, P.A., and Scullin, V.J., "General Chemical Kinetics Computer Program for Static and Flow Reactions, with Application to Combustion and Shock-Tube Kinetics", *NASA Technical Note, NASA TN D-6586* (1972).

29. Andrews, G.E. and Bradley, D., "The Burning Velocity of Methane-Air Mixtures", *Combustion and Flame, Vol. 19*, (1972) p. 275-288.

30. Niksa, S., Heyd, W., Russel, B., and Saville, D., "On the Role of Heating Rate in Rapid Coal Devolatilization", *presented at the 1984 Spring Meeting of the Western States Section of the Comb. Inst.*

31. Scholte, T.G., and Vaags, P.B., "The Burning of H_2-Air Mixtures and Mixtures of Some Hydrocarbons with Air", *Combustion and Flame, Volume 3, No. 4*, December, 1959.

32. Scholte, T.G. and Baags, P.B., "The Influence of Small Quantities of H_2 and H_2 Compounds on Burning Velocity of CO Flames", *Combustion and Flame, Vol. 3, No. 4*, December, 1959.

33. Scholte, T.G. and Baags, P.B., "Burning Velocities of Mixtures of Hydrogen, CO, CH_4 with Air", *Combustion and Flame, Vol. 3, No. 4*, December, 1959.

34. Lee, J.H.S., Chan. C. and Knystautas, R., "Hydrogen-Air Deflagrations: Recent Results", *Proceedings of the Second International Conference on the Impact of Hydrogen on Water Reactor Safety, U.S. Nuclear Regulatory Commission* (1982).

LIST OF FIGURES

Figure 1 - Schematic of long horizontal tube (LHT).

Figure 2 - Photomicrographs of cornstarch from samples with and without the fluidizing agent.

Figure 3 - Particle size distribution of cornstarch from samples with and without the fluidizing agent.

Figure 4 - Effect of ignition delay time upon dust explosion.

Figure 5 - Actual pressure-time history and ion probe signals of a 9% methane-air explosion and a schematic of the flame shape.

Figure 6 - Comparison of the pressure-time history for explosions in initially quiescent and turbulent methane-air mixtures.

Figure 7 - Maximum explosion pressure for different methane-air mixtures, theory and experiment.

Figure 8a- Burnout time for different methane-air mixtures.

Figure 8b- Comparison of heat loss in the LHT versus the burnout time for a gas explosion.

Figure 9 - Maximum explosion pressure for different cornstarch-air mixtures.

Figure 10 - K_{st} factor for different cornstarch-air mixtures, comparison with other investigators.

Figure 11 - K_{st} factor using characteristic length of flame travel instead of $V^{1/3}$.

Figure 12 - Maximum explosion pressure for different cornstarch-air concentrations with 0%, 2%, 4%, and 6% admixed methane.

Figure 13 - Maximum explosion pressure for different cornstarch-air concentrations with 9% methane.

Figure 14 - Maximum explosion pressure for different methane-air mixtures with 100 g/m^3, 200 g/m^3, 300 g/m^3 and 600 g/m^3 starch.

Figure 15 - Estimated values for maximum explosion pressure of different methane-air mixtures with 100 g/m^3 and 300 g/m^3 starch.

Figure 16 - Rate of pressure rise for different starch concentrations with 0%, 2%, 4% and 6% admixed methane.

Figure 17 - Flame speed for different starch concentrations with 0%, 2%, 4% and 6% admixed methane.

Figure 18 - Rate of pressure rise for different methane concentrations with 100 g/m^3, 200 g/m^3, 300 g/m^3 and 600 g/m^3 starch.

Figure 19 - Flame speed for different methane concentrations with 100 g/m^3, 200 g/m^3, 300 g/m^3 starch.

Figure 20 - Rate of pressure rise for different starch concentrations with 9% methane.

Figure 21 - Flame speed for different starch concentrations with 9% methane.

Figure 22 - Laminar burning velocity and flame temperature for different methane-air mixtures.

Figure 23 - Comparison of normalized dP/dt and S_L data for different starch-air mixtures.

Figure 24 - Comparison for normalized $\dot{R}_f$ and S_L data for different starch-air mixtures.

Figure 25 - Comparison of normalized S_L, $\dot{R}_f$ and (dP/dt) data for different methane-air mixtures with 200 g/m^3 admixed starch.

Figure 26 - Comparison of normalized S_L, $\dot{R}_f$ and (dP/dt) data for different methane-air mixtures with 300 g/m^3 admixed starch.

Figure 27 - Comparison of normalized S_L, $\dot{R}_f$ and (dP/dt) data for different methane-air mixtures with 600 g/m^3 admixed starch.

Figure 28 - Maximum explosion pressure for 9% methane-air with different concentrations of aluminum-oxide.

Figure 29 - Rate of pressure rise for 9% methane-air with different concentrations of aluminum-oxide.

Figure 30 - Flame speed for 9% methane-air with different concentrations of aluminum-oxide.

Figure 31 - Comparison of normalized S_L, $\dot{R}_f$ and (dP/dt) for 9% methane-air with different concentrations of aluminum-oxide.

Figure 32 - Maximum explosion pressure for 100 g/m^3 starch with different hydrogen-air mixtures.

Figure 33 - Rate of pressure rise for 100 g/m^3 starch with different hydrogen-air mixtures.

Figure 34 - Lower explosible concentrations of cornstarch in atmospheres containing methane.

FIGURES

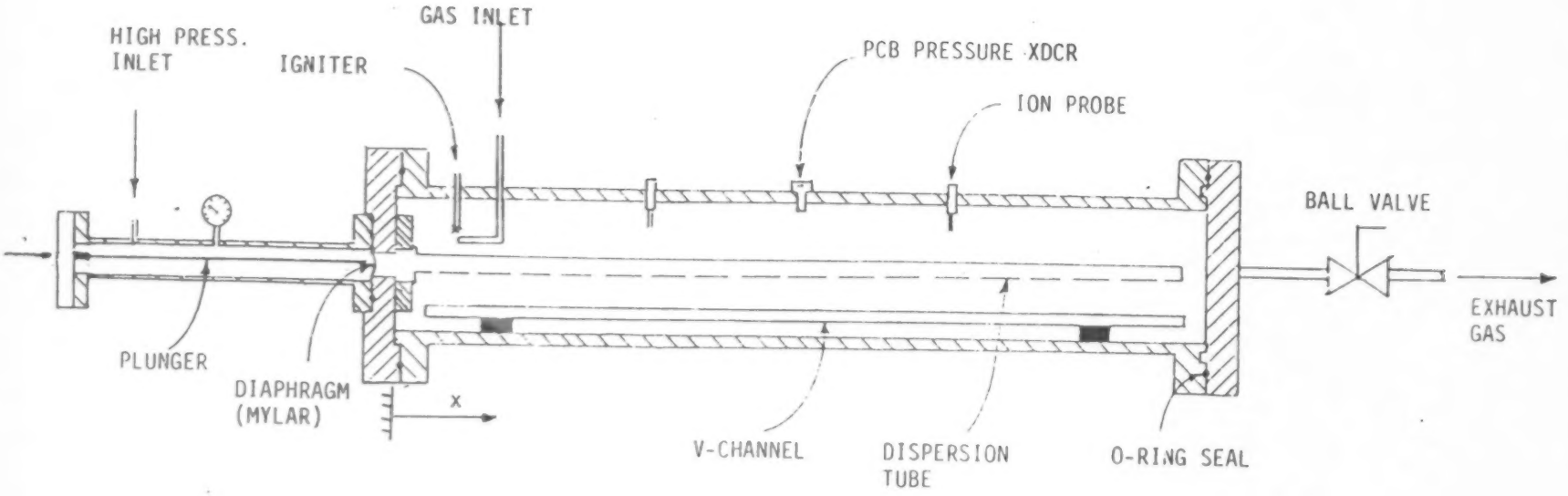

Figure 1 - Schematic of long horizontal tube (LHT)

1)

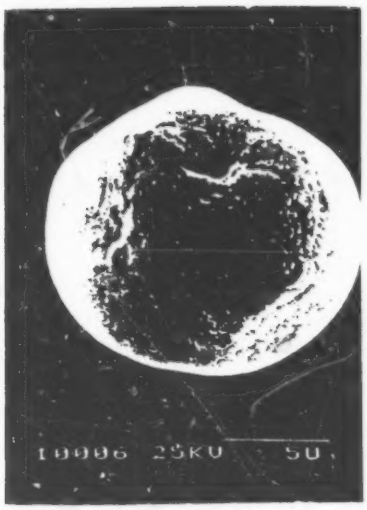

2)

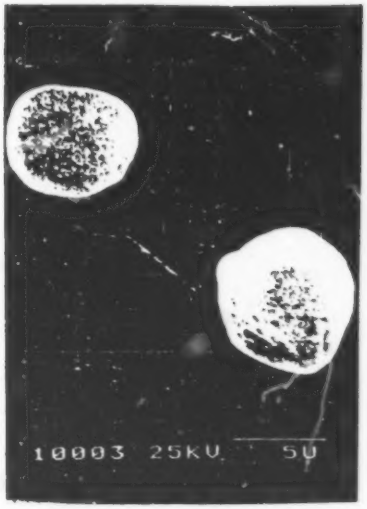

3)

4)

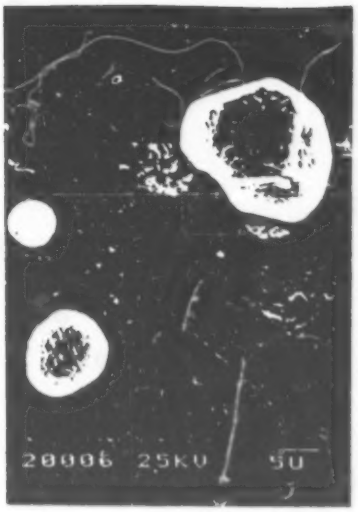

Samples 1) and 2) do not contain powder fluidizing agent while samples 3) and 4) do contain powder fluidizing agent. Note that the bars at the lower right corner of each micrograph represent 5×10^{-6} m.

Figure 2 - Photomicrographs of cornstarch

Particle Size Distribution of Cornstarch

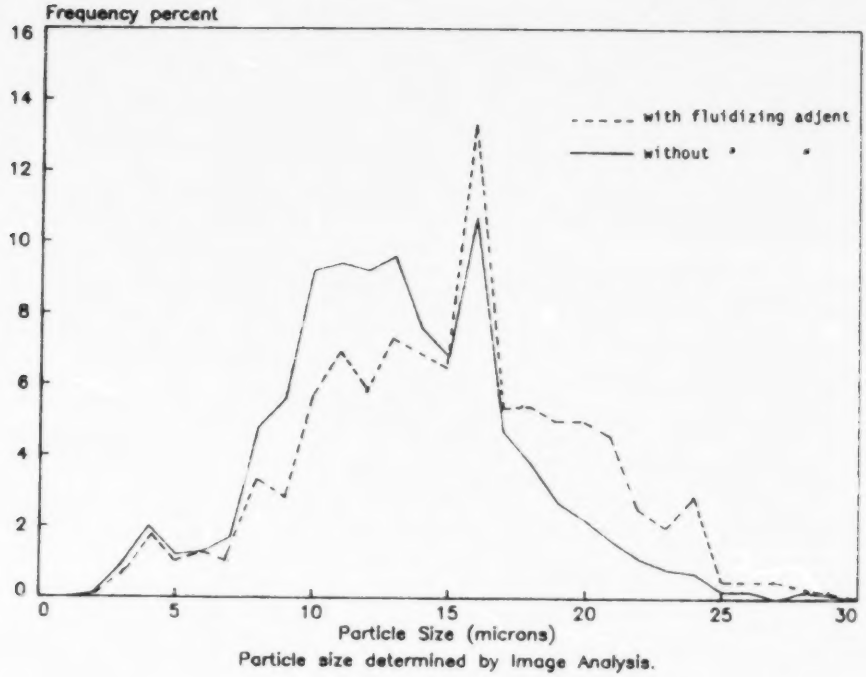

Particle size determined by Image Analysis.

Particle Size Distribution of Cornstarch

Frequency Percent for Particle Size Interval (Microns)

Lot	0-1	1-2	2-3	3-4	4-5	5-6	6-7	7-8	8-9	9-10	10-11	11-12	12-13	13-14
Cornstarch #1	0.0	0.1	0.9	2.0	1.2	1.3	1.7	4.8	5.6	9.2	9.4	9.2	9.6	7.6
Cornstarch #2**	0.0	0.1	0.7	1.7	1.0	1.2	1.0	3.3	2.8	5.6	6.9	5.7	7.3	6.8

	14-15	15-16	16-17	17-18	18-19	19-20	20-21	21-22	22-23	23-24	24-25	25-26
Cornstarch #1	6.8	10.7	4.7	3.8	2.7	2.2	1.6	1.1	0.8	0.7	0.2	0.2
Cornstarch #2	6.4	13.3	5.3	5.4	5.0	4.9	4.5	2.5	2.0	2.9	0.5	0.5

	26-27	27-28	28-29	29-30	*Mean	Dev.	Min.	Max.
Cornstarch #1	0.0	0.?	0.1	0.0	12.7	4.3	1.8	31.9
Cornstarch #2	0.5	0.3	0.2	0.2	14.7	5.1	1.8	42.5

*Mean = arithmetic mean
Dev. = standard deviation
Min. = minimum particle size
Max. = maximum particle size

**Sample #2 contains 1% fumed silica fluidizing adjent.

Figure 3

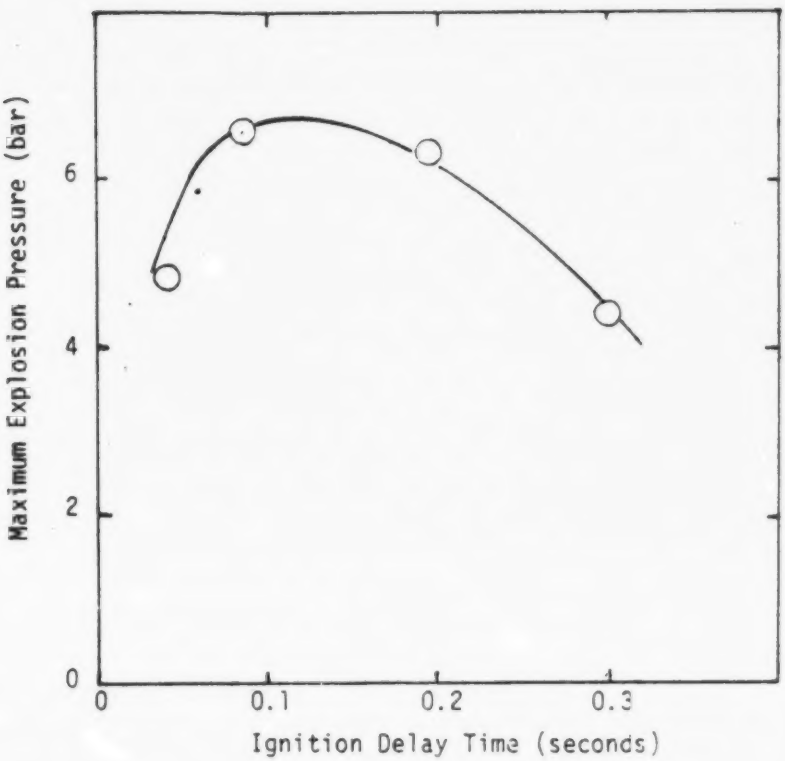

Figure 4 - Effect of ignition delay time upon dust explosion

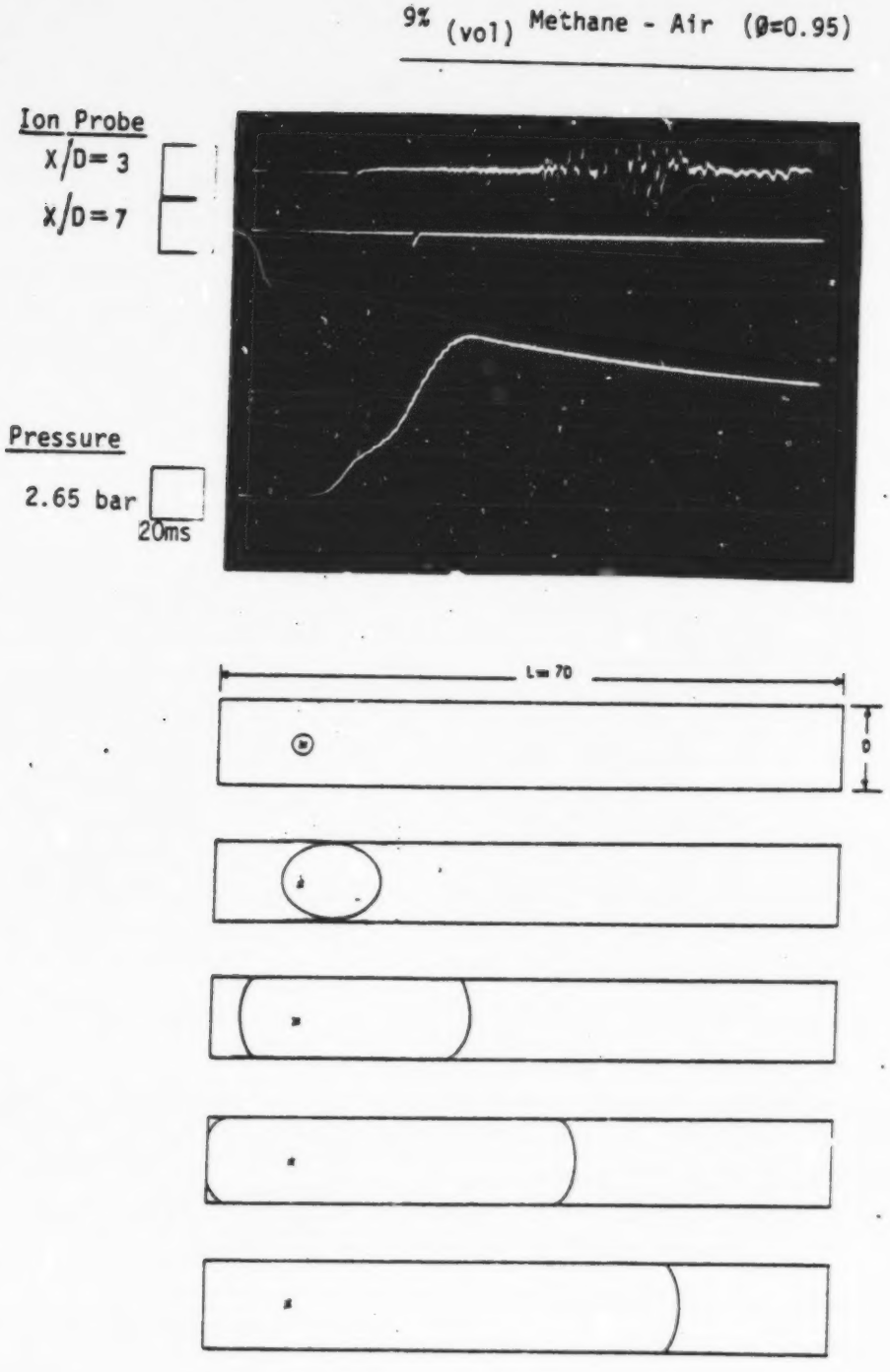

Figure 5 - Actual pressure-time history and ion probe signals of 9% methane-air explosion and a schematic of the flame shape

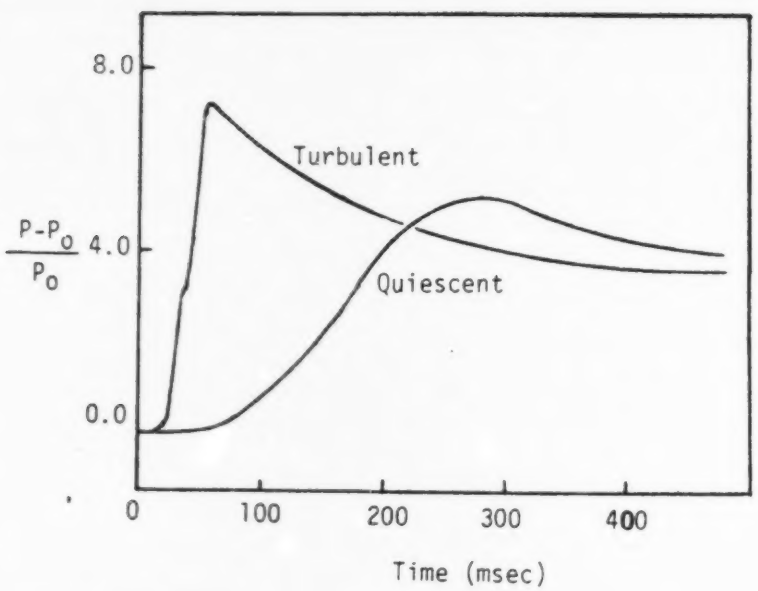

Figure 6- Comparison of turbulent and quiescent burning of 9% methane-air in the Long Horizontal Tube.

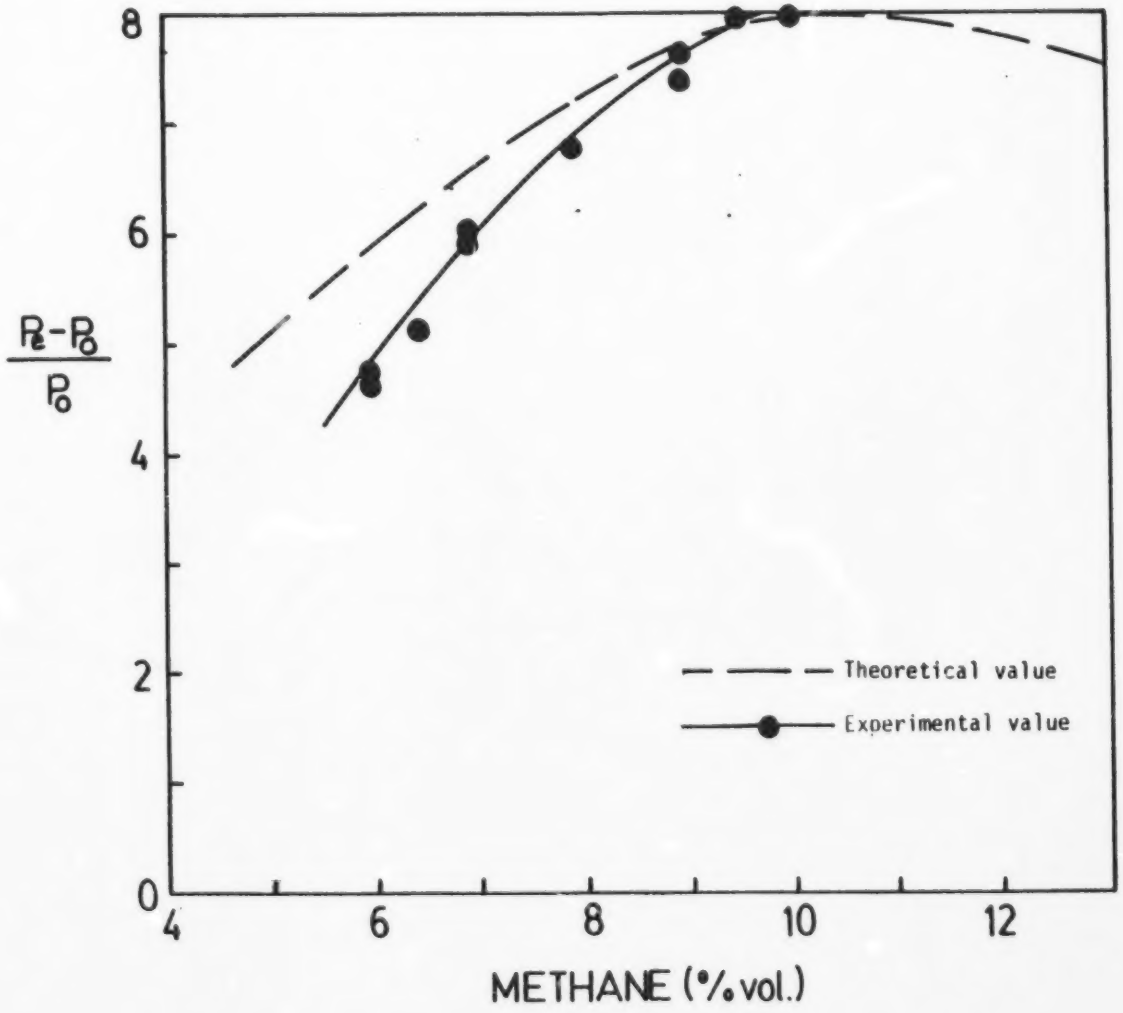

Figure 7 - Maximum explosion pressure for different methane-air mixtures, theory and experiment

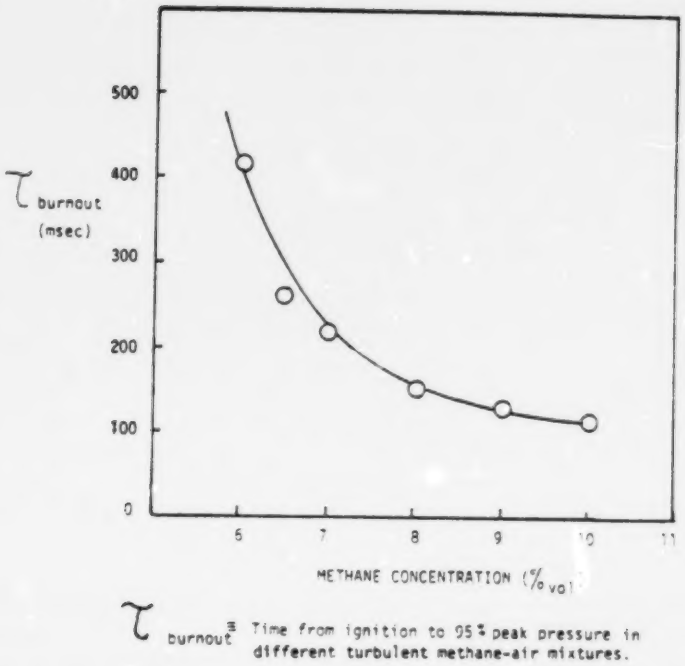

Figure 8a - Burnout time for different methane-air mixtures

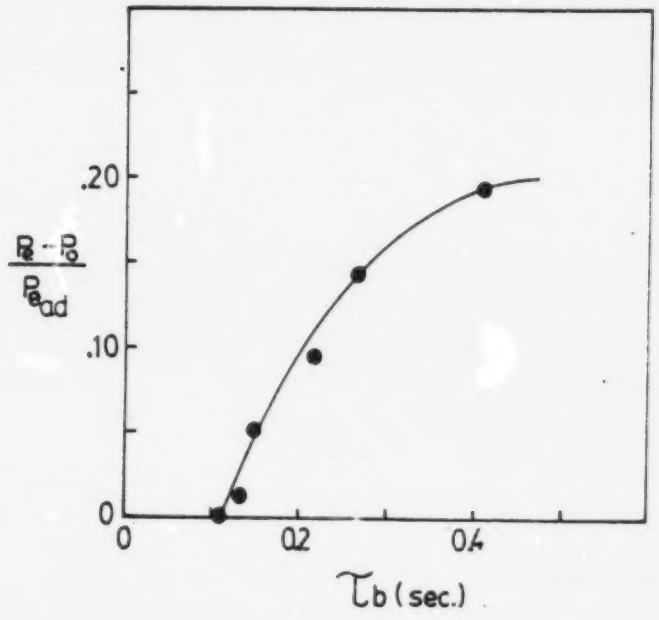

Figure 8b - Comparison of heat loss in the LHT versus the burnout time for a gas explosion

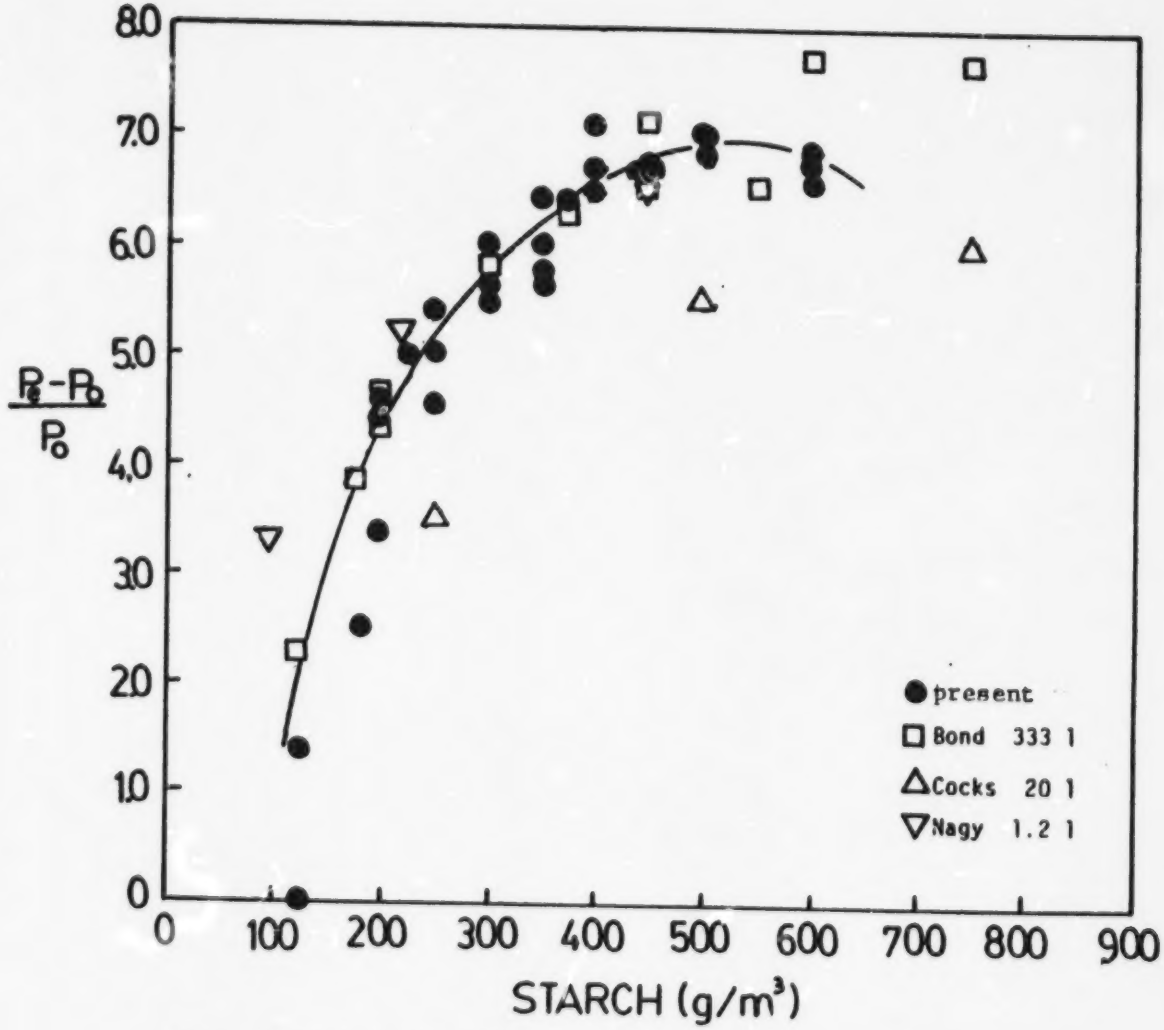

Figure 9 - Maximum explosion pressure for different cornstarch-air mixtures

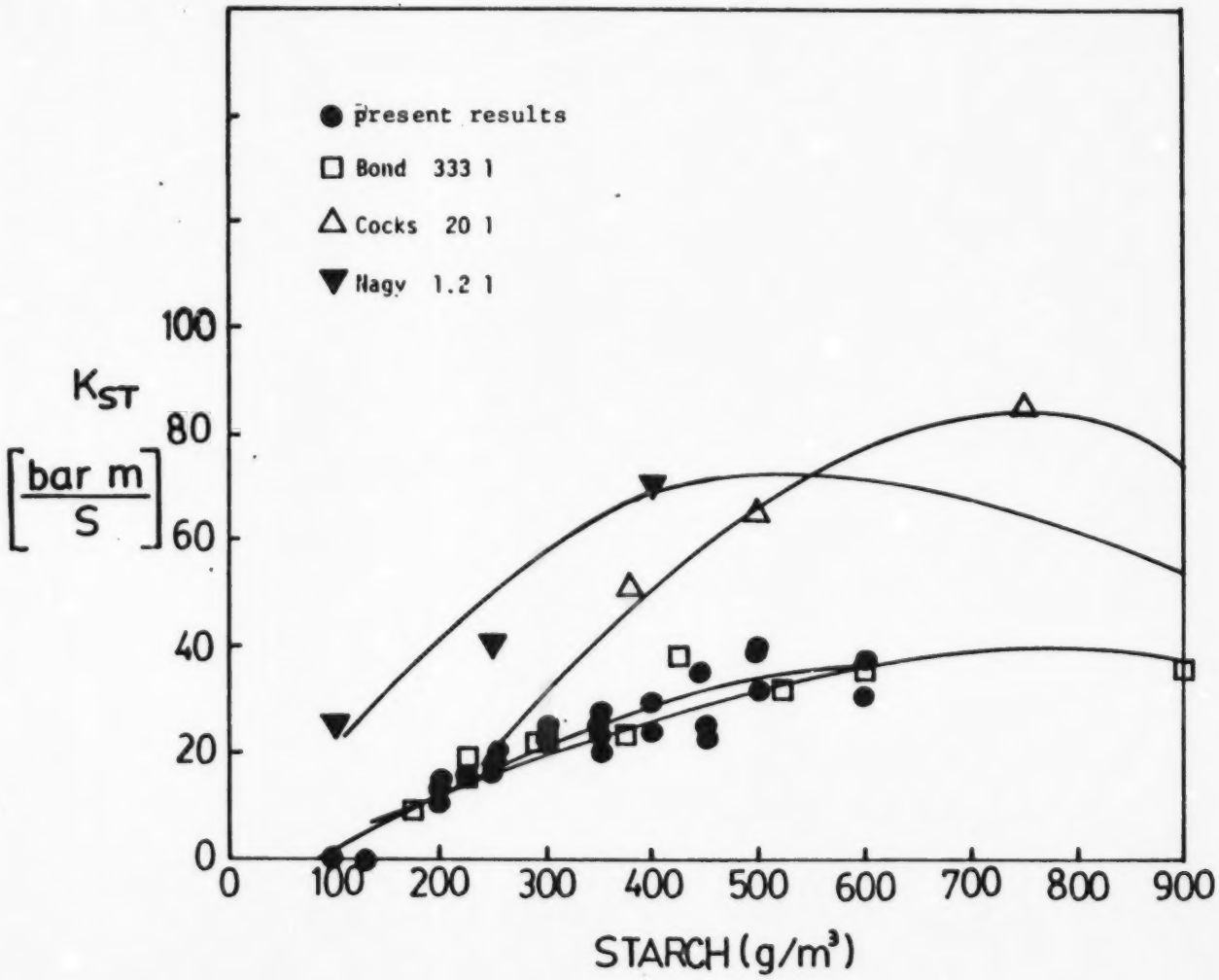

Figure 10 - K_{st} factor for different cornstarch-air mixtures, comparison with other investigators

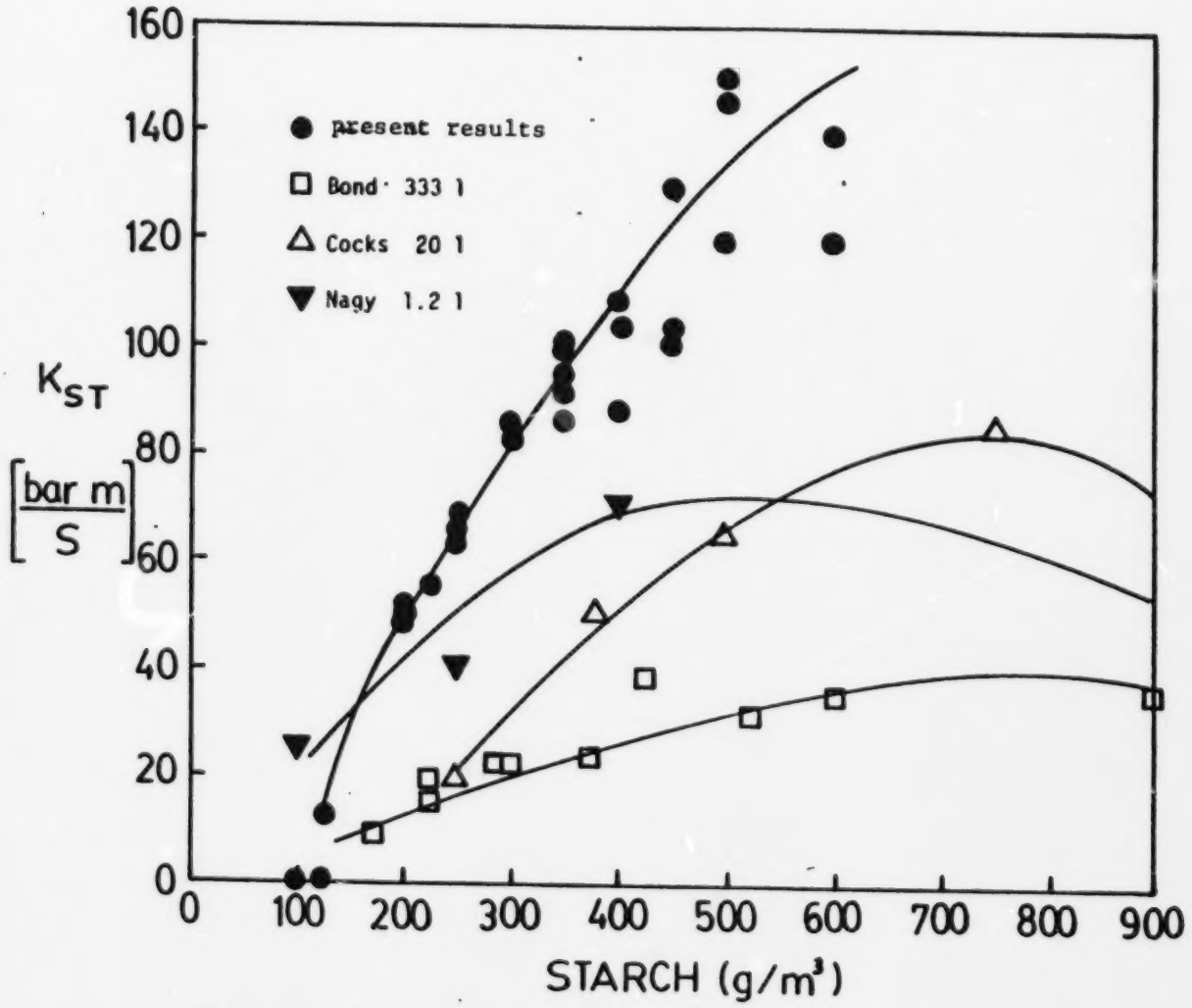

Figure 11 - K_{st} factor using characteristic length of flame travel instead of $V^{1/3}$

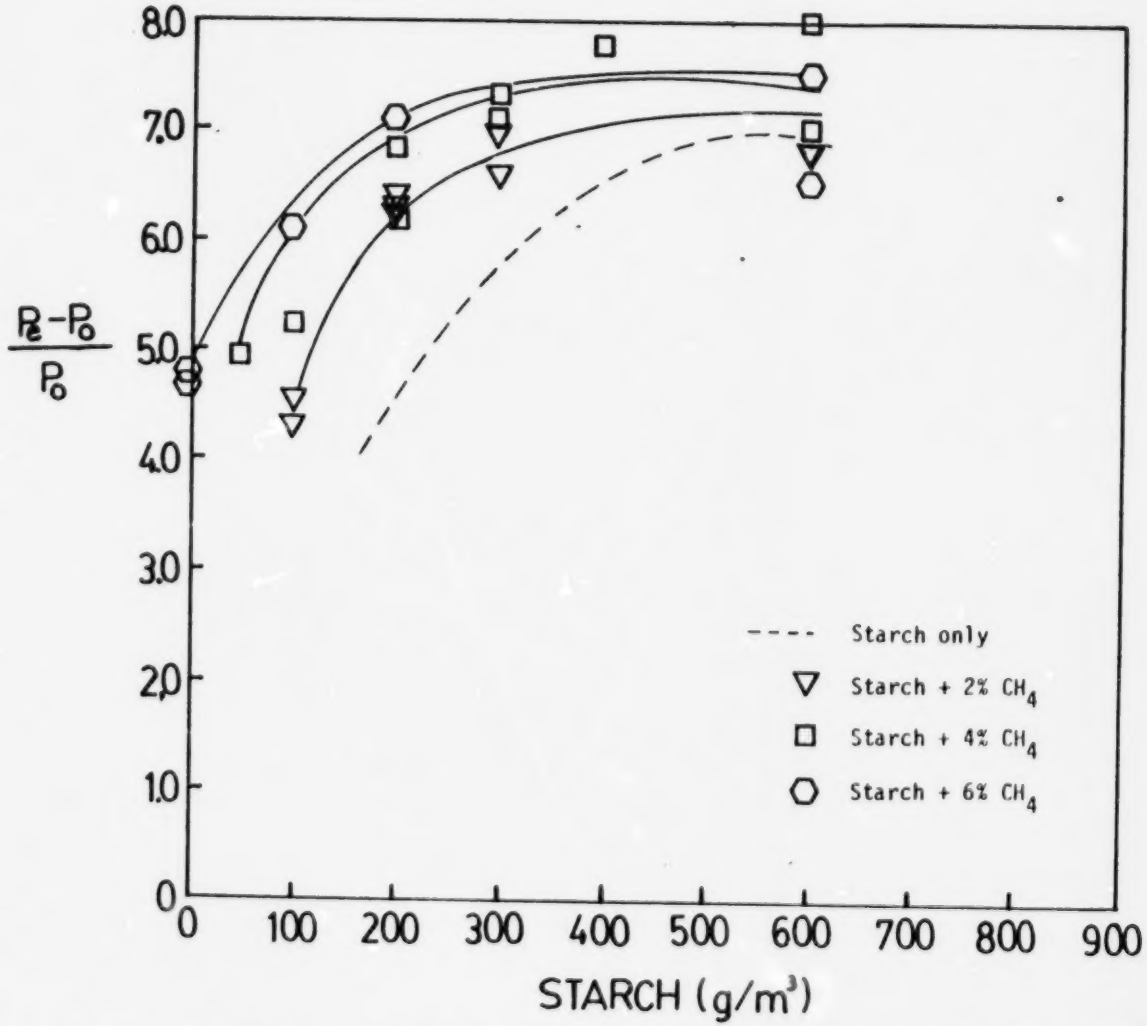

Figure 12 - Maximum explosion pressure for different cornstarch-methane-air mixtures

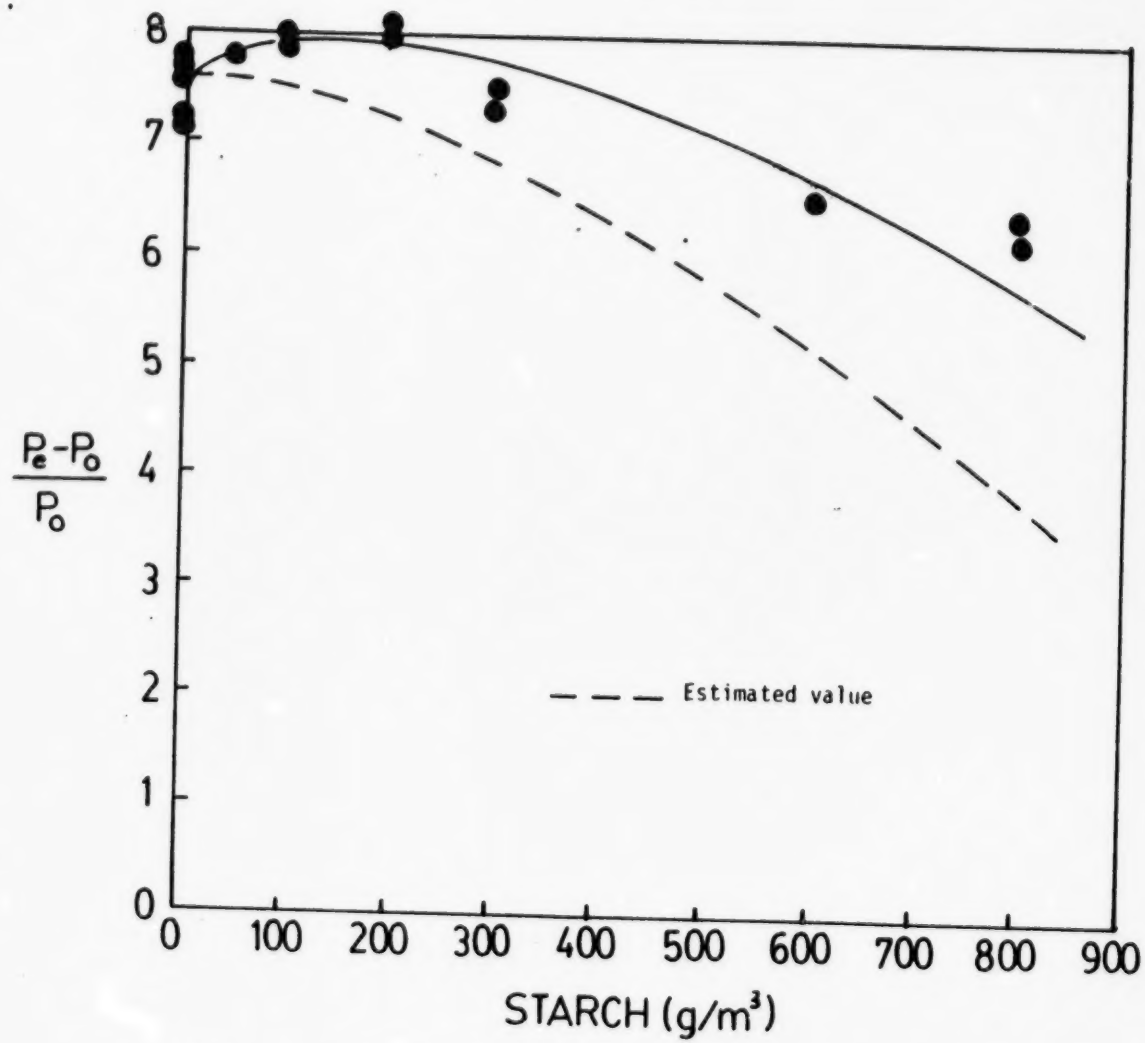

Figure 13 - Maximum explosion pressure for different cornstarch-air concentrations with 9% methane

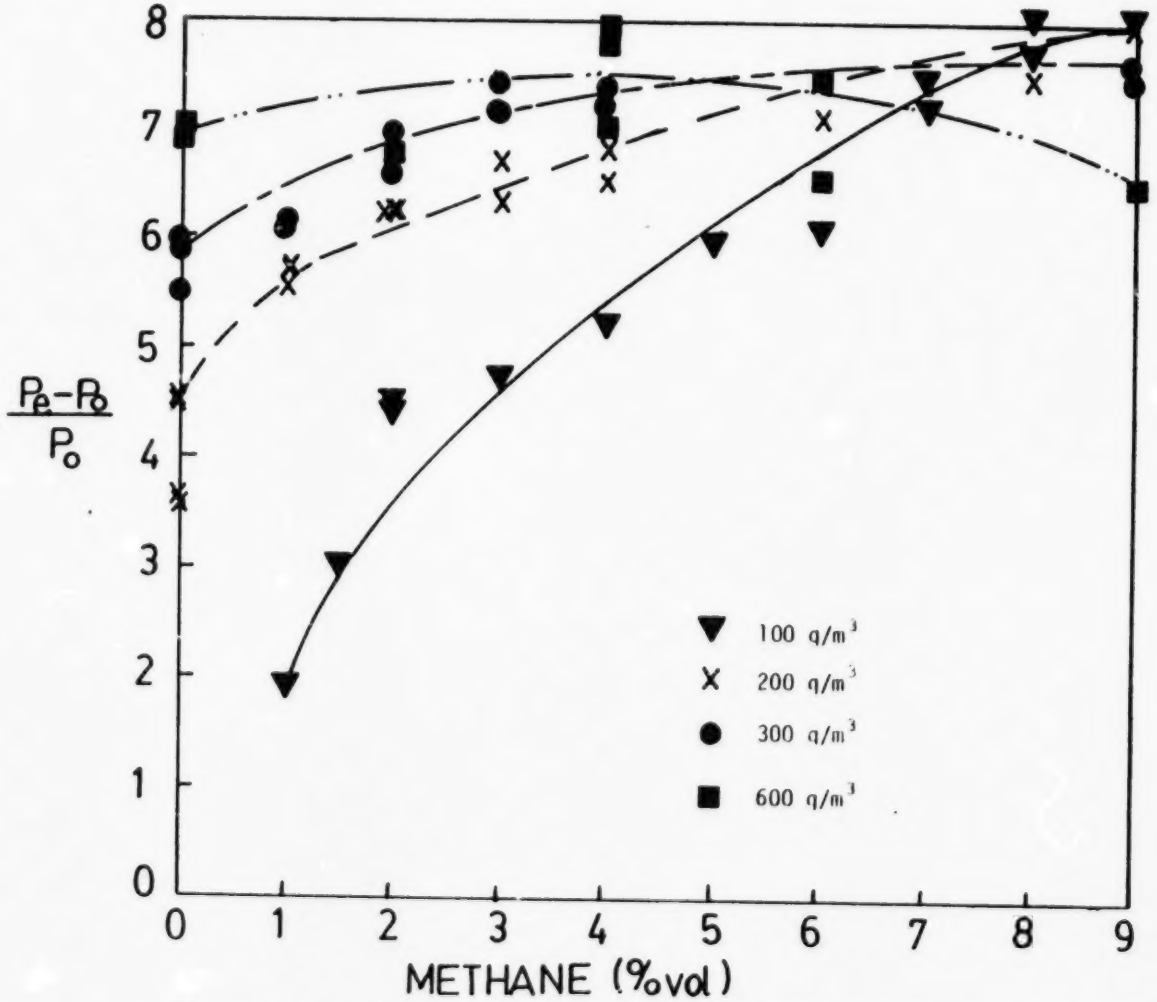

Figure 14 - Maximum explosion pressure for different cornstarch-methane-air mixtures

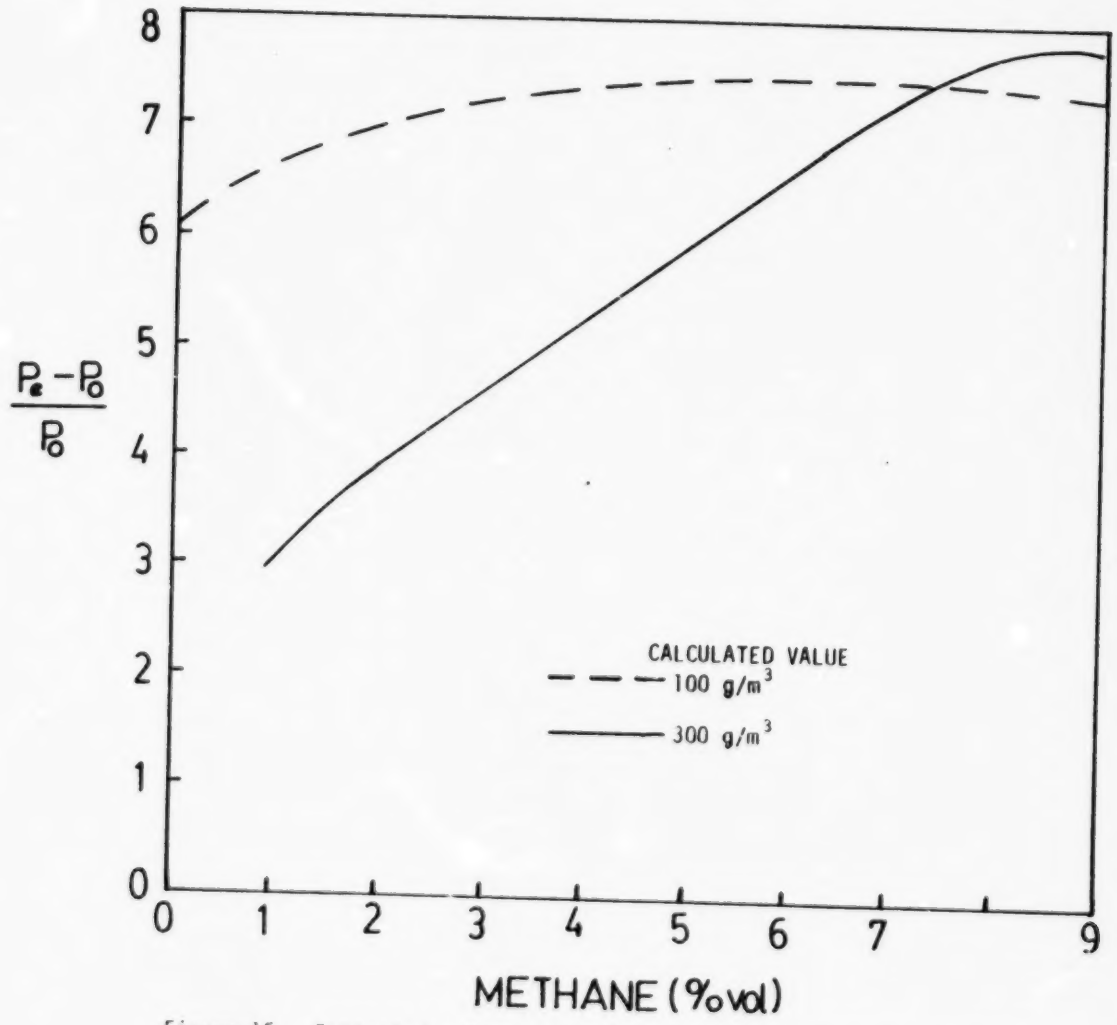

Figure 15 - Estimated values for maximum explosion pressure of different methane-air mixtures with 100 g/m³ and 300 g/m³ starch

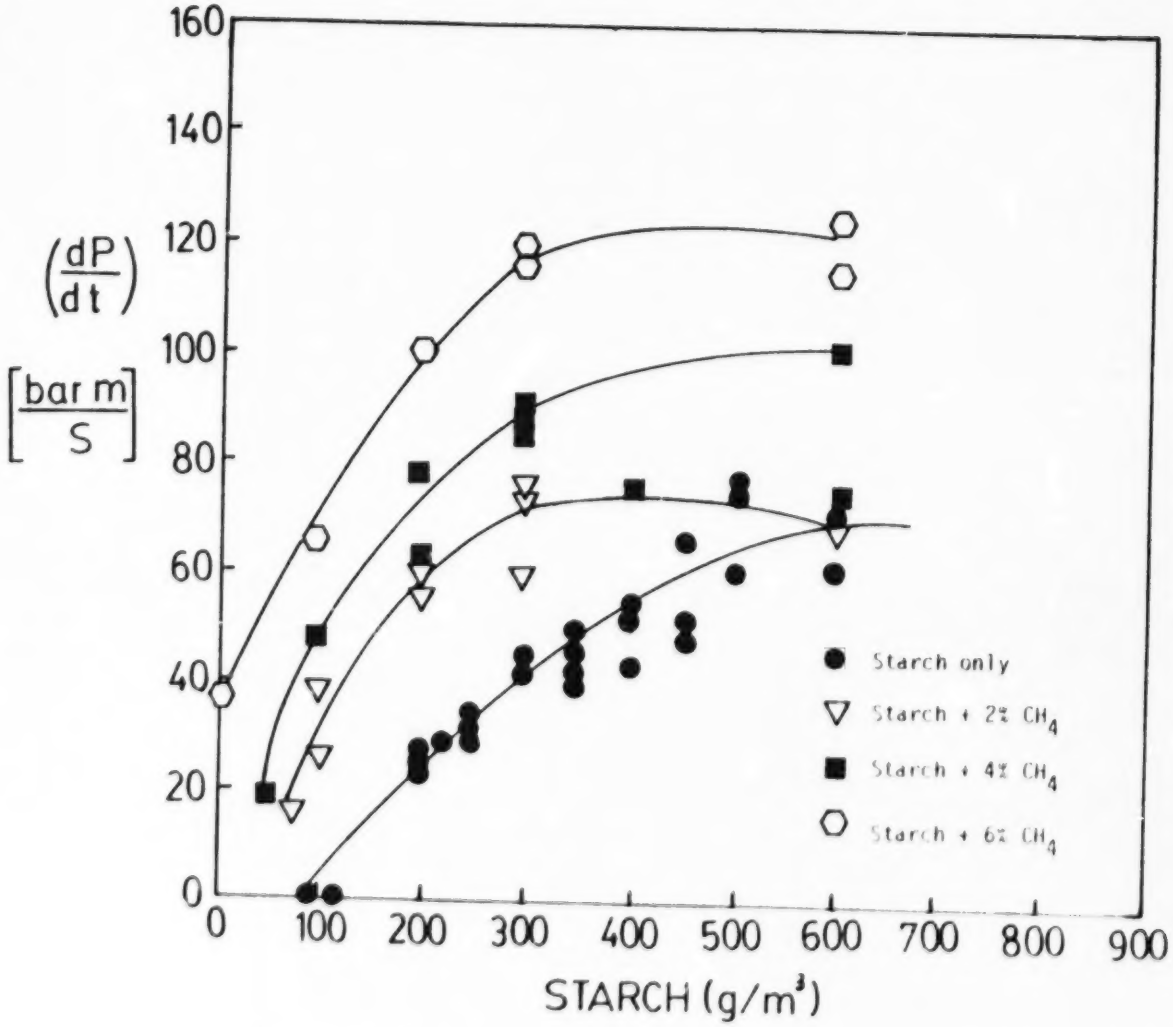

Figure 16 - Rate of pressure rise for different cornstarch-methane-air mixtures

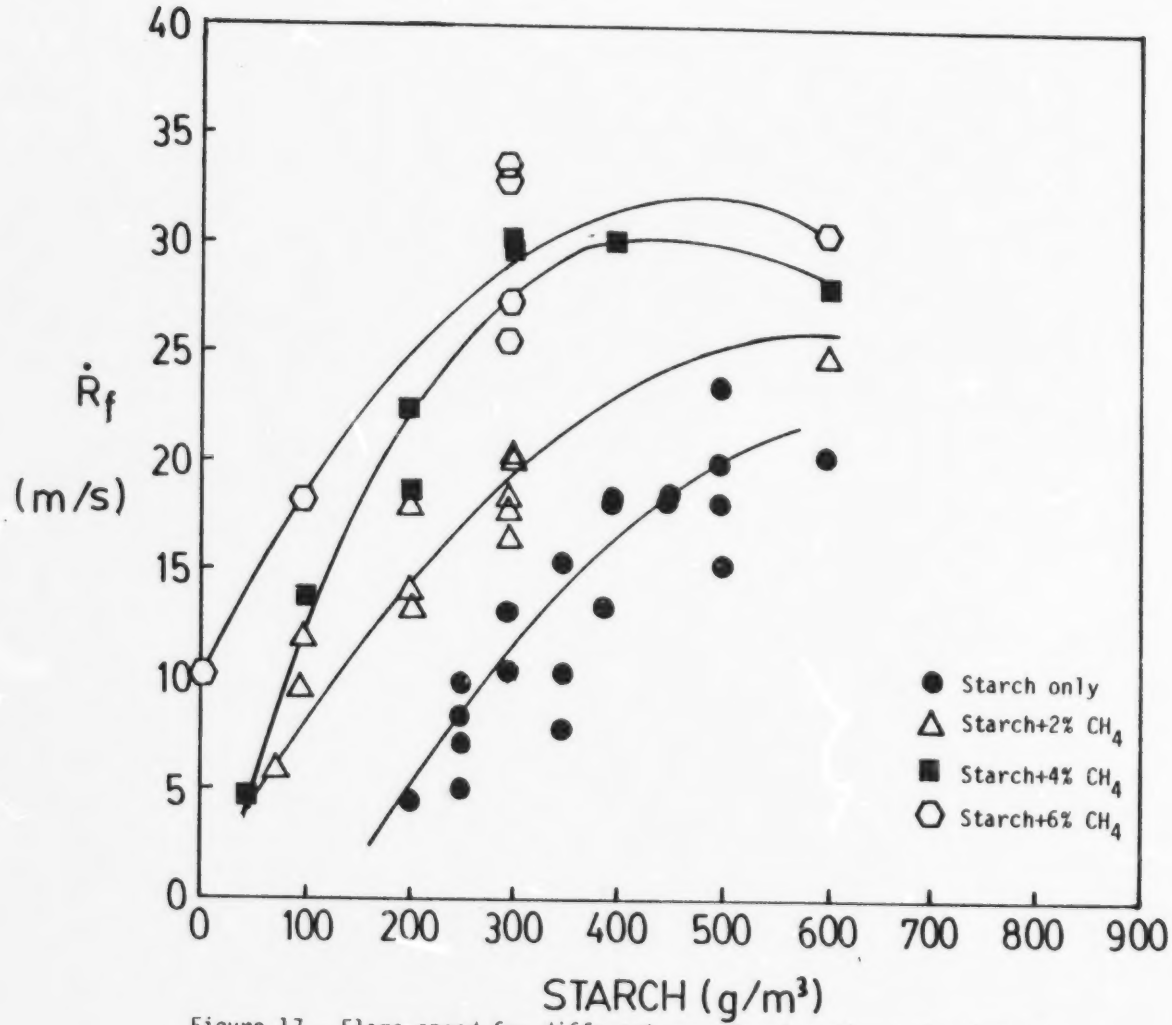

Figure 17 - Flame speed for different cornstarch-methane-air-mixtures

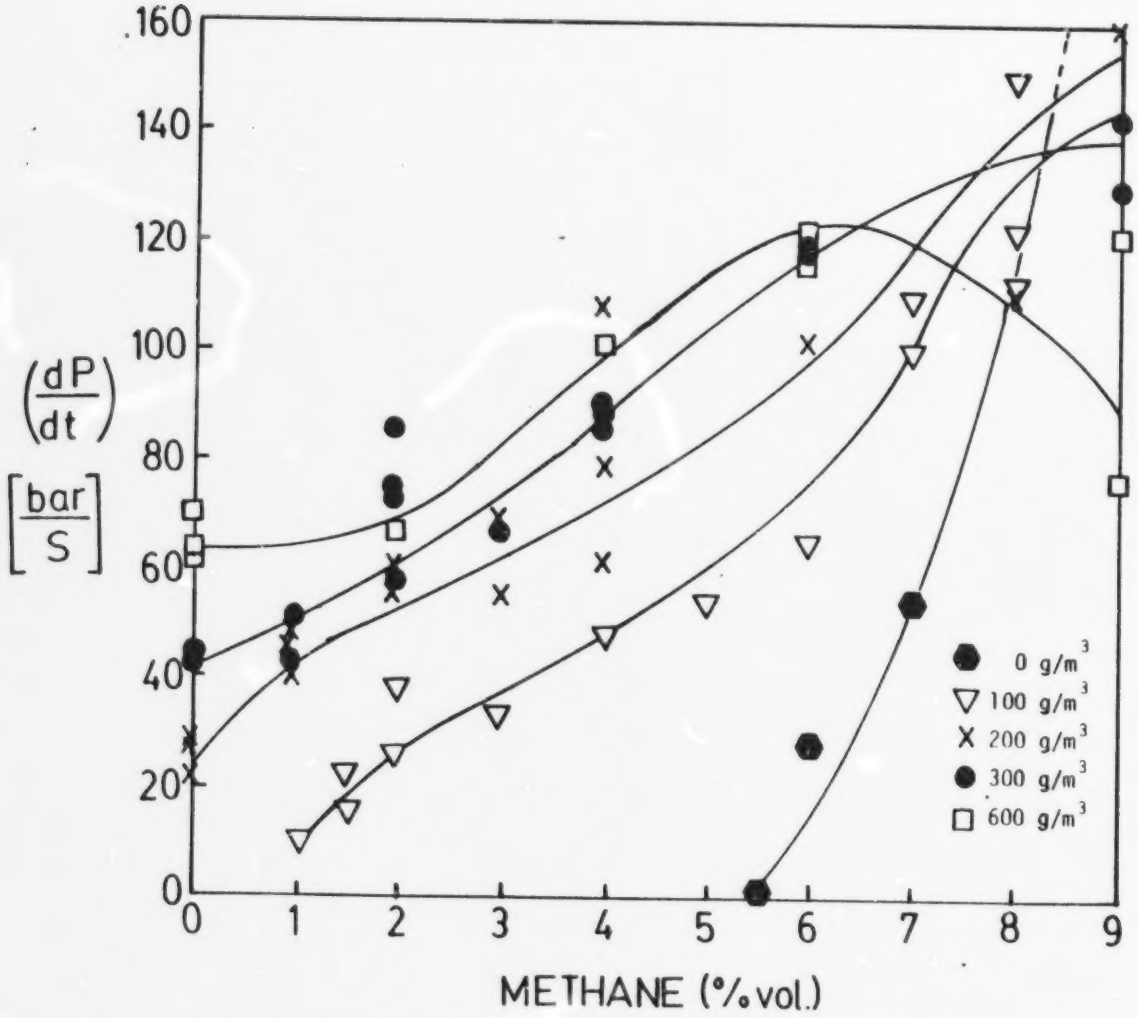

Figure 18 - Rate of pressure rise for different cornstarch-methane-air mixtures

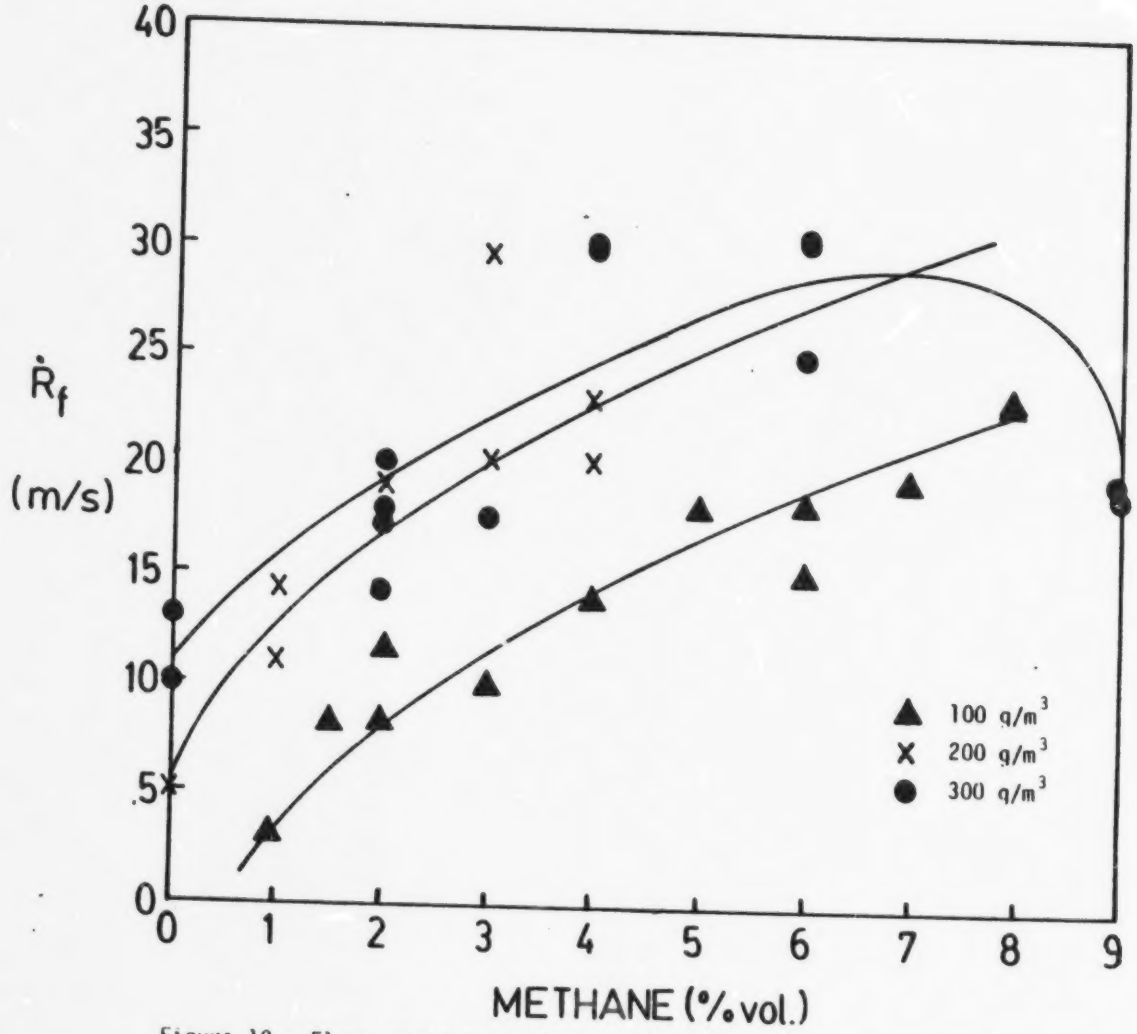

Figure 19 - Flame speed for different cornstarch-methane-air mixtures

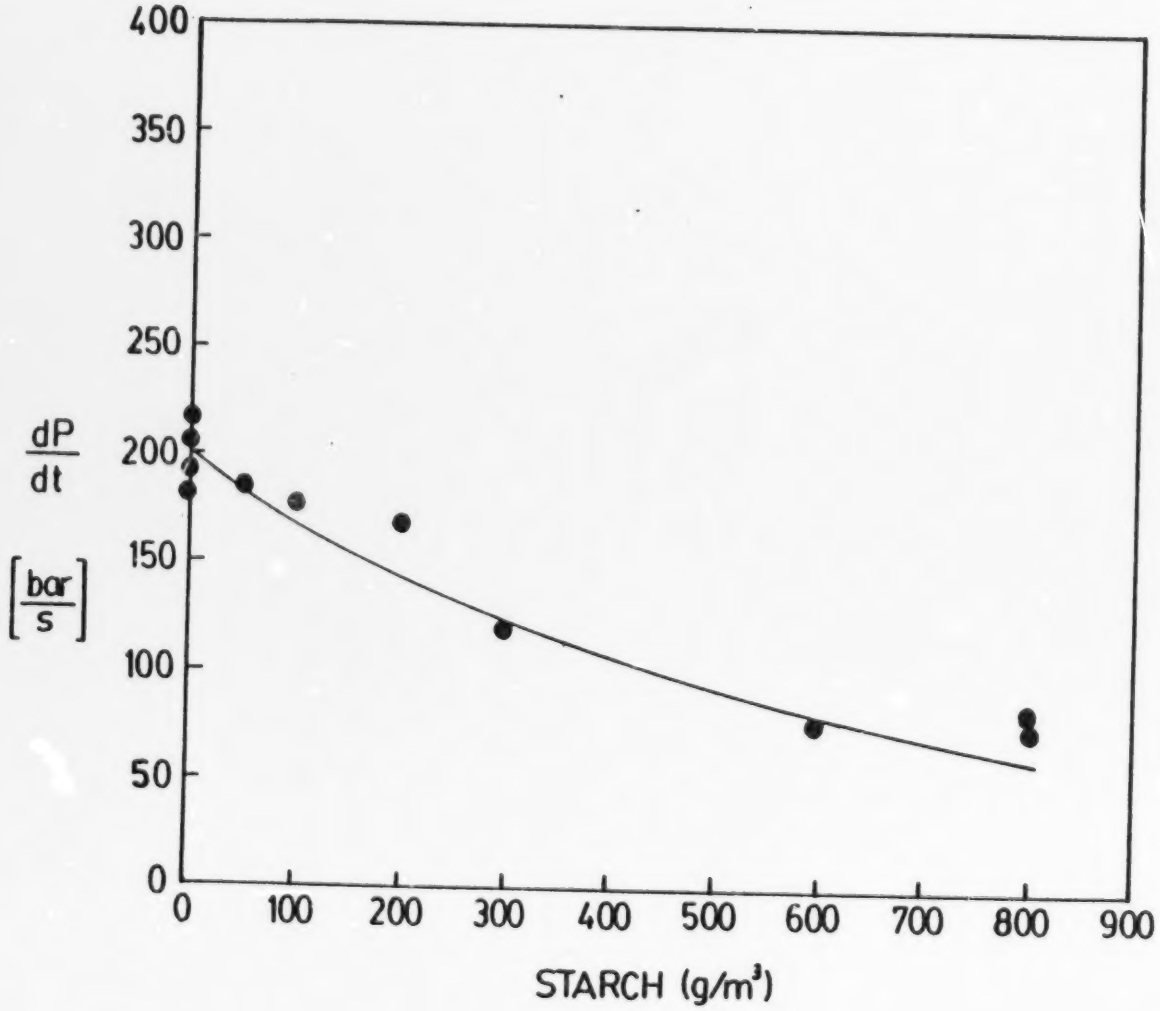

Figure 20 - Rate of pressure rise for different starch concentrations with 9% methane

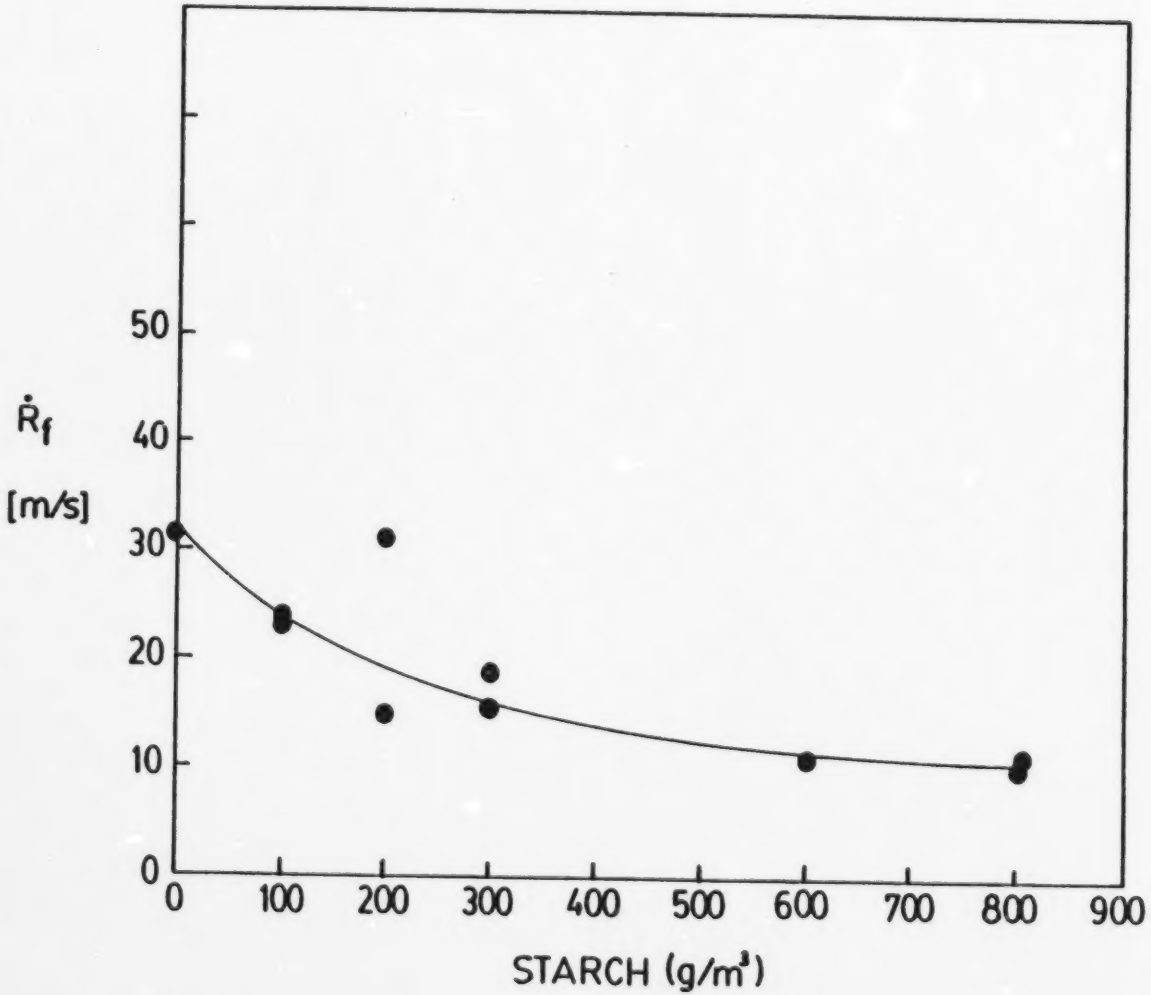

Figure 21 - Flame speed for different starch concentrations with 9% methane

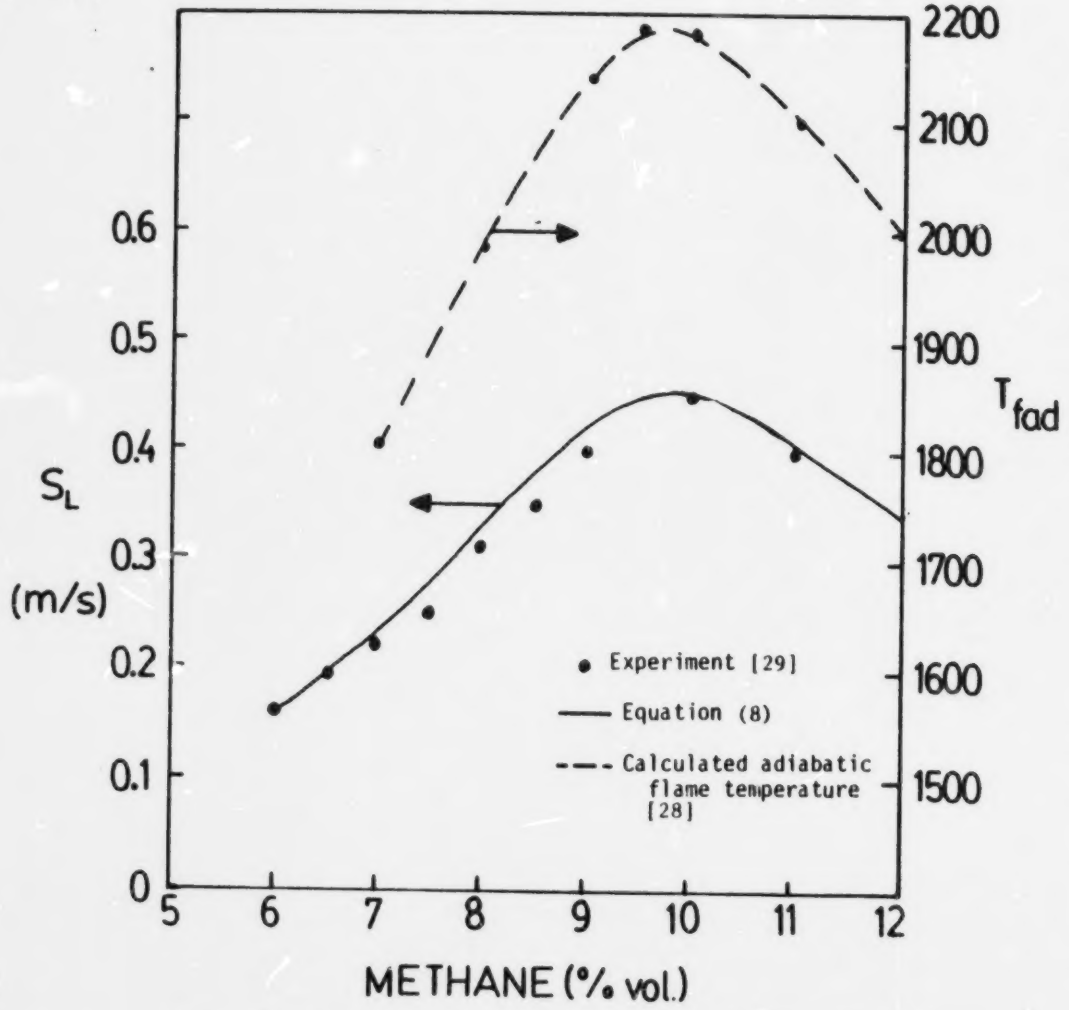

Figure 22 - Laminar burning velocity and flame temperature for different methane-air mixtures

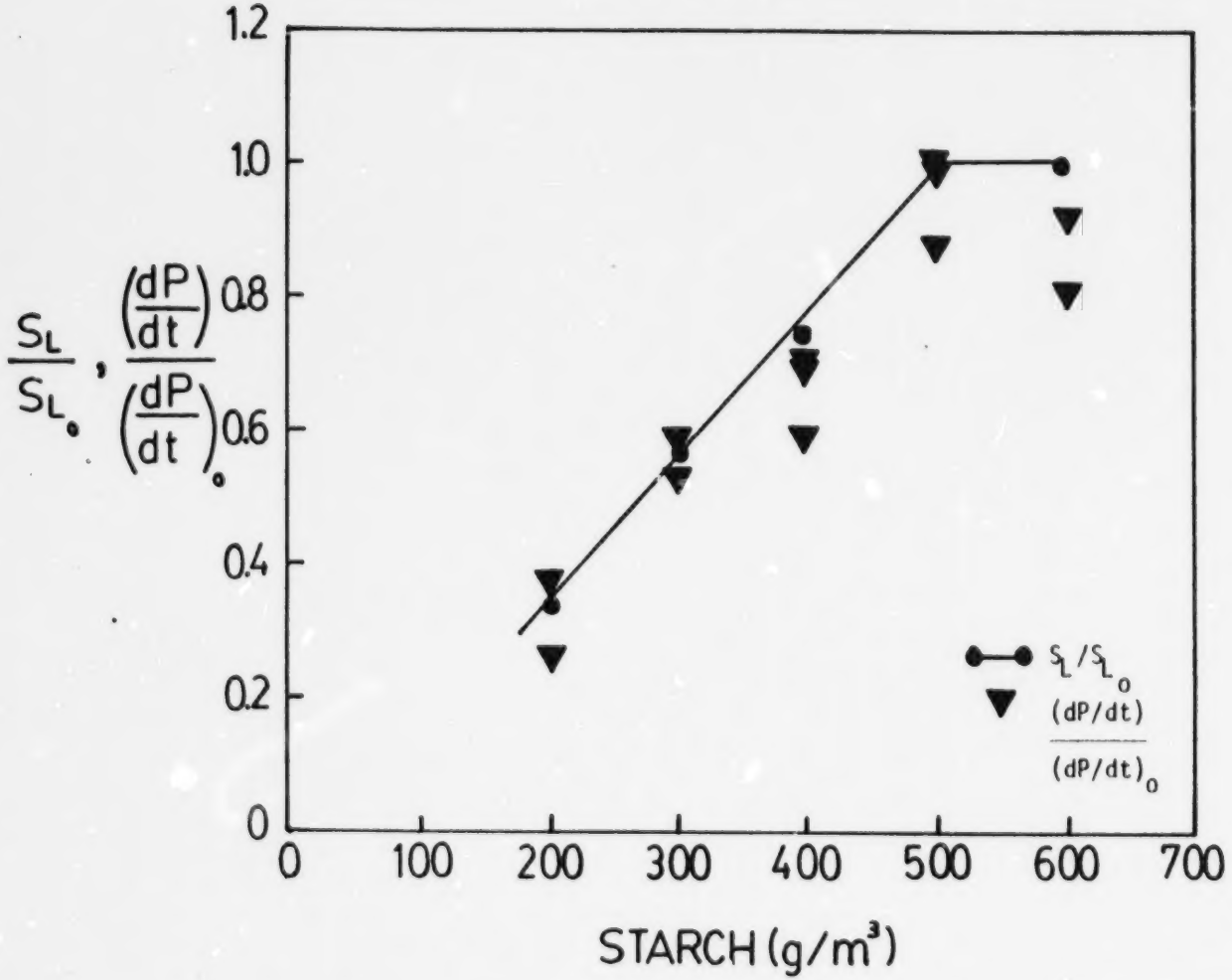

Figure 23 - Comparison of normalized dP/dt and S_L data for different starch-air mixtures

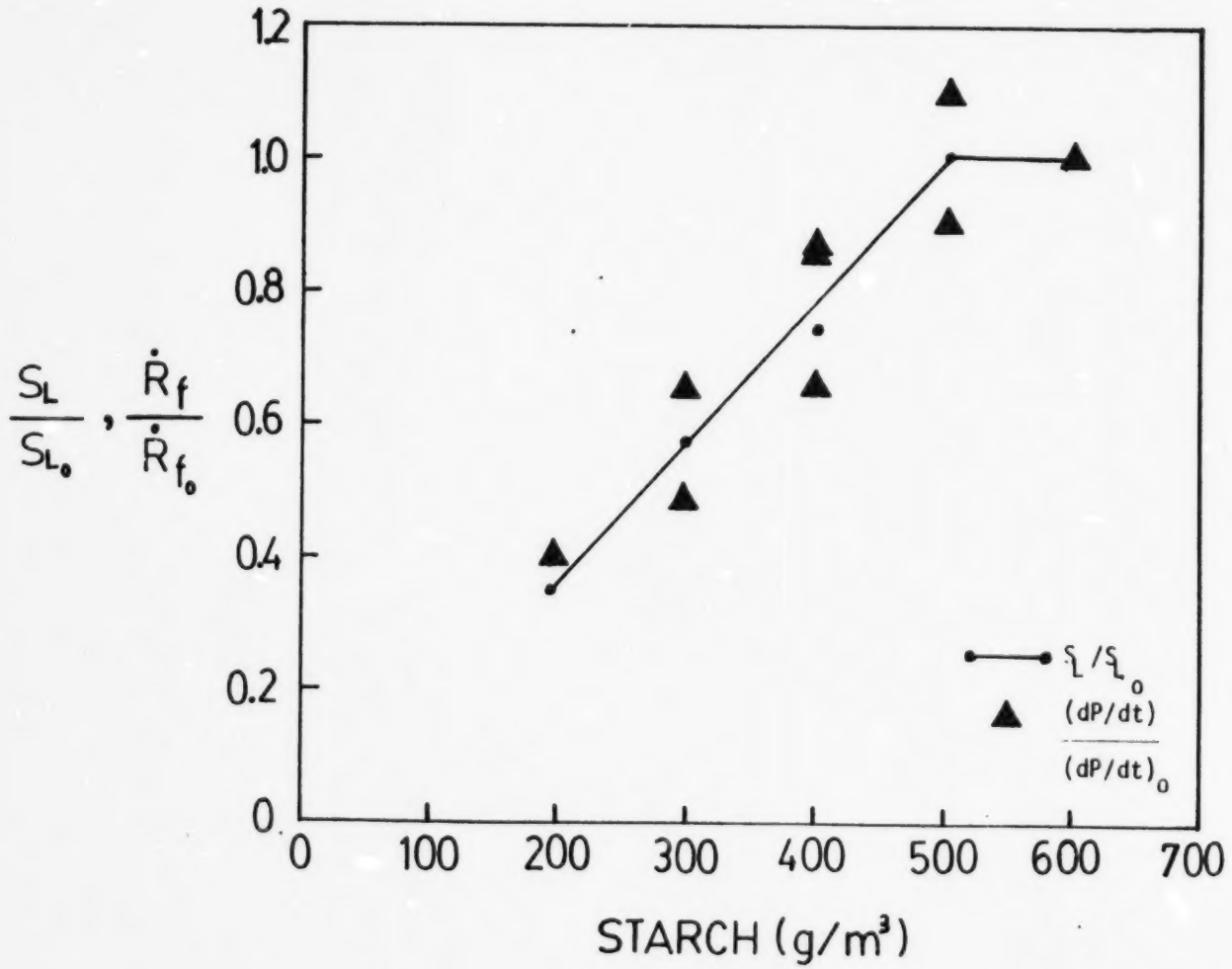

Figure 24 - Comparison for normalized $\dot{R}_f$ and S_L data for different starch-air mixtures

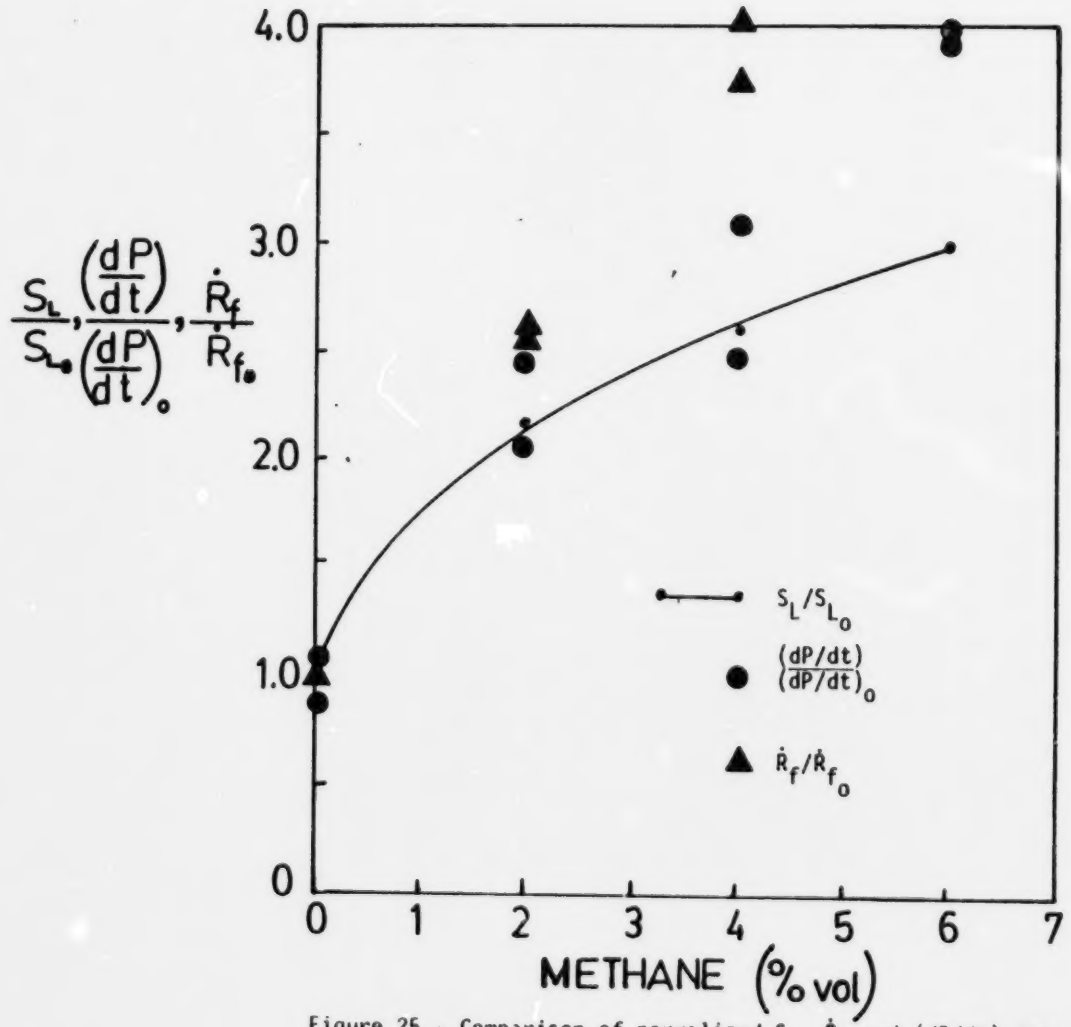

Figure 25 - Comparison of normalized S_L, $\dot{R}_f$ and (dP/dt) data for different methane-air mixtures with 200 g/m^3 starch

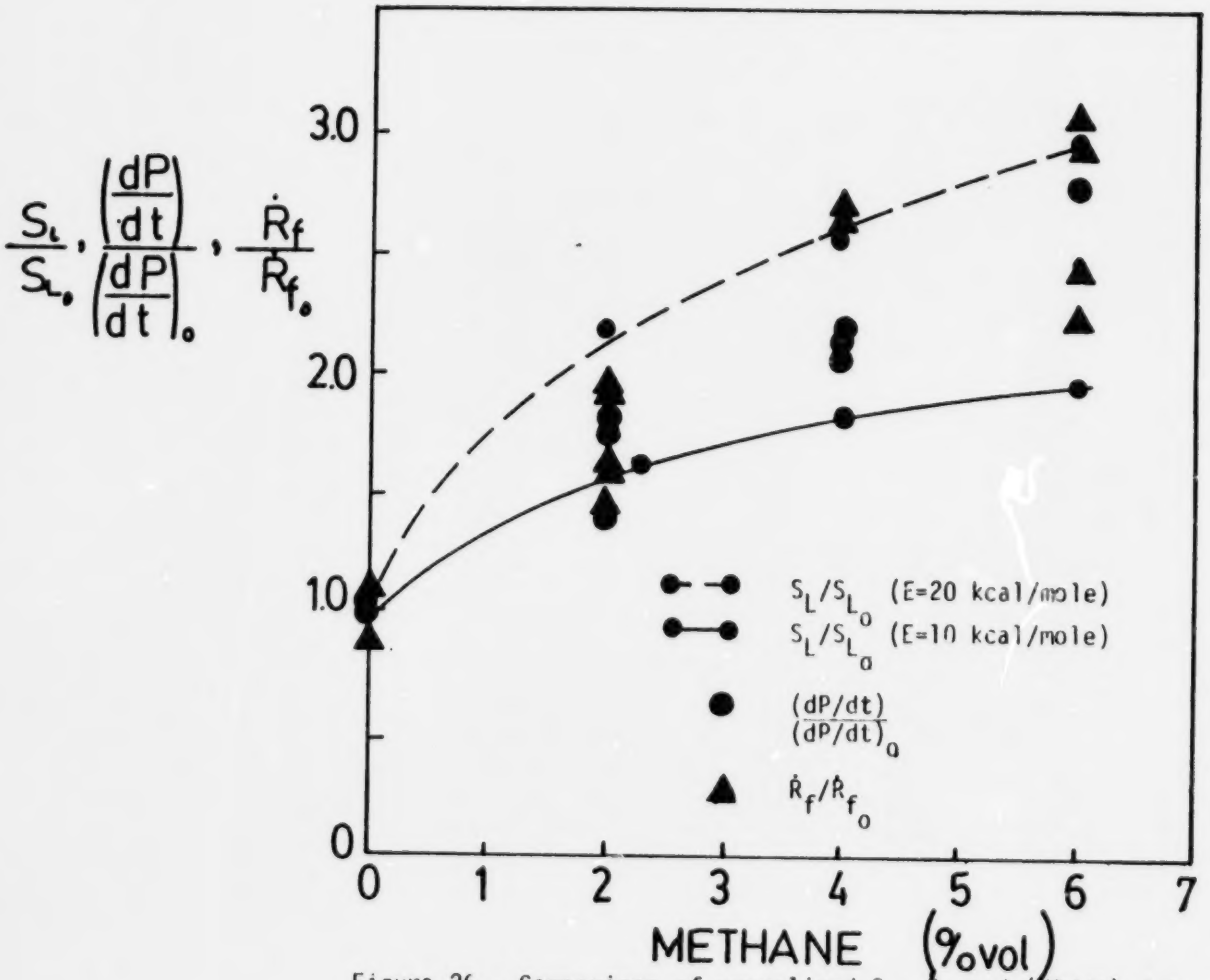

Figure 26 - Comparison of normalized S_L, $\dot{R}_f$ and (dP/dt) data for different methane-air mixtures with 300 g/m^3 starch

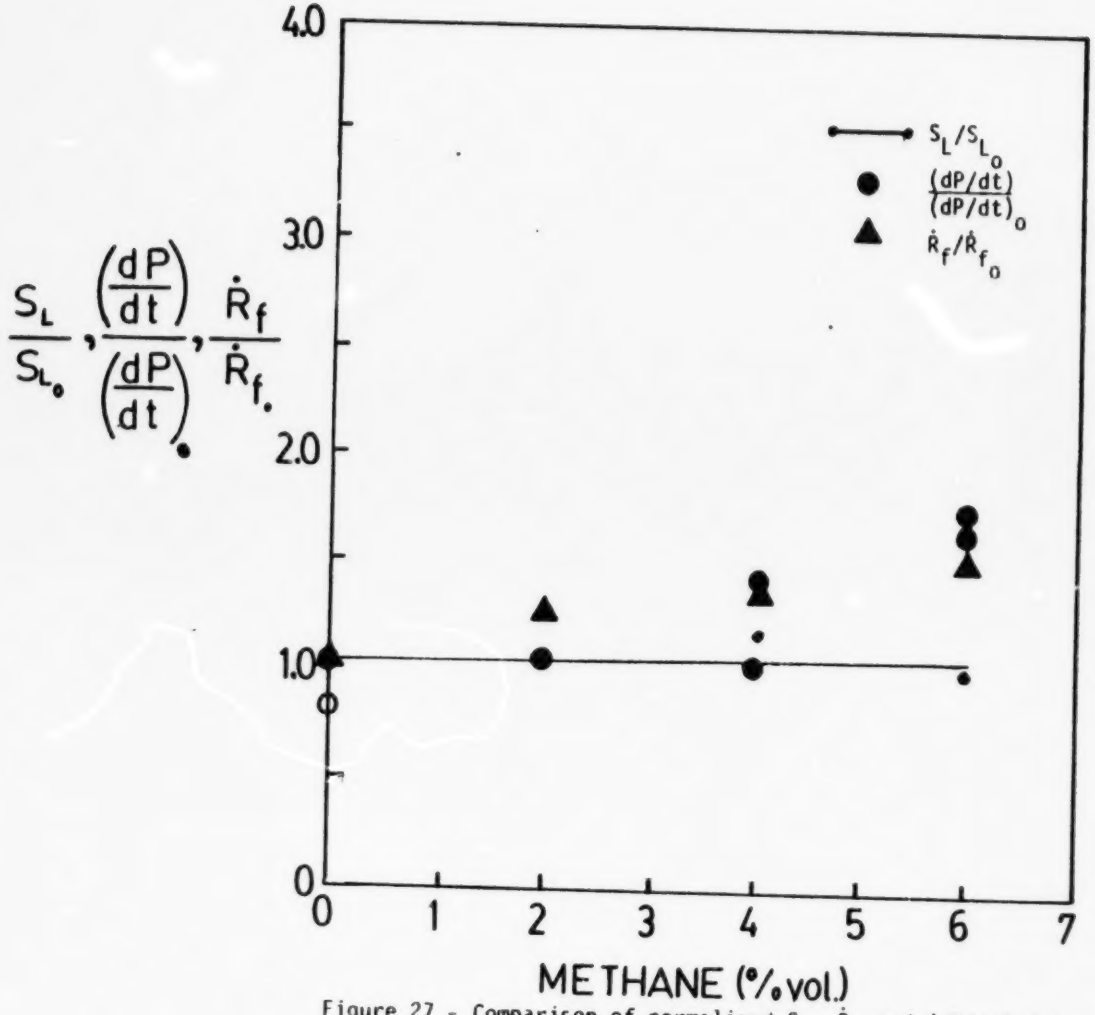

Figure 27 - Comparison of normalized S_L, $\dot{R}_f$ and (dP/dt) data for different methane-air mixtures with 600 g/m^3 starch

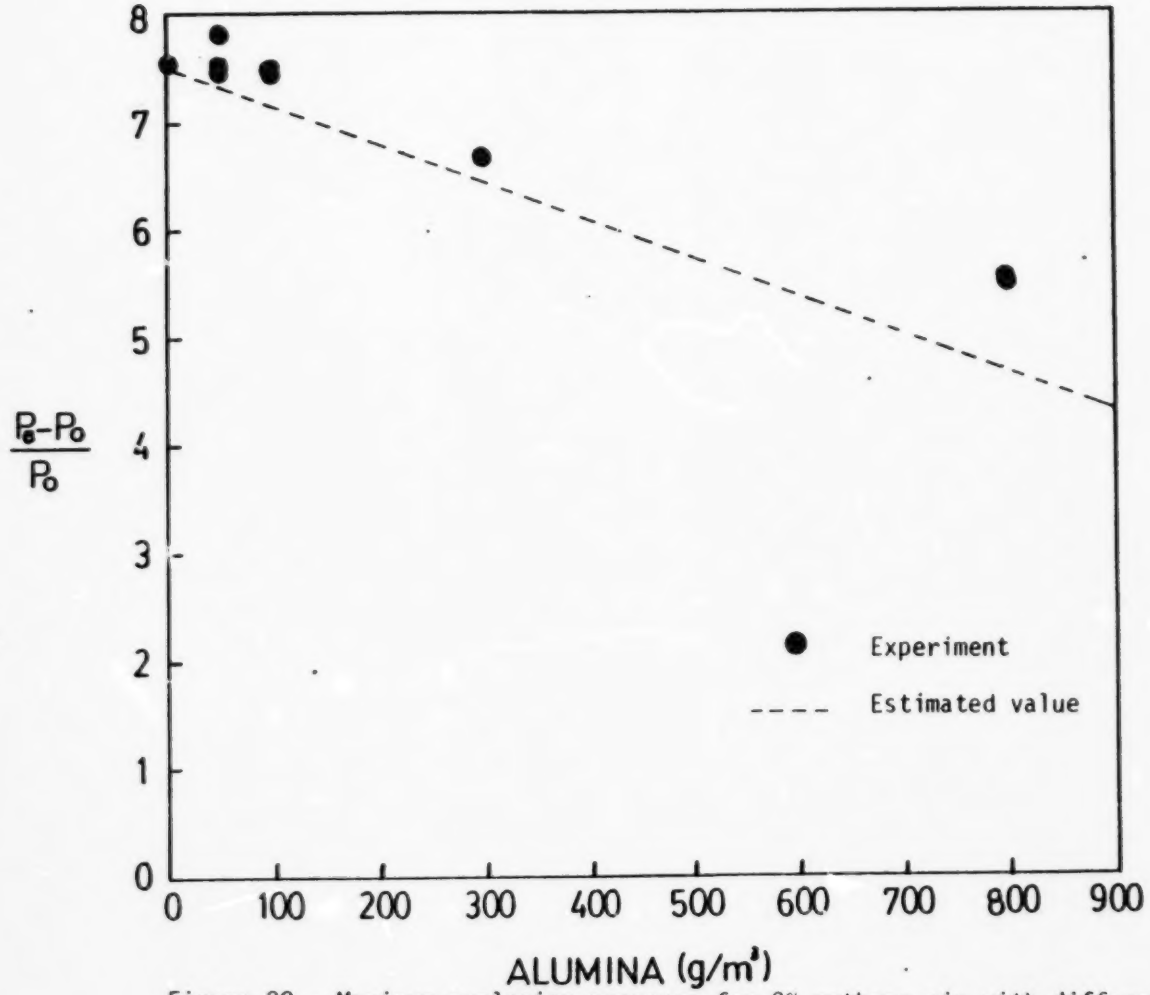

Figure 28 - Maximum explosion pressure for 9% methane-air with different concentrations of aluminum-oxide

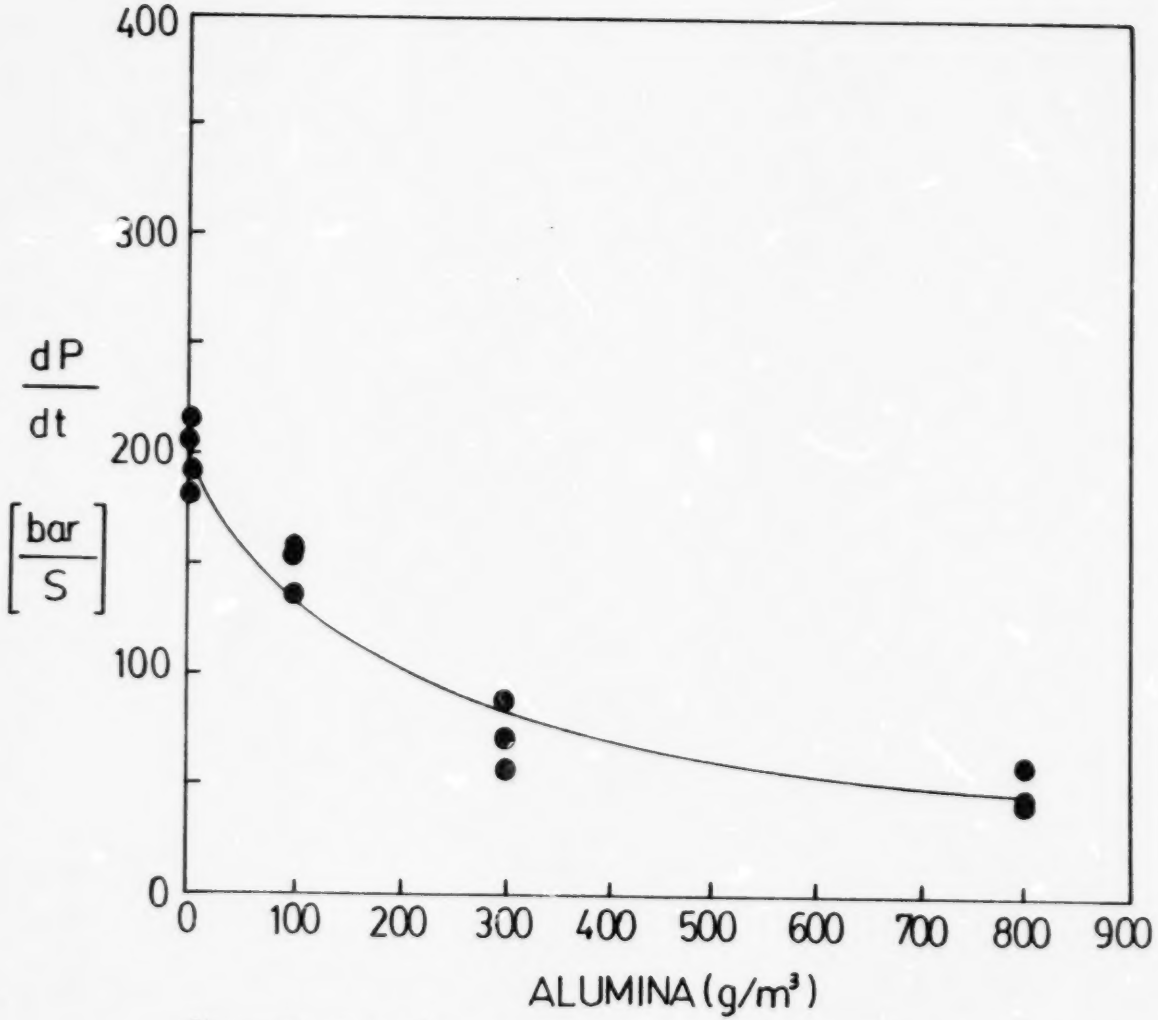

Figure 29 - Rate of pressure rise for 9% methane-air with different concentrations of aluminum-oxide

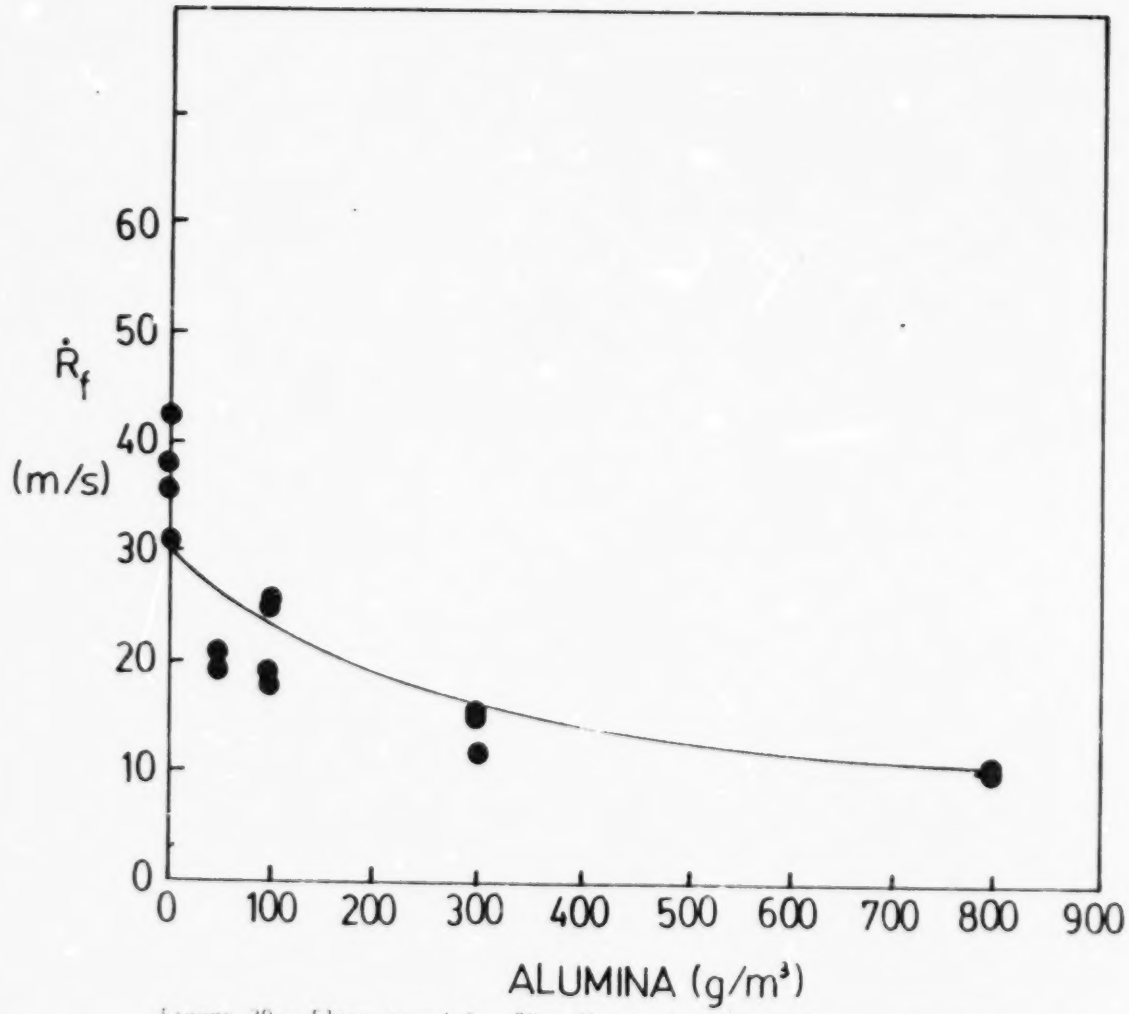

Figure 30 - Flame speed for 9% methane-air with different concentrations of aluminum oxide

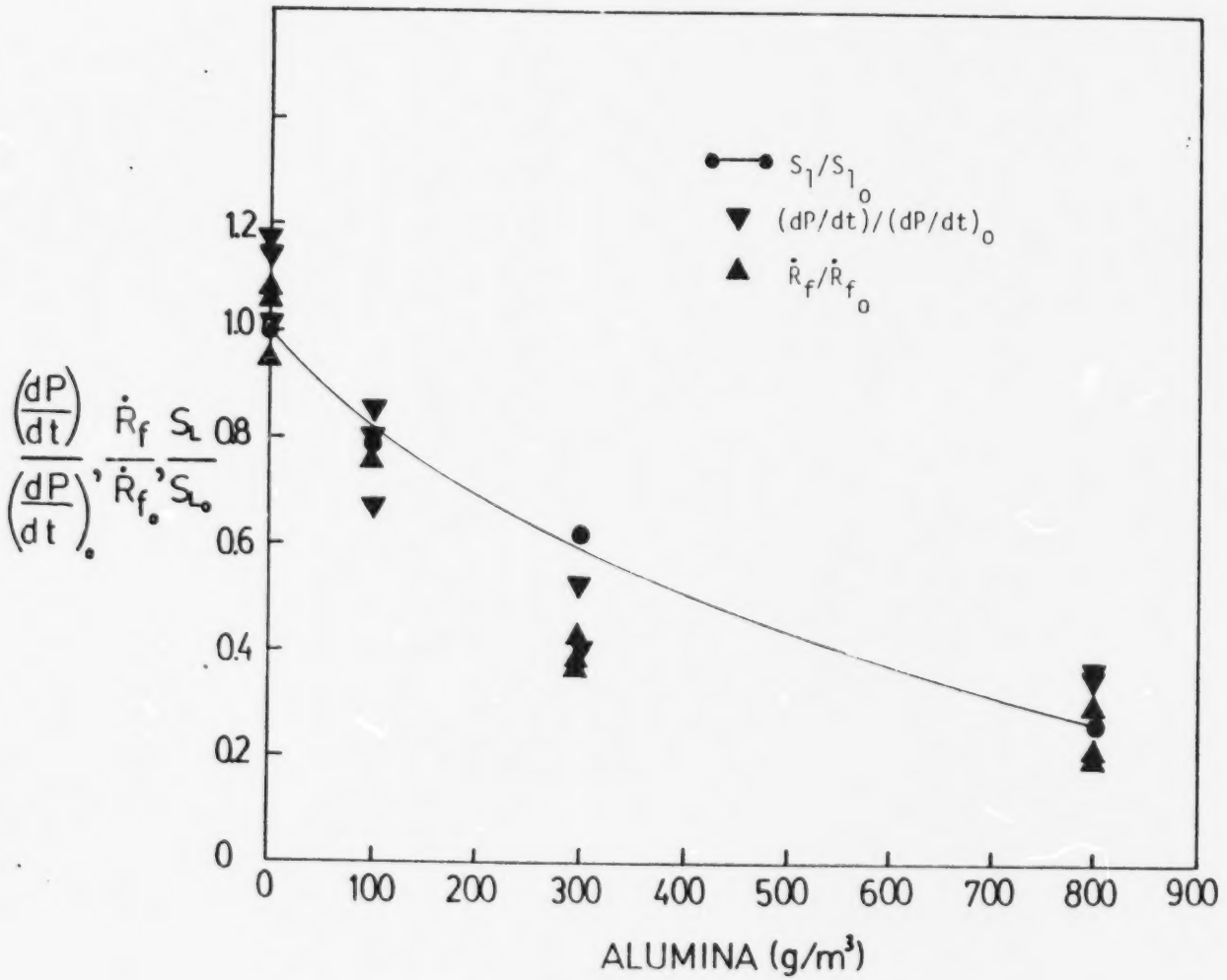

Figure 31 - Comparison of normalized S_l, $\dot{R}_f$ and (dP/dt) for 9% methane-air with different concentrations of aluminum-oxide

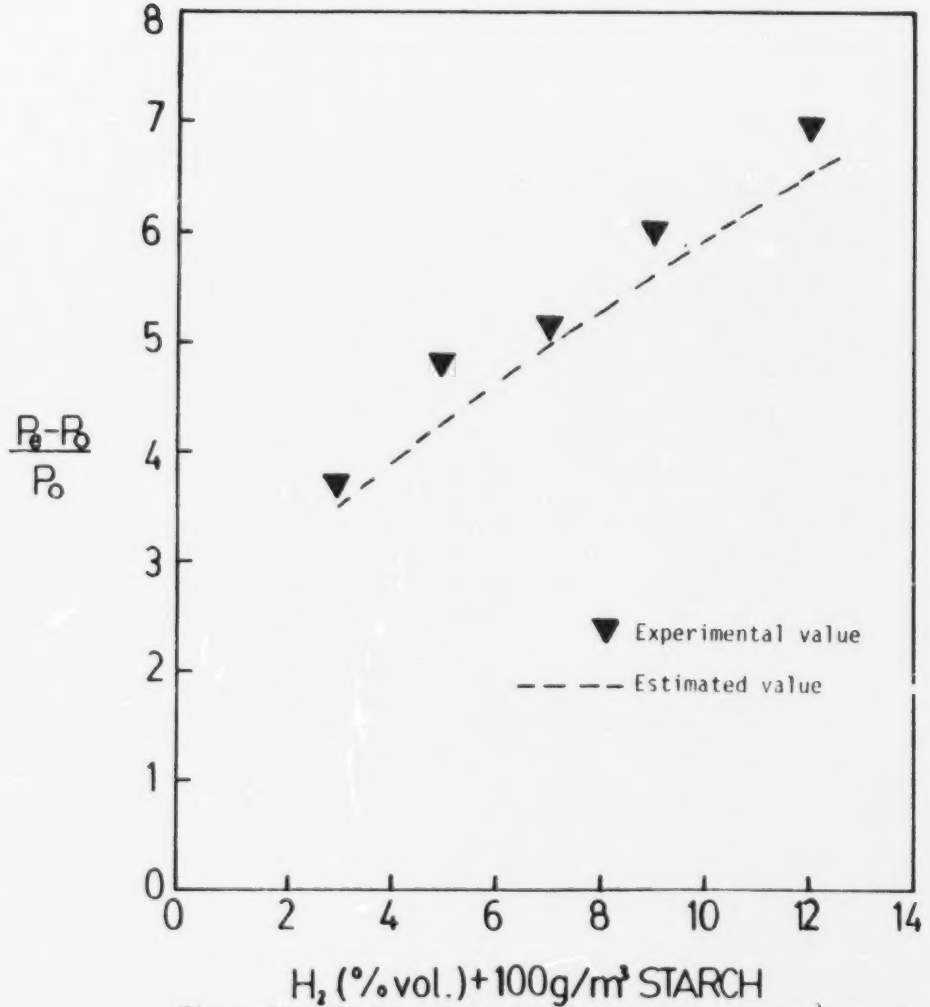

Figure 32 - Maximum explosion pressure for 100 g/m^3 starch with different hydrogen-air mixtures

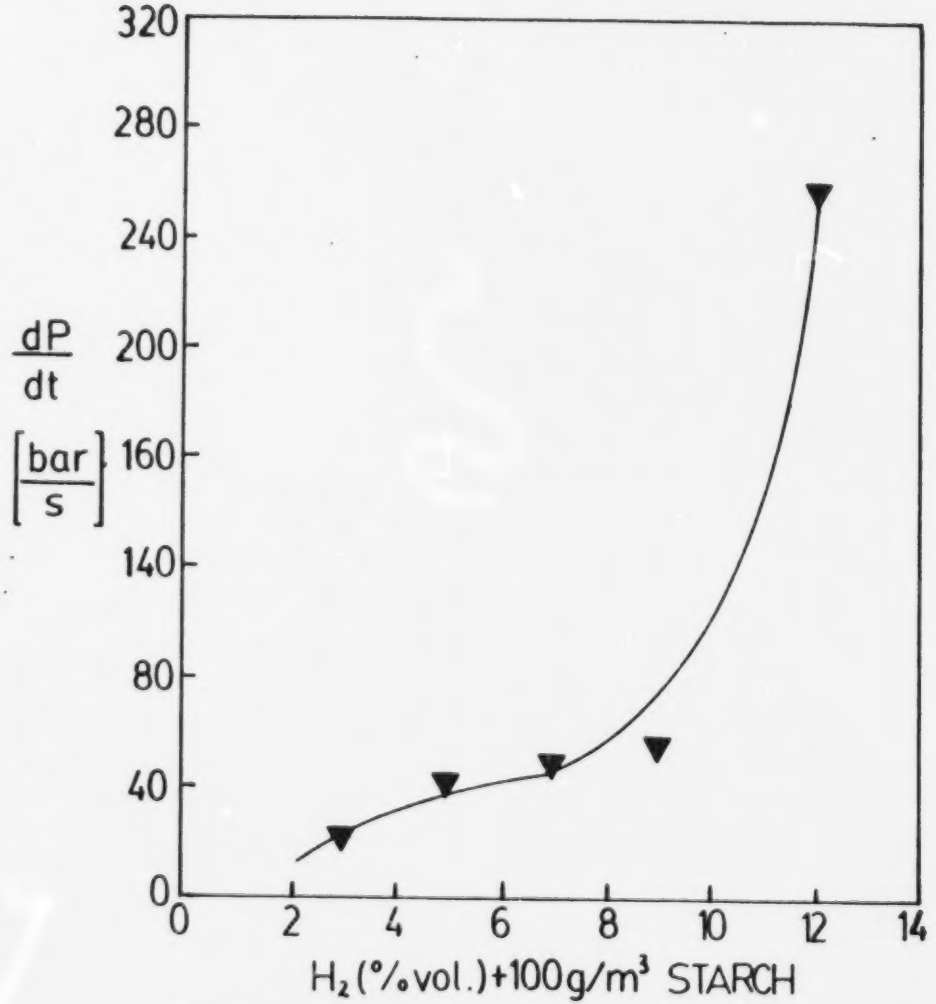

Figure 33 - Rate of pressure rise for 100 g/m^3 starch with different hydrogen-air mixtures

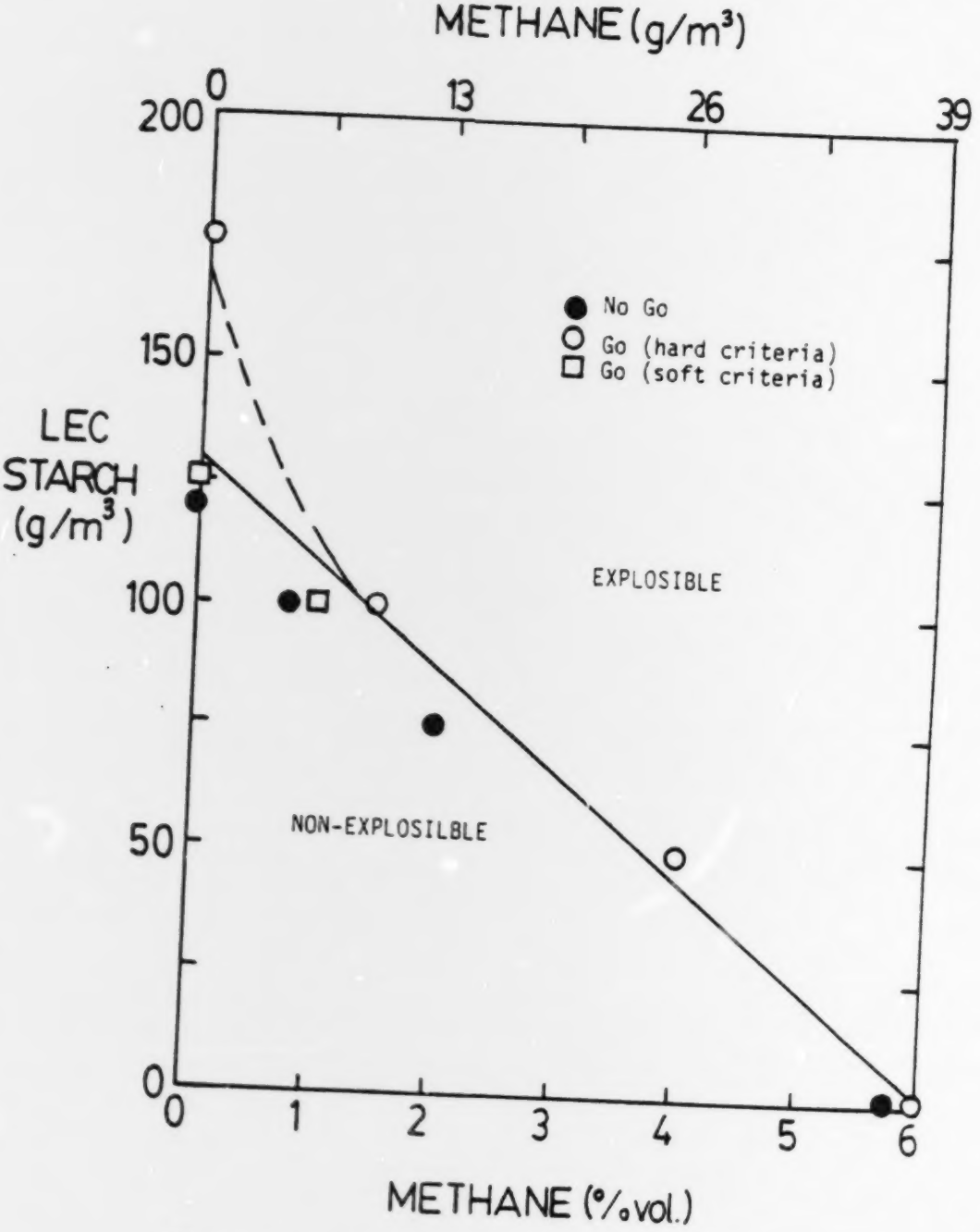

Figure 34 - Lower explosible concentrations of cornstarch in atmospheres containing methane